Regulation of a Prion-Induced Immune Response by MiRNA-146a

by

Shantel Gushue, BSc

A Thesis submitted to the Faculty of Graduate Studies of

The University of Manitoba

In partial fulfillment of the requirements for the degree of

MASTER OF SCIENCE

Department of Medical Microbiology

University of Manitoba

Winnipeg, Manitoba

Table of Contents

Abstract

Prion diseases are curious neurodegenerative diseases characterized by the conversion of a cellular protein, PrP^{C}, into an infectious isoform, PrP^{Sc}. One of the earliest hallmarks of disease and concurrent with prion deposition, is the activation of the brain's principal immune effector cells, microglia. In prion disease, activated microglia synthesize fairly low levels of pro-inflammatory cytokines, presumably to ameliorate the severe pathology that can arise in host tissue as a result of an acute inflammatory response. The specific stimuli and signaling pathways that lead to this modulation of function are as yet unknown. However, the involvement of miRNAs, a recently identified class of regulatory molecules, is likely. Recently, miR-146a was found to be upregulated in the brains of prion infected mice. In addition, its expression was found to be enriched in cells of microglial origin. It was hypothesized that, given the immunomodulatory role ascribed to miR-146a in macrophages, upregulation of miR-146a may function to attenuate the microglial immune response to prion infection.

The first objective was to identify inflammatory related miRNAs associated with prion disease in microglia. Using Taqman Low Density Arrays, allowing for the detection of hundreds of miRNAs at once, the miRNAs of microglia treated with inflammatory agonists were profiled. The miRNA profile of activated microglia was found to be similar to that of macrophages. Furthermore, among the miRNAs profiled, miR-146a and miR-155 were the most highly induced and persistently expressed over 24 hours.

The second objective was to investigate miR-146a induction. Therefore, microglia were treated with various agonists and miR-146a expression was determined using

Taqman miR-146a assays. Although treatment with a PrP-mimic did not induce miR-146a expression, stimulation of TLRs 1, 2, 4, and 5, resulted in significant over-expression similar to what has been described previously. Moreover, in contrast to the rapid and transient induction of inflammatory mediators, miR-146a follows alternate kinetics functioning to prolong the dampening of the innate immune response following activation via TLR4 and TLR2.

By employing a functional proteomic strategy, the third objective was to identify miR-146a regulated proteins. First, miR-146a expression was manipulated using miR-146a mimics and miR-146a inhibitors. Secondly, the functional model was validated by confirming decreased expression of IL6 by ELISA in miR-146a over-expressing microglia cells. Lastly, using Tandem Mass Tag labels to discriminate between treatment group (miR-146a mimic and TLR2 agonist) and control group (scrambled-miR and TLR2 agonist), the effect of miR-146a on the proteome was determined. In total, 172 proteins were identified as being miR-146a regulated and gene ontology assignment resulted in an over-representation of proteins involved in cellular dynamics capable of altering the activation state of microglia. After filtering for bioinformatically predicted targets and those implicated in a similar genomic study, it was decided to further investigate proteins ARF6, RhoA and NOS2 based on their role in modulating the phagocytic potential of microglia.

The final objective was to validate miR-146a putative direct targets identified from the proteomics analysis. Luciferase expression of the 3'UTR of targets upon transfection with miR-146a were determined. Based on luciferase analysis, NOS2 appears to be directly targeted by miR-146a and this was also confirmed by western blot.

While production of NOS2 by microglia under an acute activation state serves to support and protect CNS homeostasis, chronic expression of this factor can lead to neurotoxicity. Therefore, miR-146a appears to have an overarching role in altering microglial activation during prion disease thus protecting neurons from bystander damage.

Taken together, these results suggest that miR-146a could play an important role in the prion disease process by specifically attenuating the microglial induced immune response. Therefore, manipulation of miR-146a may represent a novel therapeutic strategy. Furthermore, given that miR-146a de-regulation has been observed in other neurodegenerative diseases, these results may well extend beyond the realm of prion disease. Lastly, although practical limitations relating to the sensitivity of the comparative proteomics methodology meant that it alone were not sufficient to identify miRNA targets, an integrated approach that takes into consideration genomic and bioinformatic strategies is most promising.

Acknowledgements

I would like to take this opportunity to express my sincere appreciation and gratitude to my supervisor, Dr. Stephanie Booth, Adjunct Professor in the Department of Medical Microbiology and Infectious Diseases, Faculty of Medicine, University of Manitoba and the Head Research Scientist, Molecular Pathbiology, Public Health Agency of Canada, for her guidance, direction, expertise and support during the course of this project and preparation of the thesis. It was a longer road than expected, but because of her encouragement and patience, I finally made it to the light at the end of the tunnel. I would also like to thank Dr. Booth's financial support during the course of this project.

I would like to thank my committee members Dr. Keith Fowke, Head and Professor in the Department of Medical Microbiology and Infectious Diseases, and Dr. Sam Kung, Associate Professor in the Department of Immunology, both of the Faculty of Medicine, University of Manitoba, for their insightful discussions during our meetings and for reviewing this thesis.

To the members of Dr. Booth's lab (past and present) including Sarah Medina, Reuben Saba, Rhiannon Harris Huzarewich, Kathy Manguiat, Anna Majer, Amrit Boese, Clark Phillipson, Bernie Abrenica, Kathy Frost, Yulian Niu, Kyle Caligiuri, and Debra Sorenson, thank you for all of your help and assistance over the years and for some very special memories I will cherish for the rest of my life.

I would like to extend a heartfelt thank you to my family including: Dad (Boris) and wife (Debbie); Aunt (Vera) and husband (Stan); Baba (Liliana); Mom (Denise) and

partner (Pete); Sister (Charisse) and partner (Dan); and nephews (Joey and Daniel) for providing me with the love and support that guided and encouraged me to complete this chapter in my life. You were with me every step of the way and words cannot express how much it meant to me.

Lastly, I would like to thank the Alevizos family, especially Dino, for providing me with unconditional love, inspiration, drive and opportunity that ultimately lead to the completion of this thesis.

Dedication

This thesis is dedicated my Baba, Liliana Nakarow. You are an inspiration to me and will continue to be for the rest of my life. I would not be the person I am today, nor would I have experienced the amount of happiness, joy and success in my life, had it not been for you. I love you and will forever appreciate how much you have positively influenced every aspect of my life.

List of Tables

List of Figures

1. Introduction

1.1 Prion disease

Prion diseases, or transmissible spongiform encephalopathies (TSEs), represent a group of lethal neurodegenerative disorders that affect humans and a wide range of animal species. In humans, they comprise kuru, Creutzfelt-Jakob disease (CJD), fatal familial insomnia (FFI), Gerstmann-Straussler-Scheinker disease (GSS), and the recently described variably protease-sensitive prionopathy (VPSPr). In animals, they include scrapie in sheep and goats, bovine spongiform encephalopathy (BSE), chronic wasting disease (CWD) in deer and elk, transmissible mink encephalopathy (TME), exotic ungulate spongiform encephalopathy (EUE), feline spongiform encephalopathy (FSE), and transmissible spongiform encephalopathy (NHP) in non-human primates.

Prion diseases belong to a growing group of disorders that are a consequence of protein misfolding and aggregation, which include Alzheimer's disease (AD), Parkinson's disease, Huntington disease (HD), systemic amyloidosis, and many others. Distinct from these disorders, prion diseases have a wide phenotypic spectrum, multiple apparent etiologies, and have a high degree of transmissibility within and between species. They are extremely curious diseases that behave similarly to conventional infectious agents and occur in a variety of strains characterized by distinctive clinical and neuropathological features. However, despite inherent differences among prion strains, all share a common and intriguing feature, the conversion of a normal cellular protein, known as the cellular prion protein (PrP^{C}), into an abnormal isoform that is infectious, known as the scrapie prion protein (PrP^{Sc})(Prusiner, 1982).

1.2 Etiology

Prion diseases can occur as a result of a sporadic, genetic or acquired event (Table 1.1). In sporadic forms of the disease, the source of infection is of an idiopathic nature and, therefore, undetermined. Possible explanations are somatic mutations of the *PRNP* gene or spontaneous conversion of PrP^{C} to PrP^{Sc} (Prusiner, 1998). Sporadic CJD is the most common form of human prion disease. It accounts for 85% of all CJD cases with an annual worldwide incidence of 1-2 cases/million population. This disease occurs equally between the sexes and the average age of onset is 60 years old (R. T. Johnson, 2005; Mead et al., 2003; Sikorska & Liberski, 2012). However, some younger (below 20 years) and older (above 90 years) cases have been reported (Sikorska & Liberski, 2012). Sporadic CJD progresses very rapidly, with the median time to death being 5 months after the initial onset of symptoms (R. T. Johnson, 2005; Sikorska & Liberski, 2012).

Genetic forms of the disease are inherited and are associated with mutations in the *PRNP* gene. Over 50 different mutations in *PRNP* have been identified in individuals with familial CJD. However, 95% are due to four point mutations at codons 102, 178, 200, and 210, and insertions of five or six octapeptide repeats (Capellari et al., 2005). On the other hand, FFI is associated with a single mutation in *PRNP* at codon 178 (Medori, Montagna et al., 1992; Medori, Tritschler et al., 1992). However, this mutation is not unique and has been found in typical familial CJD (Goldfarb et al., 1992).

The last form of disease, and probably most infamous and feared, is acquired. Acquired forms comprise disorders with suspected or proven external prion exposure through either dietary or iatrogenic means. This form has received considerable attention

with regard to Bovine Spongiform Encephalopathy (BSE), it's detrimental impact on the cattle industry, and potential threat to humans given that beef is a common food source. The first cases of human prion disease of BSE origin, known as variant CJD (vCJD), were reported in April 1996 in the UK (Will et al., 1996). As of 2012, a total of 224 patients with vCJD from 12 countries have been identified worldwide (J. Lee, Kim, Hwang, Ju, & Woo, 2013). A similar but recent emerging threat to humans, has been the dramatic rise in Chronic Wasting Disease (CWD) among deer and elk populations (Belay et al., 2004). The Canadian Food Inspection Agency state that while at this time there is no scientific evidence to suggest that CWD can be transmitted to humans, precautions must be taken and human exposure to the CWD infectious agent be avoided as they continue to evaluate any potential health risk (Canadian Food Inspection Agency of Canada, 2012).

Iatrogenic transmission of the prion agent has been recognized as early as 1970 and has reportedly occurred through contaminated neurosurgical instruments, intracerebral electroencephalographic electrodes, human pituitary hormone, corneal transplant, or dura mater grafts (Duffy et al., 1974). Advancements in the field of medicine have greatly decreased the incidence of transmission due to iatrogenic means; however, a new type of iatrogenic CJD has emerged and become a significant public health concern. In 2004, the first case of human-to-human secondary transmission of vCJD via blood transfusion was reported in the UK (Llewelyn et al., 2004). As a result, Canada has implemented much more stringent requirements for blood donation such as refusal to accept blood from those who have travelled to Britain or France for an extended period of time (Canadian Blood Services, 2005).

Table 1.1. Etiology of prion diseases.

DISEASE	ACRONYM	HOST	ETIOLOGY
Scrapie	Scrapie	Sheep, Goats	Infection with Prions of unknown origin
Transmissible Mink Encephalopathy	TME	Mink	Infection with Prions of either sheep or cattle origin
Chronic Wasting Disease	CWD	Cervids	Infection with Prions of unknown origin
Bovine Spongiform Encephalopathy	BSE	Cattle	Infection with Prions of unknown origin
Exotic Ungulate Spongiform Encephalopathy	EUE	Nyala, Kudu	Infection with Prions of BSE origin
Feline Spongiform Encephalopathy	FSE	Cats	Infection with Prions of BSE origin
Transmissible Spongiform Encephalopathy in Non-Human Primates	NHP	Lemurs	Infection with Prions of BSE origin
Kuru	Kuru	Human	Ritualistic Cannibalism
Sporadic Creutzfelt-Jacob Disease	sCJD	Human	Spontaneous $PrP^{C} \rightarrow PrP^{Sc}$ conversion or somatic mutation
Familial Creutzfelt-Jacob Disease	fCJD	Human	Mutations in *PRNP*
Gerstmann-Staussler-Scheinker Syndrome	GSS	Human	Mutations in *PRNP*
Iatrogenic Creutzfelt-Jacob Disease	iCJD	Human	Infection with Prions of human origin by cadaveric corneal grafts, hGH or dura mater
Fatal Familial Insomnia	FFI	Human	*PRNP* haplotype 178N-129M
Variant Creutzfelt-Jacob Disease	vCJD	Human	Infection with Prions of BSE origin
Sporadic Fatal Insomnia	sFI	Human	Spontaneous $PrP^{C} \rightarrow PrP^{Sc}$ conversion or somatic mutation
Variably Protease-Sensitive Prionopathy	VPSPr	Human	Spontaneous $PrP^{C} \rightarrow PrP^{Sc}$ conversion or somatic mutation

1.3 PrP^{Sc}

It is clear that prion diseases have become an important issue from a public health perspective but, in addition, the unique biological features of the prion agent has captivated the scientific community. While the molecular structure of PrP^{Sc} is poorly understood, what is known is that it is identical in its primary sequence to the PrP^{C} molecule from which it originates. Furthermore, PrP^{Sc} is vastly different in its secondary structure than that of PrP^{C}. Unlike the cellular form, which is approximately 40% α-helical and 3% β-sheet, PrP^{Sc} is heavily β-pleated (approximately 40%)(Pan et al., 1993; Prusiner, 1998). Although many approaches have been used to further study the structure of PrP^{Sc}, the inherent biochemical properties pose significant challenges to traditional and existing methods. Contrary to the biochemical properties of PrP^{C}, PrP^{Sc} is detergent insoluble, proteinase K resistant, and forms protein aggregates in a similar fashion to that of amyloid in Alzheimers diseased brains (Cohen & Prusiner, 1998; Prusiner, 1998).

1.4 Mechanism of PrP^{Sc} replication and conversion

Prion replication begins when PrP^{Sc} interacts with host PrP^{C}, thereby catalyzing its conversion to the pathogenic form of the protein. The precise molecular mechanism of PrP^{C} to PrP^{Sc} conversion are not completely understood; however, historically, two models have been proposed. They are the nucleation-polymerization model and the template assisted model indicated in **Figure 1.1**. According to the nucleation-polymerization model, PrP^{Sc} is a small oligomer that acts as a seed for recruiting, converting and stabilizing the misfolding of monomeric PrP^{C} molecules which then become incorporated into the polymer (Jarrett & Lansbury, 1993). In the template-

assisted model, monomeric PrP^{C} unfolds to some extent and refolds under the influence of monomeric PrP^{Sc} and this reaction is thought to be facilitated by an enzyme or a chaperone and an energy source (Prusiner, S.B., 1991). While neither model have been shown *in vivo*, available data support a nucleation-polymerization model (Caughey, 2003; Soto, Saborio, & Anderes, 2002; Soto, Estrada, & Castilla, 2006). The question remains, however, whether or not prion replication requires a cellular co-factor. Several pieces of evidence indicate that co-factors indeed play a role in this process (Abid & Soto, 2006). For example, lipids and polyanions have been identified as minimal components required for the amplification of PrP^{Sc} (Deleault, Harris, Rees, & Supattapone, 2007).

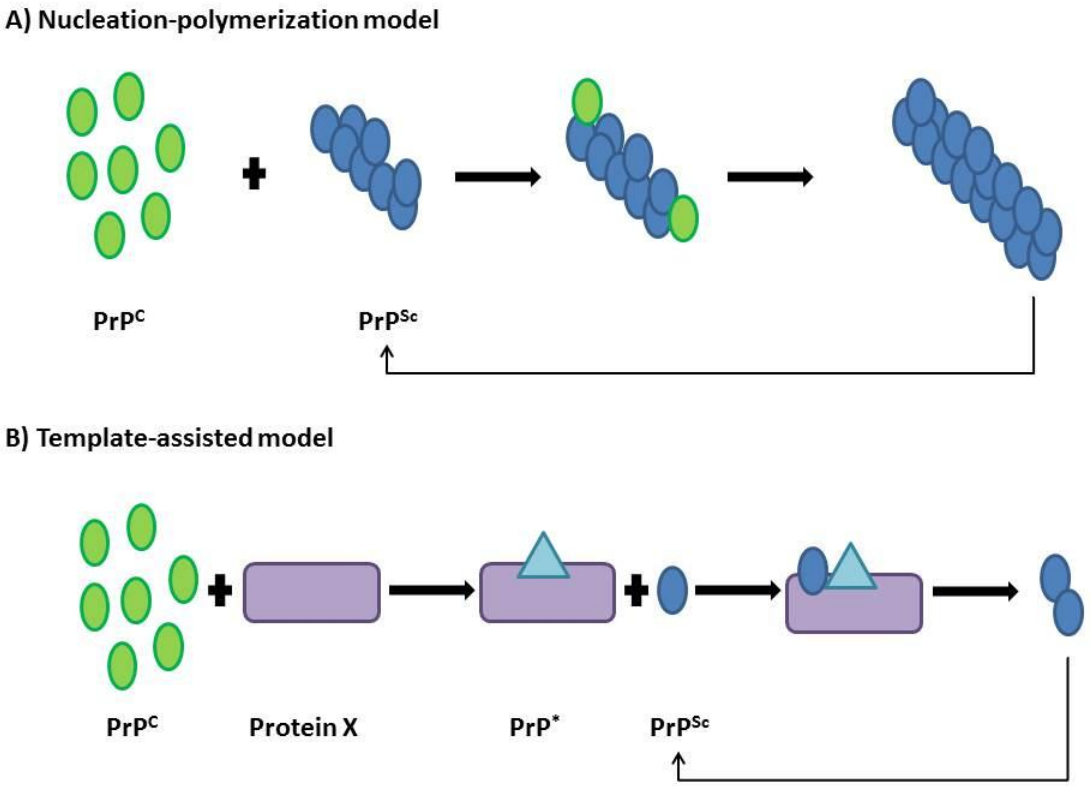

Figure 1.1. Models for conversion of PrP^{C} to PrP^{Sc} **A.** Nucleation-polymerization model. The infectious PrP^{Sc} is a small oligomer that acts as a seed for recruiting, converting and stabilizing the misfolding of the normal PrP^{C} **B.** Template-assisted model. Key step includes the formation of an intermediate state (PrP*) on binding to a molecular chaperone (protein X). This intermediate can interact with PrP^{Sc} (monomeric or oligomeric), which acts as a template for its conversion. Adapted from Soto (2004).

1.5 Role of PrP^C

PrP^C is a normal cellular glycophosphatidylinositol (GPI) anchored membrane protein encoded on the *PRNP* gene locus of hosts. Although it is expressed in a wide range of tissues such as muscle, heart, lymphoid tissues, kidney, digestive tract, skin, mammary gland, and endothelia, it is especially concentrated in the brain (Ford, Burton, Morris, & Hall, 2002; Linden et al., 2008; Miele et al., 2003; Tichopad, Pfaffl, & Didier, 2003). In the brain, maximal expression of PrP^C is observed in neuronal and glial populations of the hippocampus, thalamus and neocortex (Bailly et al., 2004; Ford et al., 2002; Harris et al., 1993; Laine, Marc, Sy, & Axelrad, 2001; Moser, Colello, Pott, & Oesch, 1995; Radovanovic et al., 2005).

The *PRNP* gene is highly conserved among mammals and paralogue genes have been described in chicken, amphibians, reptiles and fish, suggesting an important role in cellular and biological processes (Nicolas, Gavin, & del Rio, 2009). Initial independent studies with several null mouse strains failed to find developmental or anatomical gross abnormality which lead to the temporary conclusion that PrP^C does not fulfill any important biological function (Manson et al., 1994; Moore et al., 1999; Rossi et al., 2001; Sakaguchi et al., 1996). However, studies focusing on the nervous system have revealed that PrP^C is indeed a multifaceted protein involved in a variety of biological functions including: copper and/or zinc ion transport or metabolism, neuroprotection, lymphocyte activation, cellular signaling and proliferation, membrane excitability, synaptic transmission and plasticity, neuritogeneisis, and apoptosis (D. R. Brown, 2002; Cashman et al., 1990; Chiarini et al., 2002; Maglio, Perez, Martins, Brentani, & Ramirez, 2004; Mouillet-Richard et al., 2000; Sakaguchi et al., 1996; Steele, Emsley, Ozdinler,

Lindquist, & Macklis, 2006). How the functions ascribed to PrP^{C} specifically relate to prion pathogenesis remains largely unknown. What is known, however, is that PrP^{C} is indispensable to the replication and conversion process of prion diseases. In addition, the amount of PrP^{C} available is directly proportional to the extent to which conversion to the infectious form occurs. This is supported by the observation that PrP-deficient mice do not develop prion disease when inoculated with the infectious agent and, conversely, PrP-overexpressing mice exhibit significantly shortened incubation time of disease (Bueler et al., 1992; Fischer et al., 1996; Manson et al., 1994; Sakaguchi et al., 1996; Scott et al., 1989)

1.6 Prion pathogenesis

Given the abundant expression of PrP^{C} in the central nervous system (CNS), it is not surprising that prion pathogenesis occurs in the brains of infected hosts resulting in progressive and fatal neurodegeneration. Unclear, however, is the mechanism of neuronal loss. It's possible that continuous conversion of PrP^{C} to PrP^{Sc} may result in functional impairment of the former, so that its assumed neuroprotective effects are lost. This is central to the proposed ''loss of function hypothesis''. Another possibility, known as the "gain of function hypothesis", is that the physiological function of PrP^{C} is not actually linked to toxicity, but rather, toxicity is related to a gain in toxic activity of PrP^{Sc}. Support for this hypothesis stem from observations with other protein misfolding neurodegenerative diseases whereby brain damage occurs in areas where protein aggregates accumulate. In addition, *in vitro* experiments have shown that misfolded oligomers are directly toxic to neurons in culture (El-Agnaf et al., 1998; Forloni et al., 1993; Loo et al., 1993). However, in the absence of PrP^{C}, PrP^{Sc} is innocuous, suggesting

that PrP oligomers and fibrils are not toxic *per se* and that PrP^C may act as a mediator of the toxic signal (Brandner et al., 1996).

1.7 Clinical and pathological features of prion disease

In humans with prion disease, impaired brain function becomes increasingly evident prior to death and include symptoms such as loss of coordination, insomnia and rapid dementia. Symptoms such as irritability and ataxia are exhibited in humans and animals alike. Other distinct characteristics associated with prion-induced neurodegeneration are observed at the microscopic level. They are: neuronal loss, prominent gliosis, deposition of prion amyloids, and the presence of round empty spaces that generates a spongiform appearance in brain tissue. Interestingly, gliosis, which encompasses the activation of astrocytes and especially microglia, is one of the earliest hallmarks of disease. In many instances, this feature precedes clinical symptoms as well as other typical neurodegenerative changes such as spongiosis, neuronal cell death, and prion deposition (Giese et al., 1998). Not surprising, microglia have been implicated as playing a role in the prion-induced neurodegenerative process, particularly with regard to the observed neuroinflammation.

1.8 Microglia and prion disease

Microglia are crucial components of the innate immune response. They typically exist as quiescent entities of the brain, but when antagonized by even subtle disturbances in CNS homeostasis that may result from infection, autoimmunity, ischemia, hemorrhage, wounds, and degenerative diseases, can respond quite aggressively. They alter from a resting state to an activated one involving numerous changes which include

morphological changes, proliferation, chemotaxis, phagocytosis and the production of numerous cytokines and chemokines involved in inflammatory and immunomodulatory responses (Ghoshal et al., 2007; B. Liu & Hong, 2003; Streit, 2002a; Streit, 2002b). Such an inflammatory milieu has been recognised in the prion infected brain for some time; however, whether the activation of this innate immune response contributes to neurodegeneration versus neuroprotection in prion-like pathologies, is still unknown.

Upon accumulation of PrP^{Sc} deposits, microglia are activated and attracted to the site of injury, sometimes involving migration of the cells within the brain (Williams, Lawson, Perry, & Fraser, 1994). After activation, microglia upregulate certain proteins including complement factors, proteins of the major histocompatibility complex, proinflammatory cytokines including TNFα and interleukins such as IL6 and IL-1β (D. R. Brown, 2001). If there is excessive and chronic activation of these factors, the immune system goes into overdrive and produces oxidative stress, fostering neuronal apoptosis and neurodegeneration. Alternatively, lines of evidence indicate that PrP^{Sc} can be efficiently cleared from the brain and that phagocytosis by activated microglia represents a prominent clearing mechanism (Beringue et al., 2000; Luhr et al., 2004; McHattie, Brown, & Bird, 1999). Further supporting a beneficial role, microglia secrete neurotrophic factors such as brain derived neurotrophic factor (BDNF) which functions to promote neuronal growth and recovery in the face of a neurodegenerative state. Increasing evidence suggests that microglial cells may be multi-functional, playing roles in brain tissue repair and neurogenesis, as well as in immunity (Wyss-Coray & Mucke, 2002).

1.9 Prion-induced inflammatory response

In prion disease, the activation of microglia cells appear to be of a chronic and atypical nature. This activated phenotype, which has been referred to as anti-inflammatory or benign, shows low levels of the inflammatory cytokines IL6, IL-1β and TNFα, and readily detectable levels of TGF-β and PGE2 (Cunningham et al., 2003; V. H. Perry, Cunningham, & Boche, 2002). This specific cytokine profile has been observed in macrophages during phagocytosis of apoptotic cells, representing a phagocytic phenotype (Fadok, McDonald, Bratton, & Henson, 1998). Furthermore, while there is no evidence that the enhanced levels of PGE2 are detrimental, nor that TGF-β is injurious, there is evidence suggesting microglia are in a "primed state" and capable of producing a heightened pro-inflammatory profile in the presence of systemic inflammation. Indeed, when prion-infected mice were challenged systemically with bacterial endotoxin to mimic an intercurrent infection, there was a dramatic switch in the microglial phenotype to an aggressive inflammatory cytokine profile and increased neuronal apoptosis (Cunningham et al., 2009). The rapid switching of the microglia phenotype illustrates the inherent plasticity of these cells and also illustrates that these cells are subject to tight regulation.

1.10 Involvement of toll-like receptors (TLRs)

The contribution of toll-like receptors (TLRs), a family of proteins that are central players in the stimulation of innate immune responses, has been investigated in relation to prion disease progression. Upon recognition of their ligands, TLRs transduce intracellular signals via intermediary proteins including MyD88, TIRAP, TRIF, and TRAM, and

signaling molecules such as IRAK4, IRAK1, and TRAF6. These signals translate to the production of inflammatory cytokines and interferons (IFNs) (**Figure 1.2**).

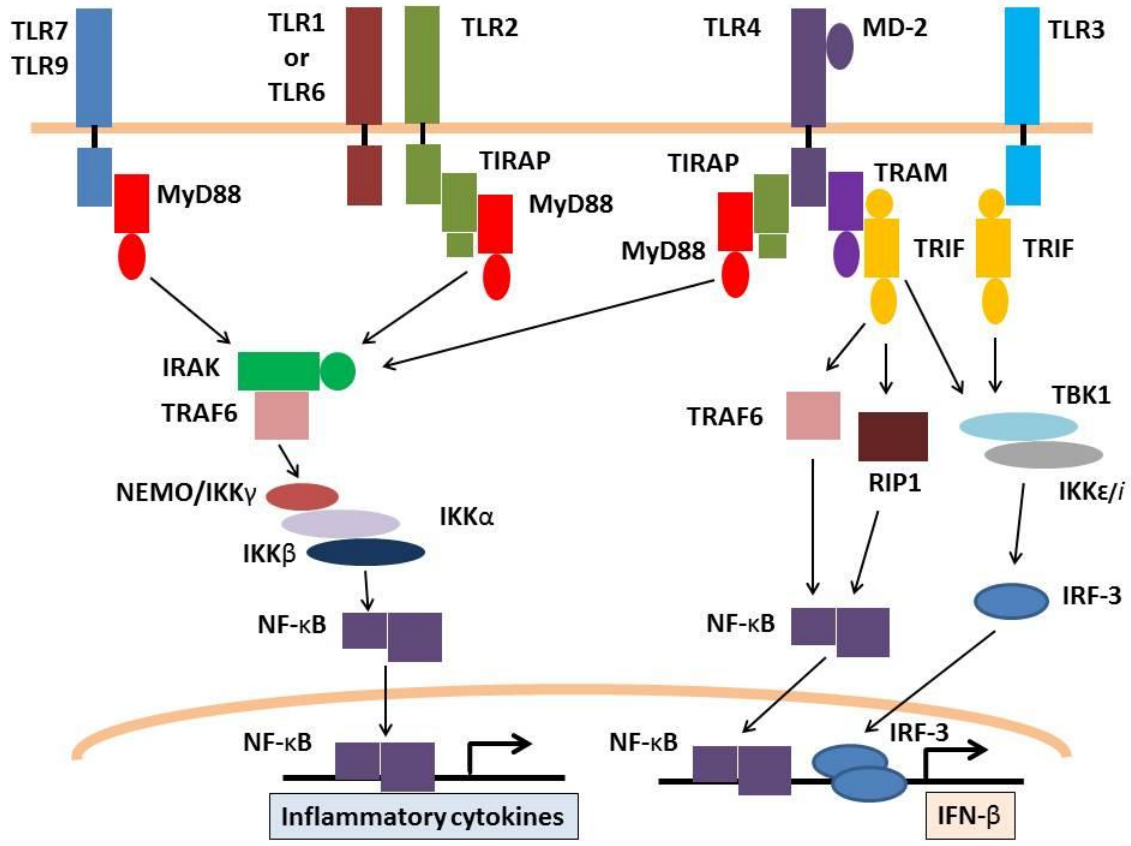

Figure 1.2. Simplified TLR signaling pathway. TLR2 in concert with TLR1 or TLR6 discriminates between the molecular patterns of triacyl and diacyl lipopeptide, respectively. TLR3 recognizes dsRNA. TLR4 recognizes bacterial LPS. TLR7 mediates recognition of imidazoquinolines and ssRNA. TLR9 recognizes CpG DNA of bacteria and viruses. TLR1/2 and TLR2/6 utilize MyD88 and TIRAP as essential adapters. TLR3 utilizes TRIF. TLR4 utilizes four adapters, including MyD88, TIRAP, TRIF and TRAM. TLR7/8, TLR9 use only MyD88. The MyD88-dependent pathway controls inflammatory responses, while TRIF mainly mediates type I IFN responses. Adapted from Takeda and Akira (2004).

An increasing amount of data is emerging that describes the involvement of TLRs in the pathogenesis of prion diseases. It has been reported that pretreatment with immune activators such as un-methylated CpG DNA and complete Freund's adjuvant, both of which are known to activate immune response-mediated TLR2 and TLR9 signaling, delayed the onset of prion disease in mice inoculated with Rocky Mountain Laboratory (RML) strain (Sethi, Lipford, Wagner, & Kretzschmar, 2002; Spinner et al., 2007; Tal et al., 2003). Furthermore, Spinner et al (2008) found that ablation of TLR4 signaling in mice, causing cause them to be hyporesponsive to lipopolysaccharide (LPS), significantly accelerated the rate of prion disease development in comparison to their wild-type counterparts (Spinner et al., 2008). They also found that the anti-prion mechanisms induced by TLR4 signaling appear to be functional in the CNS rather than the periphery. In addition, a study by Prinz et al (2003) confirmed that pathogenic changes in prion disease are independent of MyD88, a major adaptor signaling molecule of TLRs (Prinz et al., 2003). Recently, a MyD88-independent transcription factor known as interferon regulatory factor 3 (IFN3) was implicated as having a protective role against prion infection (Ishibashi, Atarashi, & Nishida, 2012). Although the mechanism for the anti-prion effects mediated by IRF3 has yet to be clarified, certain interferon responsive genes might be involved.

TLRs are known to be expressed by innate immune response cells and play a critical role in their activation against foreign pathogens. In particular, microglial TLRs are crucial as a first line of defence against bacterial or viral infection in the CNS and are capable of mediating different pathways leading to their neuroprotective or neurotoxic phenotypes. For example, the activation of microglial TLR2 by the Alzheimers amyloid β

(Aβ) peptide is associated with neuronal injury through the release of cytotoxic inflammatory mediators and nitric oxide (NO)(K. Chen et al., 2006; Tahara et al., 2006). Conversely, when TLR2 is inhibited, phagocytosis of Aβ is enhanced, improving neuronal function in AD mice (K. Chen et al., 2006; Tahara et al., 2006). Indeed, the regulation of microglial activation state by TLRs is undeniable and warrants further investigation with regard to prion disease. A new layer of regulation by small RNA molecules, known as microRNAs (miRNAs), have also been implicated in altering microglial functioning during prion-induced neurodegeneration.

1.11 MicroRNAs and their biogenesis

Recent evidence suggests that miRNAs are capable of regulating gene expression post-transcriptionally and play important roles in modulating the response of immune cells to stimuli (O'Connell, Rao, Chaudhuri, & Baltimore, 2010). They are short non-coding RNA molecules of approximately 22 nucleotides in length that bind to one or more locations in the untranslated region (UTR) of mRNA targets (Bartel, 2004). While binding to the 5'UTR of transcripts have been observed, miRNAs most commonly bind the 3'UTR.

MiRNAs are the products of enzymatic processing of longer precursor RNA molecules transcribed largely by RNA polymerase II from intergenic noncoding transcripts or noncoding regions of protein-coding transcripts (Cai, Hagedorn, & Cullen, 2004; S. M. Johnson, Lin, & Slack, 2003; Johnston & Hobert, 2003; Y. Lee et al., 2004). Processing from intragenic regions by RNA polymerase III have also been reported (C. Z. Chen, Li, Lodish, & Bartel, 2004). The precursors typically contain imperfect inverted repeats that are capable of folding back on themselves to generate stem-loop structures.

The stem loop structures are cleaved at their base by the microprocessor complex consisting of the enzyme Drosha and its interacting partner, DGCR8/Pasha, within the nucleus (Y. Lee et al., 2003). The stem-loop structures, known as pre-miRNAs, are actively exported to the cytoplasm by Ran-GTPase/Exportin 5 and further processed by the highly conserved Dicer enzyme to release double-stranded RNA molecules corresponding to the stem region (Basyuk, Suavet, Doglio, Bordonne, & Bertrand, 2003; Y. Lee et al., 2003). This duplex molecule is then selected and incorporated into the RNA-induced silencing complex (RISC) or the microribonucleoprotein complex (miRNP), where the strand with the least thermodynamically stable 5' end is used to activate the complex and guide it to complementary mRNA targets (Mourelatos et al., 2002). Depending on the degree of homology between the miRNA and its target sequence, miRNA-mediated regulation of gene expression is achieved either by degradation or translational repression of the target molecule. For example, precise pairing with complementary nucleotide sequences in the 3'UTR of target mRNAs results in mRNA degradation, whereas the association of the miRNA seed sequence at their 5'end (nucleotides 2-8) with the 3'UTR of target mRNAs results in translational repression (Doench, Petersen, & Sharp, 2003; Khvorova, Reynolds, & Jayasena, 2003; Schwarz et al., 2003). A simplified illustration of miRNA biogenesis is provided in **Figure 1.3**.

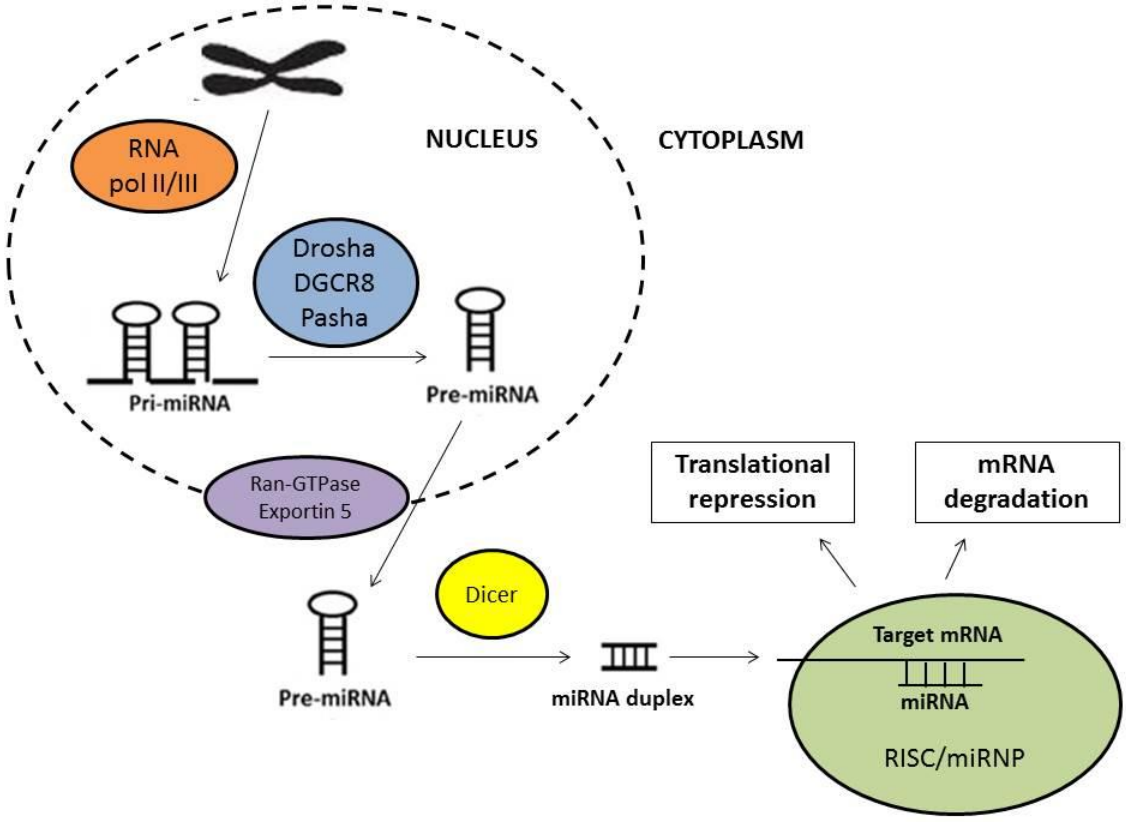

Figure 1.3 Biogenesis of miRNAs. The miRNA gene is transcribed to generate a primary miRNA (pri-miRNA) precursor molecule that undergoes nuclear cleavage to form a precursor miRNA (pre-miRNA). The pre-miRNA is cleaved in the cytoplasm to create a miRNA duplex containing the mature miRNA. The duplex unwinds and the mature miRNA assembles into RISC (or miRNP). The miRNA base-pairs with target mRNA to direct gene silencing via mRNA degradation or translational repression based on the level of complementarity between the miRNA and the mRNA target

The notion that target-site recognition is primarily determined by multiple instances of nucleotides 2-8 implies that miRNAs influence the expression of a remarkably large number of different mRNAs. Indeed, a single miRNA is capable of targeting hundreds to thousands of transcripts (Lewis, Shih, Jones-Rhoades, Bartel, & Burge, 2003). Likewise, a single target may have multiple binding sites for various miRNAs. Another interesting and relatively new regulatory concept, is the potential for a miRNA to regulate another miRNA (Lai, Wiel, & Rubin, 2004).

1.12 Relevance of miRNAs

In general, well over a third of human genes appear to be regulated by miRNAs either indirectly or directly. These estimates are also expected to be much higher as more miRNAs are identified and the sensitivity of computational target finding programs increases. In addition, miRNAs are highly conserved among species suggesting strong selective pressure likely driven by important biological or cellular functioning. Bernstein et al (2003) found that mice lacking Dicer, the enzyme essential for the production of mature miRNAs, die at embryonic day 7.5 and lack multipotent stem cells (Bernstein et al., 2003). Taken together, it is not surprising that miRNAs are currently known to be involved in almost all biological processes and developmental programs. Perhaps even more important, however, is that they have been implicated in many human diseases including those with a neuroinflammatory/degenerative component such as AD, HD, and prion disease.

1.13 MiRNAs and neurodegeneration

Despite the fact that miRNAs have only recently (within the last decade) been detected and characterized in the brain, there exists astounding evidence for their role in

various neurodegenerative conditions. Under healthy conditions, miRNAs have been implicated in a wide variety of brain functions that collectively result in the proper development and maintenance of brain tissue. They are crucial for a system's ability to cope with external and internal perturbations, as they regulate the mRNA expression profile by reinforcing transcription, reducing defective and overabundant transcript copy number. Disturbances in gene expression as a result of perturbed transcription or post-translational regulation, is one of the main causes of cellular dysfunction that underlies different disease states. Therefore, the involvement of miRNAs in disease, in addition to their altered expression, is not surprising.

Aberrant miRNA expression patterns have been described in several neurodegenerative diseases which may represent the main etiologic factor underlying disease or, at the very least, provide novel insight into the pathogenesis of disease. In HD, altered expression of miR-29a, miR-330, miR-218, miR-132, miR-9, and miR-124a in progression of the disease have been identified (R. Johnson et al., 2008; Packer, Xing, Harper, Jones, & Davidson, 2008). Both genes and miRNAs have also been found to be differentially expressed in prion disease and, interestingly, some of the largest groups of genes de-regulated during the prion disease process are inflammatory related genes (Saba, Goodman, Huzarewich, Robertson, & Booth, 2008). Among the miRNAs found to be differentially expressed in the brains of prion infected animals, miRNA-146a (miR-146a) was found to be significantly upregulated (Saba et al., 2008; Saba et al., 2012). Given the innate immune function ascribed to this particular miRNA, it's reasonable to propose that some of the prion-induced alterations in gene expression are due to the indirect or direct effects of miR-146a.

1.13 MiRNA-146a

Most vertebrates have two copies of the gene encoding miR-146, miR-146a and miR-146b. Although structurally similar, only deviating by just 2 nucleotides in their mature sequence, they are located on different chromosomes, 5 and 10, respectively. In spite of the structural similarities, they differ greatly in biological activity. Expression profiling has shown that miR-146a is found at high levels in the trachea, lung, thymus, colon, kidney, prostate, skin and the brain. Given the ubiquitous expression, it is not surprising that miR-146a has been shown to play various cellular roles, driven largely by the identification of targets.

It was shown that miR-146a is scarcely expressed in naïve T cells, while abundantly expressed following T cell activation via T cell receptor stimulation (Curtale et al., 2010). During T cell activation, miR-146a was shown to play an anti-apoptotic role, mediated through the targeting of FADD mRNA (Curtale et al., 2010). Production of IL-2 was also found to be regulated by miR-146a in this study (Curtale et al., 2010). Based on these observations, it was suggested that miR-146a play a role in the modulation of adaptive immunity.

MiR-146a has also been reported to be a tumor suppressor in various cancers including gastric, pancreatic, breast and prostate cancer through the regulation of cellular proliferation, survival and differentiation. In prostate cancer cells, ROCK1, one of the key kinases for the activation of the hyaluronan, was found to be targeted by miR-146a, resulting in the reduction of proliferation, metastasis and invasiveness (Lin, Chiang, Chang, & Ying, 2008). A study by Hurst et al (2009) showed that upregulation of miR-146a induces the expression of Breast Cancer Metastasis Suppressor 1 (BRMS1) protein

resulting in the reduction in metastic potential of breast cancer cells (Hurst et al., 2009). They also found that miR-146a upregulation was associated with a down regulation of the Epidermal Growth Factor Receptor (EGFR)(Hurst et al., 2009). This was also confirmed in pancreatic and gastric cancer cells by two independent studies (Kogo, Mimori, Tanaka, Komune, & Mori, 2011; Li et al., 2010). Interestingly, upregulation of miR-146a has also been shown to target ERB4, a member of the EFGR family. However, this was found to elicit cardiotoxic effects in cardiomyocytes (Horie et al., 2010). Inhibition of glioma development has also been associated with miR-146a expression through direct targeting of NOTCH1 (Mei, Bachoo, & Zhang, 2011). Targeting of the chemokine receptor CXCR4 by miR-146a has also been reported. Downregulation of miR-146a in leukemic cell lines and normal megakaryocytes, have important consequences for malignancy through enhanced CXCR4 expression (Labbaye et al., 2008). Direct targeting of CXCR4 mRNA by miR-146a was also confirmed by another study showing that the Karposi's sarcoma-associated herpesvirus-encoded viral FLICE inhibitor protein (v-FLIP) mediates CXCR4 suppression through miR-146a upregulation (Punj et al., 2010). MiR-146a functioning in cellular proliferation and differentiation goes beyond cancer and has implications in other cellular processes through direct targeting of specific molecules. For example, miR-146a modulation of Kruppel-like factor 4 (KLF4) has an important role in promoting vascular smooth muscle cell proliferation (Sun et al., 2011).

Perhaps most notorious role ascribed to miR-146a, is the regulation of the innate immune response. In fact, miR-146a was the first miRNA shown to have a direct role in the regulation of innate immune responses (Taganov, Boldin, Chang, & Baltimore, 2006).

Taganov and colleagues (2006) showed that there are two NF-κB binding sites in the promoter regions of miR-146a. Moreover, the authors showed that mir-146a was the effector arm of a negative feedback mechanism of inflammatory signaling pathway initiated by NF-κB (TNF-α activation) and that miR-146a directly targets IL-1 receptor-associated kinase 1 (IRAK1) and TNF receptor-associated factor 6 (TRAF6) for post transcriptional regulation (Taganov et al., 2006). IRAK1 and TRAF6 are key adapter molecules in TLR and IL-1 receptor signaling cascades which can mediate the activation of NF-κB. Therefore, it appears that by post-transcriptionally regulating TRAF6 and IRAK1, miR-146a can fine tune the immune response and, in the process, keep the immune response to pathogens "in check". Induction of miR-146a by the TLR system has been reported through TLR1, 2, 4, and 5 (Taganov et al., 2006). In addition to stimulation of TLRs, IL-1β induced increases of miR-146a expression have also been reported (M. M. Perry, Moschos, Williams, Shepherd, Larner-Svensson, & Lindsay, 2008a). In this study, miR-146a expression was found to negatively regulate the release of chemokines, IL-8 and RANTES. Significantly, this negative feedback inhibition was only seen at high IL-1β concentrations, which indicated that this might be an important mechanism during severe inflammation. Taken together, miR-146a is now often thought to be a negative regulator during the innate immune response.

1.13 MiR-146a and prion disease

As mentioned previously, microglia cells are the primary effectors of the innate immune response in the brain and their activation is one of the first pathological features of disease. They synthesize fairly low levels of pro-inflammatory cytokines; presumably as a defense mechanism to prevent the severe pathology that can arise in host tissue as a

result of an acute inflammatory response induced by rampant signaling in phagocytes (V. H. Perry et al., 2002). The specific stimuli and signaling pathways leading to this modulation of functions are as yet unknown. However, given the regulatory role played by miRNA's, their involvement is likely. Recently, the upregulation of miR-146a during prion induced neurodegeneration in mouse models of disease was reported (Saba et al., 2008; Saba et al., 2012). Also reported was that its expression in the CNS is highly enriched in cells of microglial origin (Saba et al., 2012). MiR-146a functionality has been explored in macrophages but its role in microglia is just beginning to emerge. In order fully elucidate the role of miR-146a in microglia cells and its role in prion disease, identification of functionally important miR-146a targets is warranted.

1.14 MiRNA target identification approaches

Computational algorithms and bioinformatics have been the major driving force in predicting miRNA targets. There are numerous programs readily available, each taking into consideration one or several key features of miRNA and target binding. Some of these key features include, but are not limited to; complete sequence complementarity, imperfect complementarity, secondary structure of the target, allosteric hindrance by other RNA binding elements, and positioning of the 3'UTR (Grimson et al., 2007; Kertesz, Iovino, Unnerstall, Gaul, & Segal, 2007). However, the relevance of these programs are often under scrutiny as these programs have a high degree of false positives, hence the need for more reliable and biologically appropriate methods.

Currently, a common approach in identifying target genes has been at the transcriptional level using microarrays and qRT-PCR. The drawback of this particular approach is the fact target mRNAs that are not susceptible to mRNA degradation would

be missed. MiRNAs are capable of regulating many of their targets at the translational level without affecting mRNA abundance. Since proteins are the major direct executors of life processes and might reflect gene function more directly than mRNA, proteomic methods are best suited for revealing the full spectrum of miRNA targets.

Proteomic technologies enable the exhaustive analysis of the protein content of a tissue or sample allowing the measurement and detection of phenotypic characteristics of disease. Only in recent years has technological advances facilitated the differential measurement of protein abundance levels between multiple conditions at a given time, and just as importantly, provided sufficient "through-put" to attach statistical significance. Therefore, high-throughput proteomic approaches are an important tool to identify functionally important miRNA targets in order to uncover miRNA function and determine its effect on a disease process.

1.15 Rationale, hypothesis and project objectives

Given that microglia during prion infection synthesize a unique profile of inflammatory mediators, including low levels of many cytokines that are characteristic of infection, it was hypothesized that miR-146a, a known regulator of the innate immune response in human monocytes, plays a role in modulating microglial functionality. The primary objective was to investigate the role of miRNA-146a in microglia cells during prion-induced neurodegeneration with the following specific aims:

1. **To identify inflammatory related miRNAs associated with prion disease in microglia**
2. **To investigate miR-146a induction in microglia**
3. **To identify miR-146a targets using a functional proteomic strategy**
4. **To validate miR-146a targets**

2. Materials and Methods

2.1 Cell culture

Two mouse microglial cell lines were employed in this study, BV2 and EOC 13.31 cells. The BV-2 cells were kindly provided by Dr. Yoon-Seong Kim (Department of Neurology/Neuroscience, Weill Medical College of Cornel University, New York) and the EOC 13.31 cells were obtained from the American Type Culture Collection Centre (ATCC). Both cell lines were grown and maintained in DMEM (ATCC) supplemented with 10% heat-inactivated FBS (Sigma) in a humidified incubator containing 5% CO2 at 37°C. However, the EOC 13.31 cells were additionally supplemented with 20% LADMAC conditioned media. LADMAC conditioned media was made from LADMAC cells purchased from ATCC that secrete CSF-1 as per manufacturer's instructions.

2.2 MiRNA profiling in activated microglia cells

2.2.1 MiRNA profiling in microglia cells activated with LPS and IFN-γ

Both EOC 13.31 and BV2 cells were seeded on 6-well plates. However, due to differences in their proliferation rates, EOC 13.31 cells were plated at a density of 1×10^6 cells/well and BV2 cells at 1×10^5 cells/well. Cultures were incubated overnight in a humidified incubator containing 5% CO_2 at 37°C and then stimulated for 6 and 24 hours with 100 ng/ml LPS (*E. coli* 055:B5, Sigma-Aldrich, Cat. 62326) and 100U IFN-γ (Recombinant, expressed in *E. coli*, Sigma-Aldrich, Cat. I4777). The experiment was performed in triplicate and negative controls consisted of mock stimulation with PBS (Gibco).

2.2.2 MiRNA profiling in microglia cells activated with a TLR2 agonist

BV2 cells were seeded on 6 well plates at a seeding density of 1×10^5 cells/well. Cells were incubated overnight in a humidified incubator containing 5% CO_2 at 37°C and

then stimulated for 8, 12 and 24 hours with 10^8 cells/ml of heat-killed *Listeria monocytogenes* (HKLM)(Invivogen, Cat. tlrl-hklm), a TLR2 agonist. The experiment was performed in triplicate and negative controls consisted of mock stimulation with PBS (Gibco).

2.2.3 RNA isolation

Total RNA was extracted from cell culture using the miRVana miRNA Isolation kit (Ambion) according to manufacturer's instructions. Briefly, cells were lysed in 600 µl lysis/binding buffer and RNA were extracted using an equal volume acid-phenol:chloroform solution. Ethanol was then applied to the aqueous phase and passed through a filter. The filter was washed several times and RNA eventually eluted in 100 µl nuclease free water. The quality and concentration was tested on the 2100 Bioanalyser (Agilent Technologies) where typical concentrations were 40-50 ng/µl and RNA Integrity Numbers (RIN) were 9.8-10. Preparation of the samples and the gel were performed using the Agilent RNA 6000 Nano Kit (Agilent Technologies) according to manufacturer's instructions.

2.2.4 TaqMan Low Density Array (TLDA)

MiRNAs were profiled using Taqman Rodent MicroRNA Array A from Applied Biosystems as per manufacturer's instructions. Briefly, TaqMan® MicroRNA Reverse Transcription Kit and Megaplex™ RT Primers "Pool A" were used to synthesize single-stranded cDNA from 500 ng of total RNA. Thermocycler conditions were as follows: 2 min. at 16°C, 1 min. at 42°C and 1 sec. at 50°C for 40 cycles, followed by 5 min. at 85°C and 4°C for ever. Next, 6 µl of the RT product was combined with 450 µl of TaqMan® Universal PCR Master Mix, No AmpErase® UNG, 2× and 444 µl of nuclease free

water. The Taqman miRNA array was then loaded and run on an Applied Biosystems 7500 Real Time PCR System using the 384 well TaqMan Low Density Array default thermal-cycling conditions.

2.2.5 Significance analysis of TLDA

TLDA cards were analyzed using RQ manager (Applied Biosystems) and StatMiner (Intergromics). Average threshold cycle (Ct) values were obtained using RQ manager and amplification curves were analysed to check for errors. Those targets failing quality analysis were removed from further investigation. In addition, only highly abundant miRNAs with Ct values between 20 and 32 were selected for further analysis. To determine the differential expression of miRNAs between experimental and control groups, fold change was calculated using the $2^{-\Delta\Delta Ct}$ method: $2^{-\Delta Ct\ Experimental - \Delta Ct\ Control}$ with ΔCt = average Ct target miRNA – average Ct U6.

To identify miRNAs that were most significantly different in expression between the experimental and control group, a moderated T-Test (limma parametric) with a false discovery rate (FDR) < 2% was performed using StatMiner. Only miRNAs with p-value < 0.05 and fold change > 1.4 were considered significant.

2.3 MiR-146 induction in microglia cells

BV-2 cells were plated on 24-well plates at a seeding density of 2×10^4 cells/well and incubated overnight in a humidified incubator containing 5% CO_2 at 37°C. The cells were then stimulated with various molecules/agonists for a specified time. In all instances, mock-treated cells (stimulated with PBS) were used as a negative control and the experiments were performed in triplicate.

2.3.1 PrP-beta

BV2 cells were treated with 0.05 µM and 1 µM of PrP-beta (Alicon, Cat. P0027), a synthetic peptide said to mimic PrP^{Sc}, for 6 and 24 hours using serum free media.

2.3.2 TLR1/2 agonist

BV2 cells were stimulated for 24 hours with a synthetic triacylated lipopeptide (LP) that mimics the acylated amino terminus of bacterial LPS, known as Pam3CSK4 (Invivogen, Cat. tlrl-pm2s), at a concentration of 0.25, 0.5 and 1 µg/ml.

2.3.3 TLR2 agonist

BV2 cells were stimulated over a 72 hour period with 10^8 cells/ml of heat-killed *Listeria monocytogenes* (HKLM)(Invivogen)(Cat. tlrl-hklm). EOC13.31 cells were also tested using this agonist. However, EOC 13.31 cells were plated at a seeding density of 2 x 10^4 cells/ well.

2.3.4 TLR4 agonist

BV2 cells were stimulated for 8 hours with 0.1-100 ng/ml LPS (*E. coli* 055:B5, Sigma-Aldrich, Cat. 62326). Furthermore, BV2 cells were stimulated with 100 ng/ml LPS over a 72 hour time period.

2.3.4.1 Analyzing TLR4 agonist preparation for contaminants

EOC 13.31 cells were employed in this particular experiment to determine if the working LPS stock possessed contaminants. EOC 13.31 cells are TLR4 deficient making them hyporesponsive to treatment with LPS. Therefore, EOC 13.31 cells were treated with 0.1-100 ng/ml of two LPS preparations; LPS (*E. coli* 055:B5, Sigma-Aldrich, Cat. 62326) and an ultra-pure LPS (*E.coli*, serotype EH100 (Ra), Enzo Life Sciences, Cat.

ALX-581-010-L002)). Additionally, to determine if the contaminant was stimulating TLR2, both the EOC 13.31 and BV2 cells were incubated for 30 min. with various concentrations of purified monoclonal antibody to mouse TLR2 (Invivogen, Cat. mab-mtlr2) followed by 24 hour stimulation with 100 ng/ml LPS (*E. coli* 055:B5, Sigma-Aldrich, Cat. 62326).

2.3.5 TLR5 agonist

BV2 cells were stimulated for 24 hours with flagellin isolated from *Salmonella typhimurium*, known as FLA-ST (Invivogen, Cat. tlrl-stfla), at a concentration of 0.25, 1 and 10 µg/ml.

2.3.6 RNA isolation

Total RNA was isolated from cell culture using the miRVana miRNA Isolation kit (Ambion) according to manufacturer's instructions. Briefly, cells were lysed in 300 µl lysis/binding buffer and RNA were extracted using an equal volume acid-phenol:chloroform solution. Ethanol was then applied to the aqueous phase and passed through a filter. The filter was washed several times and RNA eventually eluted in 50 µl nuclease free water. The quality and concentration of the extracted RNA was determined using a Nanodrop^{TM} 1000 spectrophotometer (Thermo Scientific). Typical RNA yields were 30-40 ng/µl and the 260/280 ratio (indicative of purity) was in the appropriate range of 1.9-2.

2.3.7 qRT-PCR

MiRNA expression was measured and quantified using the TaqMan® miR-146a miRNA Assays (Applied Biosystems) according to the manufacturer's protocol. MiRNA

expression was normalized to the U6 snRNA level which was expressed at high levels with negligible variance under the experimental conditions used in our study. Fold change was determined using the $2-\Delta\Delta Ct$ method.

2.4 Developing a miR-146a functional model

2.4.1 MiR-146a overexpression and knockdown

Overexpression and knockdown of miR-146a was achieved using a lipid-based reverse transfection system (siPORT^{TM} NeoFX, Ambion) following manufacturer's instructions. Briefly, siPORT^{TM} Neo FX^{TM} transfection agent was diluted in OPTI-MEM I medium and incubated for 10 min. at room temperature. In the meantime, pre-miR^{TM} (precursor molecule for overexpression) miR-146a molecule along with its respective pre-miR^{TM} miRNA precursor negative control #1 (Ambion) were diluted in OPTI-MEM I medium to achieve a final concentration of 30 nM. On the other hand, anti-miR (anti-miRNA molecule for knockdown) miR-146a molecule along with its respective anti-miR^{TM} negative control (Ambion) were diluted in OPTI-MEM I medium to achieve a final concentration of 50 nM. Diluted RNA was then mixed with diluted siPORT^{TM} NeoFX^{TM} transfection agent in an equal volume and the mixture was incubated for 10 min. at room temperature. After incubation, a total of 200 µl of the mixture was added to each well in a 6-well plate and a 2.3 ml BV2 cell suspension (serum free DMEM) was then overlaid in each well to a final cell count of 2×10^5 cells/well. The plates were then placed into a humidified incubator containing 5% CO_2 for 8-48 hours at which time RNA was extracted using the mirVana miRNA RNA Isolation Kit (Ambion). MiR-146a expression was then measured and quantified using individual miR-146a Taqman assays

(Applied Biosystems) following manufacturer's instructions and normalized to levels of U6. The experiment was performed in triplicate.

2.4.2 Functional model of miR-146a

BV2 cells were transfected with 30nM pre-miR-146a, 50nM anti-miR-146a, 30nM pre-miR negative control #1 and mock-transfected following the transfection protocol in Section 2.4.1. However, approximately 16 hours post transfection, the BV2 cells were stimulated with 10^8 cells/ml HKLM, a TLR2 agonist, and then placed into a humidified incubator containing 5% CO_2 for 24 hours. The experiment was performed in triplicate.

2.4.3 Validation of miR-146a functional model

To validate the functional model, the levels of interleukin-6 (IL-6) secreted by the BV2 cells was determined. Supernatant was collected and a solid phase ELISA (Quantikine Mouse IL-6 (R&D Systems)) was performed according to manufacturer's instructions.

2.5 Proteomic analysis of miR-146a functional model to identify miR-146a regulated proteins

BV2 cells were transfected with 30nM pre-miR-146a or pre-miR negative control #1 as previously described in Section 2.4.1. However, in order to reduce any negative effect the transfection process may incur to the cells, they were incubated for 8 hours instead of 16 hours with the transfection reagents prior to stimulation with 10^8 cells/ml HKLM for 24 hours.

2.5.1 Protein isolation

Protein was isolated from the miR-146a model described in Section 2.5 by applying 400 µl/well of the mammalian protein extraction reagent (MPER) from Thermo Scientific following manufacturer's instructions and subsequently quantified following the microplate procedure for the Pierce BCA Kit (Thermo Scientific).

2.5.2 Cartridge trypsin digestion

Protein was digested into peptides following a protocol adapted from the Mann lab protocol. Briefly, 100 µg of protein was dried down then resuspended in 45 µl of a 4% SDS lysis buffer solution and mixed with 7X volume Urea Exchange Buffer (UEB)(8 M urea in 0.5 M HEPES) in Nanosep 30K cartridges (VWR). The device was centrifuged at 10,000 x g at 20 °C for 15 min at a time, until all the liquid passed through. All following centrifugation steps were performed applying the same conditions allowing maximal concentration. The concentrate was diluted two times with 250 µl of UEB and the device was centrifuged. Subsequently, 100 µl of a 50 mM iodoacetamide (IAA) solution was added to the concentrate followed by centrifugation. The resulting concentrate was diluted with 100 µl UEB and concentrated again. This step was repeated 2 times. 150 µl of 50 mM HEPES was then applied to the filter, centrifuged and repeated. The concentrate was subjected to a 30 min. incubation at room temperature with 50 µl of a benzonase solution (1000 units of benzonase in 50 mM HEPES and 2 mM $MgCl_2$). The filter was washed and centrifuged 3 times with 100 µl of 50 mM HEPES and then transferred to a fresh tube. 50 µl of a trypsin digestion solution containing 5 µg trypsin was applied to the cartridge and was incubated overnight in a humidified incubator at 37°C. The next morning, 50 µl of 50 mM HEPES was added to the trypsin digestion and

the cartridge was inverted and centrifuged allowing the collection of peptides to the bottom of the tube. This was performed 3 times and the remaining peptide was dried down using a speed vacuum. Samples were resuspended in 30 µl 50 mM HEPES and pH was tested on alkacid papers to ensure the buffer pH was approximately 8.

2.5.3 Peptide labelling

The peptides were labelled following the Thermo Scientific TMTsixplex Isobaric and Isotopic Mass Tagging protocol with minor modifications. Briefly, each label was equilibrated to room temperature and 44 µl of acetonitrile was added. The labels were then incubated for 5 min. with occasional vortexing and 70 µl of 100% Ethanol was added. Next, samples were incubated overnight with the contents of their corresponding TMT label indicated below:

TMT Label	*Treatment*
126	*Pre-miR-146a + HKLM*
127	*Negative Control + HKLM*

The next day, 8 µl of 5% hydroxylamine was added to the labelled samples and incubated for 15 min. To ensure one-to-one mixing of all samples, equal volumes (1 µl) of each labelled sample were mixed with buffer A (2% acetonitrile, 0.1% formic acid) to a final volume of 60 µl, and analysed by nano-LC/MS/MS using a 2-hour gradient. Histograms of count versus ratio for each TMT report ion pair, where label 126 was the reference label, were generated using the peak list from Mascot Distiller (v2.4.2, Matrix Science) and an in-house Perl script. The median ratio (histogram centroid) for each

report ion pair was used to make minor corrections to the final mixing volumes, with the final mixing volumes calculated to yield unity median TMT ratios. The calculation used to determine the final mixing volumes was as follows:

$2^{\text{Median ratio}}$ = Fold Change

8µl/Fold Change = Volume of sample to be combined

(Where 8 µl is the theoretical volume per sample yielding 100 µg total protein)

Example:

Label 127

Median ratio of 0.32

$2^{0.32} = 1.25$

8 µl /1.25 = 6.4 µl

Samples were combined in volumes calculated from the labelling bias, vortexed, dried down and resuspended in 42 µl nano LC Buffer A (2% acetonitrile, 0.1% formic acid).

2.5.4 Peptide Fractionation

TMT-labelled peptide samples (100 µg) were fractionated by high-pH, C_{18}-reversed phase liquid chromatography on a micro-flow Agilent 1100/1200 series system (Agilent Technologies), using a Waters XBridge C_{18} guard column (10 mm long, 2.1 mm inner diameter, 3.5 µm particles) and a Waters XBridge C_{18} analytical column (10 cm

long, 2.1 mm inner diameter, 3.5 µm particles). Buffer B was 20 mM ammonium formate and 90% acetonitrile, pH 10. The gradient TMT started at 0% B to 75% B over 82.5 minutes, at a constant flow rate of 150 µl/min. A total of 18 fractions were collected across the peptides elution profile (10-75 min). Fractions were dried and resuspended in 40 µl of nano LC buffer A.

2.5.5 Nano-LC/MS/MS

Each fraction was separately analysed with a Thermo Scientific Orbitrap Elite hybrid mass spectrometer. The following MS and MS/MS settings were used, for Orbitrap Elite : FT: MSn AGC Target = 5e4; MS/MS = 1 µscans, 150 ms max ion time; MS = 300-1800 m/z, 120000 resolution at m/z400, MS Target = 1e6; MS/MS = Top 10 Data-Dependent™ acquisition HCD, Dynamic Exclusion enabled, repeat count 1, Duration 30 sec, Exclusion duration 120 sec; HCD Parameters: Collision Energy = 30%; resolution 15000, MS/MS Mass Range: 100–2000 m/z Isolation: 1.2 Da.

2.5.6 Data processing (Mascot and Scaffold)

The Thermo Scientific Proteome Discoverer Bio-software suite 1.3 with Mascot™ search engine and Swiss-Prot database was used for data analysis. Results were filtered using 80% confidence for peptides, 99% confidences for proteins, and at least 2 peptides per protein. The FDR was less than 2%. Fold change was generated by comparing the proteomic profile of miR-146a overexpressing cells to control cells (transfected with the scrambled sequence known as pre-miR negative control #1). Fold changes of > 1.1 and q-value of < 0.02 were considered significant.

2.6 Functional analysis of miR-146a regulated proteins

Proteomic data was uploaded into Ingenuity Pathway Analysis (IPA) software (Ingenuity ®Systems). This software analyzes lists of genes in the context of the Ingenuity Pathway Knowledge Base (IPKB), which contains biological and chemical interactions and functional annotations created from millions of individually modeled relationships between proteins, genes, complexes, cells, tissues, drugs, and diseases. It has been cited in thousands of scientific molecular biology publications. MiR-146a regulated proteins were defined as proteins down-regulated upon miR-146a over-expression. For all analyses, Fisher's exact test was used to calculate a p-value determining probability that each biological function assigned to the data set was due to chance alone.

2.8 Determining candidate direct miR-146a targets

To discriminate between direct and indirect targets among miR-146a regulated proteins outlined in Section 2.6, the miRNA Target Filter application in IPA was employed. The microRNA target tool in IPA uses experimentally validated interactions from TarBase and miRecords, predicted microRNA-mRNA interactions from TargetScan and Ingenuity Knowledge Base to create miRNA target lists.

2.9 MiR-146a gene target validation

2.9.1 MiRNA reporter vector constructs, transfection and dual luciferase reporter assays

2.9.1.1 Cloning strategy and reporter assays for ARF6, RhoA and NOS2

In order to create 3'UTR luciferase reporter constructs, fragments, or the entirety of the particular 3'UTR were cloned into a pmirGLO Dual-Luciferase miRNA Target Expression Vector (Promega). This vector is based on Promega dual-luciferase technology, with firefly luciferase (luc2) used as the primary reporter to monitor mRNA regulation, *Renilla* luciferase cassette acting as a control reporter for normalization and an ampicillin resistance gene allowing for bacterial selection for vector amplification. The 3'UTR's were cloned from 100 ng total mouse cDNA using primers created by Invitrogen and amplified using the KAPA HiFi^{TM} HotStart ReadyMix (2X) (KAPABIOSTYSTEMS) as per manufacturer's instructions. See below for PCR details:

	NOS2	***ARF6***	***RhoA***
Base Pairs	3618-3990	1073-3740	1008-2126
Accession	NM_010927	NM_007481.3	NM_016802
Forward primer 5'→3'	gctagctctgacagcccagagttcc	*gctagccatcatcctcatcttcgcc*	*gctagccatgcggttaatttgaagtgc*
Reverse primer 5'→3'	cctgcaggaagtattagagcggcggcat	*cctgcaggtttacctcattcaaaacttactgca*	*cctgcaggggaaatttagaaaactgcctttattc*

Component	Final concentration	Volume in 25µl
Nuclease free water	-	Up to 25µl
2X KAPA HiFi HotStart ReadyMix	1X	12.5 µl
Forward primer (10µM)	0.3 µM	0.75 µl
Reverse primer (10µM)	0.3 µM	0.75 µl
Template DNA	As needed	100 ng

Step	Temperature	Time	Number of cycles
Initial denaturation	95°C	2 min	1
Denaturation	98°C	20 sec	25
Primer annealing	68°C	15 sec	
Extension	72°C	30 sec	
Final extension	72°C	5 min	1
Cooling	4°C	HOLD	1

The PCR product was run on a 2% agarose gel containing SYBR^{TM} Green I (BioRad) and images were taken using GelDoc 2000 (BioRad). The DNA product was then excised, cleaned up using the Quantum Prep Freeze N' Squeeze DNA Gel Extraction Spin Columns (Qiagen), precipitated and stained for visualization with GlycoBlue Coprecipitant (Applied Biosystems) and quantified on the NanodropTM 1000 spectrophotometer (Thermo Scientific).

The insert or PCR product was ligated into the pCR 2.1 vector (3:1 insert:vector ratio) from the TOPO ® TA cloning kit (Invitrogen) and subsequently transformed into One Shot® TOP10 Competent Cells. Transformed *E.coli* were plated on LB plates

containing 100 µg/ml carbicillin and the next day, colonies were selected at random and grown up in 3 ml LB broth (100 µg/ml carbicillin). Plasmids were isolated using QIAPrep Miniprep Kit (Qiagen) and subsequently sequenced by the Canadian Science Centre for Human and Animal Health (CSCHAH) – DNA Core Services. The presence of the particular insert was confirmed with at least 99% identity to the mouse transcript 3'UTR sequence. The recombinant plasmid (1µg) was then digested with 1µl NheI-HF™ and 1µl SbfI-HF™ (New England BioLabs Inc.) for 1 hour at 37°C. The pmirGLO Dual-Luciferase miRNA Target Expression Vector was also digested in a similar manner. Digested products from both reactions were run on 1% agarose gels and the appropriate bands were cut out. DNA was isolated using the Quantum Prep Freeze N' Squeeze DNA Gel Extraction Spin Columns (Qiagen), precipitated and stained for visualization with GlycoBlue Coprecipitant (Applied Biosystems) and quantified on the NanodropTM 1000 spectrophotometer (Thermo Scientific). The digested insert and vector were ligated in a 10:1 ratio, respectively, using the TOPO® TA cloning kit (Invitrogen). The recombinant vector was then transformed into One Shot® TOP10 Competent Cells and plated on LB plates containing 100µg/ml carbicillin from which colonies were chosen after an overnight incubation at 37°C. Each colony was then grown up in 3 ml LB broth and sequenced by DNA Core Services of the CSCHAH. A clone possessing the correct insert (>99% identity with mouse transcript 3'UTR sequence) was then grown up in 200 ml LB broth (100 µg/ml carbicillin) and plasmid was extracted using the EndoFree Plasmid MaxiPrep kit (Qiagen).

2.9.1.2 Transfection

Primary neurons were prepared from the cortical region of E18.5 pups of the CD1 strain and transfected in 24-well plates with 200 ng of vector construct and 5-100 nM of miR-146a mimic (pre-mir-146a, Ambion) or 100 nM of negative control (negative control #1, Ambion). First, 2.5 ml of cold Neurobasal® media (Life Technologies) was mixed with 50µl of Lipofectamine 2000 (Invitrogen). The solution was vortexed thoroughly and incubated for 5 min. at room temperature. 100 µl was then added to the reporter plasmid/miRNA mixture (previously combined) and left for 20 min. at room temperature permitting the formation of liposomes. During the 20 min. incubation, medium was collected from the cultured primary cells ("conditioned" media) and new media was added. After the 20 minutes, the transfection mixture was diluted 1:5 with fresh and warmed Neurobasal media. Media was then removed from the neurons, replaced with the transfection mixture (500 µl) and incubated at 37° for 2 hours. After the 2 hour incubation, the cells were then washed 2X with warmed Neurobasal media and replaced with 500 µl of media consisting of equal parts conditioned media and Neurobasal media. The neurons were then incubated for 24 hours at 37° before measuring luciferase activity. Each experimental condition was performed in triplicate.

2.9.1.3 Dual luciferase reporter assays

Firefly and *Renilla* activity was measured sequentially from a single sample following the microplate procedure of the Dual-Luciferase Reporter Assay Kit from Promega as per manufacturer's instructions. Briefly, media was removed from the cultured cells and rinsed with DPBS (GIBCO). Passive Lysis Buffer (PLB)(1X) was then added to each well (100 µl) and the plate was placed on a shaker for 15 min. at room

temperature. Next, 20µl of the PLB lysates were transferred to a 96-well plate and subsequently loaded into the GloMax®-Multi Detection System (Promega) which is equipped with 2 reagent injectors. The dual reporter assay was performed the following way and one well at a time: i) 100 µl Luciferase Assay Reagent II was injected; ii) firefly luciferase activity was measured; iii) 100 µl Stop & Glo® Reagent was injected and; iv) *Renilla* luciferase activity was measured. Results were normalised to *Renilla* activity and compared to an empty vector. A paired t-test was employed and p-value < 0.05 was considered significant.

2.9.2 Western blot

Samples were prepared and the gel was run and transferred according to the manufacturer's protocol from Invitrogen for NuPAGE Novex Bis-Tris glycine mini gels (1.0 mm X10 well) with a few modifications. Briefly, 70µg of protein was dried down and resuspended in 20 µl MPER reagent. 2.5 µl NuPAGE LDS sample buffer (4X, Invitrogen) and 1 µl Sample Reducing Agent (10X, Invitrogen) was then added to the samples and incubated for 10 min. at 70°C. Samples were loaded into the wells of the gel inside the buffer tank filled with 1X MOPS SDS Running Buffer (20X, Invitrogen) and NuPAGE Antioxidant (Invitrogen). Ladders were also loaded into wells which included 3 µl of MagicMark™ XP Western Protein Standard (Invitrogen) and 3 µl Precision Plus Protein™ Dual Color Standards (Bio-RAD). The Gel ran at 200 volts (V) for 35 min. and once it was finished, it was transferred to a 0.2 µM polyvinylidene difluoride membrane (PVDF)(mini PVDF iBlot Transfer Stack, Invitrogen) using the iBlot Gel Transfer Device from Invitrogen. Once the 7 min. transfer was complete, the membrane was then blocked for 1 hour at room temperature in 10ml of a 1% BSA Blocker (Thermo

Scientific) solution made in PBST. The membrane was then incubated in primary anti-NOS2 antibody (Rabbit polyclonal to NOS2, abcam, Cat. ab15323) at a 1:100 dilution or 2 µg/ml at 4°C on a shaker. The next morning, the membrane was washed 3X at room temperature with PBST for 10 min. on a shaker. The membrane was then incubated in Goat anti-Rabbit IgG (Fab')2 (HRP) secondary antibody (1:2000 dilution, abcam, Cat. ab6112) for 1 hour on a shaker and subsequently washed 4X with PBST at 15 min. intervals at room temperature. Detection was achieved using the Supersignal West Pico Chemilluminescent Substrate from Pierce (Thermofisher Scientific) by incubating the membrane for 5 min. at room temperature in equal amounts of Pierce Supersignal luminol/enhancer solution and Pierce Supersignal West Pico stable peroxide solution. After incubation, the membrane was slightly dried and enclosed in a laminated pouch. The western was developed and imaged using the Flour-S TM MultiImager (Bio-RAD). Amount of chemilluminescnece was detected and densitometry was performed to determine quantitative differences between samples.

After NOS2 detection was complete, the membrane was stripped and re-probed for α-tubulin as a loading control. Briefly, the membrane was washed 2X with PBST and then incubated for 10 min. on a shaker at room temperature with 10 ml of Restore Western Blot Stripping Buffer (Thermo Scientific). The membrane was then washed 2X with PBST and blocked for an hour using the same BSA blocking solution and conditions mentioned previously. It was then incubated on a shaker overnight at 4°C with mouse monoclonal anti α-tubulin antibody at a 1:1000 dilution (Sigma, Cat. T9026). The next morning, the membrane was washed in a similar manner to that of NOS2 detection and subsequently incubated with the secondary antibody (Goat anti-Mouse IgG (H+L) –

HRP, Invitrogen, Cat. 626520) at a 1:2000 dilution for 1 hour on a shaker at room temperature. Secondary washing, development and imaging was performed the same way as that of NOS2 mentioned above. However, due to the fact that 70 µg of protein was initially loaded, the α-tubulin bands were extremely saturated and imaging was actually performed the next day. In the meantime, the membrane was kept at 4°C in a sealed and light –protected plate containing PBST. Lastly, densitometry was performed on the α-tubulin to ensure proper loading of each sample on the western blot. NOS2 was then normalised to α-tubulin.

3. Results

3.1 De-regulation of miRNA expression during microglial activation

While there have been numerous studies that have looked specifically at miRNAs in macrophages, there was a lack of information with regards to those expressed in microglia cells, especially in an activated state. Therefore, the aim was to identify miRNAs expressed in microglia cells that contribute to immune function in the brain and that may be involved in the inflammatory response that is initiated during the prion disease process.

3.1.1 MiRNA profiling in microglia cells activated with LPS and IFN-γ

Firstly, two mouse microglia cell lines, BV2 and EOC 13.31 cells, were treated with a combination of LPS and IFN-γ to elicit activation. This method of activation is the most commonly cited method in the literature used to activate macrophages (Y. Zhang, Zhang, Zhong, Suo, & Lv, 2013). After 6 and 24 hours stimulation, RNA was extracted and hundreds of miRNAs were profiled using the mouse Taqman Low Density Array (TLDA) Pool A from Applied Biosystems and compared to those of mock stimulated cells. MiRNAs were scored as present in the EOC 13.31 and BV2 cells if their average Ct was > 20 and < 32 and was consistently within this range for all treatment groups including controls. The analysis could have been less stringent resulting in the identification of additional miRNAs for each of the cell line lines examined, but making this cut-off stringent, allowed for the identification of only true cell-specific and highly abundant miRNAs. However, the removal of some miRNAs from further analysis due to the stringent cut-off, does not mean they are not biologically relevant to the cell lines examined. In total, 119 miRNAs were identified in the EOC 13.31 cells and 56 miRNAs were identified in the BV2 cells for further analysis listed in **Table 3.1** and **Table 3.2,**

respectively. Also presented in these tables, are significantly deregulated miRNAs, as defined by fold change > 1.4 and p-value < 0.05. The total number of deregulated miRNAs is summarized in **Table 3.3**. Interestingly, activation of the microglia cells resulted in more miRNAs identified as being induced rather than repressed.

Table 3.1. Biologically relevant and deregulated miRNAs in EOC13.31 cells upon activation by LPS and IFN- γ. EOC 13.31 cells were stimulated with 100 ng/ml LPS and 100 U/ml IFN- γ for 6 and 24 hours and RNA was collected. MiRNAs were then profiled using the "Pool A" TaqMan Low Density Array (TLDA) from Applied Biosystems and compared to mock stimulated cells. Experiments were performed in triplicate and data was normalized to that of U6 levels. MiRNAs with Ct values > 20 and < 32 were considered biologically relevant. Fold changes > 1.4 and p-value < 0.05 were considered significant. Upregulated and downregulated miRNAs are denoted by the arrows ↑ and ↓, respectively.

MiRNA	6 Hours	24 hours
U87		
mmu-let-7a	↑	↑
mmu-let-7b	↑	
mmu-let-7c	↑	
mmu-let-7d		
mmu-let-7e		↑
mmu-let-7f		↑
mmu-let-7g		↑
mmu-let-7i	↑	
mmu-miR-100		
mmu-miR-101a	↑	
mmu-miR-103		↓
mmu-miR-106a	↑	
mmu-miR-106b	↑	
mmu-miR-10a	↓	
mmu-miR-10b	↑	↑
mmu-miR-125a-5p		
mmu-miR-125b-5p		
mmu-miR-126-3p		
mmu-miR-126-5p		↓

mmu-miR-130a		
mmu-miR-130b	↑	↓
mmu-miR-138		
mmu-miR-139-5p		↓
mmu-miR-140		
mmu-miR-142-3p	↑	↑
mmu-miR-142-5p	↑	↑
mmu-miR-143		
mmu-miR-145		
mmu-miR-146a	↑	↑
mmu-miR-146b	↑	↑
mmu-miR-151-3p	↑	
mmu-miR-152		↓
mmu-miR-155	↑	↑
mmu-miR-15a		↑
mmu-miR-15b		
mmu-miR-16		
mmu-miR-17	↑	
mmu-miR-182	↑	
mmu-miR-185		↓
mmu-miR-186		
mmu-miR-188-5p		
mmu-miR-18a		↑
mmu-miR-191		
mmu-miR-192	↑	↓
mmu-miR-193		↑
mmu-miR-193b	↓	↓
mmu-miR-195		↑
mmu-miR-196b		↓
mmu-miR-199a-3p		↑
mmu-miR-19a		
mmu-miR-19b		↑
mmu-miR-200b	↑	↑
mmu-miR-20a		
mmu-miR-20b		
mmu-miR-21		↑
mmu-miR-210		↑
mmu-miR-214		
mmu-miR-218	↑	↑
mmu-miR-221	↑	
mmu-miR-222	↑	

mmu-miR-223			↓	
mmu-miR-24				
mmu-miR-25				
mmu-miR-26a				
mmu-miR-26b				
mmu-miR-27a				
mmu-miR-27b				
mmu-miR-28				
mmu-miR-29a	↑			
mmu-miR-29b	↑			
mmu-miR-29c	↑			
mmu-miR-301a	↑			
mmu-miR-30a	↑			
mmu-miR-30b	↑			
mmu-miR-30c			↑	
mmu-miR-30d			↑	
mmu-miR-30e				
mmu-miR-31				
mmu-miR-320	↓			
mmu-miR-322	↑			
mmu-miR-324-5p				
mmu-miR-328	↑		↓	
mmu-miR-331-3p				
mmu-miR-339-3p	↑			
mmu-miR-340-5p	↑			
mmu-miR-342-3p	↓		↑	
mmu-miR-34a	↑		↑	
mmu-miR-34b-3p	↓			
mmu-miR-34c				
mmu-miR-365			↑	
mmu-miR-449a	↑		↑	
mmu-miR-467a				
mmu-miR-467b	↓			
mmu-miR-467c	↑		↑	
mmu-miR-484				
mmu-miR-486				
mmu-miR-494			↑	
mmu-miR-497				
mmu-miR-503				
mmu-miR-532-3p	↑			
mmu-miR-532-5p				

mmu-miR-547	↑	↑
mmu-miR-574-3p		↓
mmu-miR-652		
mmu-miR-669a	↑	↑
mmu-miR-674	↑	↓
mmu-miR-685		↑
mmu-miR-687		↑
mmu-miR-708	↑	↑
mmu-miR-744		
mmu-miR-872	↑	
mmu-miR-9	↑	↑
mmu-miR-92a		
mmu-miR-93	↓	↑
mmu-miR-99a		↑
mmu-miR-99b		
rno-miR-196c	↓	
snoRNA135		

Table 3.2 Biologically relevant and deregulated miRNAs in BV2 cells upon activation by LPS and IFN- γ. BV2 cells were stimulated with 100 ng/ml LPS and 100 U/ml IFN- γ for 6 and 24 hours and RNA was collected. MiRNAs were then profiled using the "Pool A" TaqMan Low Density Array (TLDA) from Applied Biosystems and compared to mock stimulated cells. Experiments were performed in triplicate and data was normalized to that of U6 levels. MiRNAs with Ct values > 20 and < 32 were considered biologically relevant. Fold changes > 1.4 and p-value < 0.05 were considered significant. Upregulated and downregulated miRNAs are denoted by the arrows ↑ and ↓, respectively.

MiRNA	6 hours	24 hours
mmu-let-7g	↓	↑
mmu-let-7i		↑
mmu-miR-15b	↓	↓
mmu-miR-16		↑
mmu-miR-18a		↓
mmu-miR-19a		
mmu-miR-19b	↓	
mmu-miR-20a	↑	
mmu-miR-20b	↑	↑
mmu-miR-24		
mmu-miR-26a	↑	
mmu-miR-26b		
mmu-miR-27a		↑
mmu-miR-30b		
mmu-miR-30c	↓	
mmu-miR-93		
mmu-miR-98	↓	↑
mmu-miR-103	↓	↑
mmu-miR-125b-5p	↓	
mmu-miR-126-3p	↑	
mmu-miR-130b		
mmu-miR-132	↑	↑
mmu-miR-139-5p	↓	↑

mmu-miR-140		↑
mmu-miR-142-3p		↑
snoRNA135		↑
mmu-miR-146a	↑	↑
mmu-miR-146b		↑
mmu-miR-182	↓	↑
mmu-miR-186		↑
mmu-miR-191		
mmu-miR-195	↑	↑
snoRNA202		↑
mmu-miR-221	↑	↑
mmu-miR-222	↑	↑
mmu-miR-223		
mmu-miR-301a		
mmu-miR-320		↑
mmu-miR-328	↓	↑
mmu-miR-331-3p	↑	↑
mmu-miR-342-3p		↑
mmu-miR-365	↓	↑
mmu-miR-484		↑
mmu-miR-532-5p		↑
mmu-miR-574-3p		↑
mmu-miR-324-3p	↓	
mmu-miR-652		↑
mmu-miR-685	↓	↑
mmu-miR-106b		
mmu-miR-155	↑	↑
mmu-miR-17		
mmu-miR-29a		↑
mmu-miR-30a		↑
mmu-miR-30e		↑
mmu-miR-92a		↑
mmu-miR-106a		

Table 3.3 Summary of the number of significantly deregulated miRNAs in EOC 13.31 cells and BV2 cells upon stimulation with LPS and IFN- γ.

Cell line	Timepoint	Upregulated	Downregulated
EOC13.31	6 Hours	44	9
EOC13.31	24 Hours	36	13
BV2	6 Hours	11	13
BV2	24 Hours	37	2

In order to further determine how similarly the selected microglial cell lines respond to stimuli, deregulated miRNAs in EOC13.31 and BV2 cells were compared to one another at both timepoints. This comparison revealed 4 similar upregulated miRNAs at 6 hours and 9 similar upregulated miRNAs at 24 hours (**Figure 3.1)**. Fold changes for these lists are indicated in **Table 3.4**. Interestingly, the greatest fold changes were observed in miR-146a and miR-155 which also happen to be the only miRNAs shared amongst both corresponding data sets. Expression of these miRNAs were also more pronounced in the BV2 cells compared to the EOC 13.31 cells, likely due to the inherent absence of TLR4 signaling in EOC 13.31 cells. When the same comparison was made between downregulated miRNAs, no miRNAs were found to be similar between the cell lines (**Figure 3.2)**.

Next, to determine miRNA persistence following activation, deregulated miRNAs at 6 and 24 hours in individual cell lines were compared to one another. Analysis revealed 8 miRNAs to be persistently upregulated over time in BV2 cells and 16 in EOC 13.31 cells (**Figure 3.3)**. Fold changes for these lists are indicated in **Table 3.5**. In the BV2 cells, substantial upregulation of greater than 4 fold were observed for miR-20b, miR-146a, miR-155, miR-221 and miR-222 at the 24 hour timepoint. Only miR-146a and miR-155 were identified as being upregulated in both cell lines over time. Comparison of downregulated miRNAs in individual cell lines revealed that miR-15b and miR-193b were persistantly downregulated over time in BV2 and EOC13.31 cells, respectively **(Figure 3.4)**.

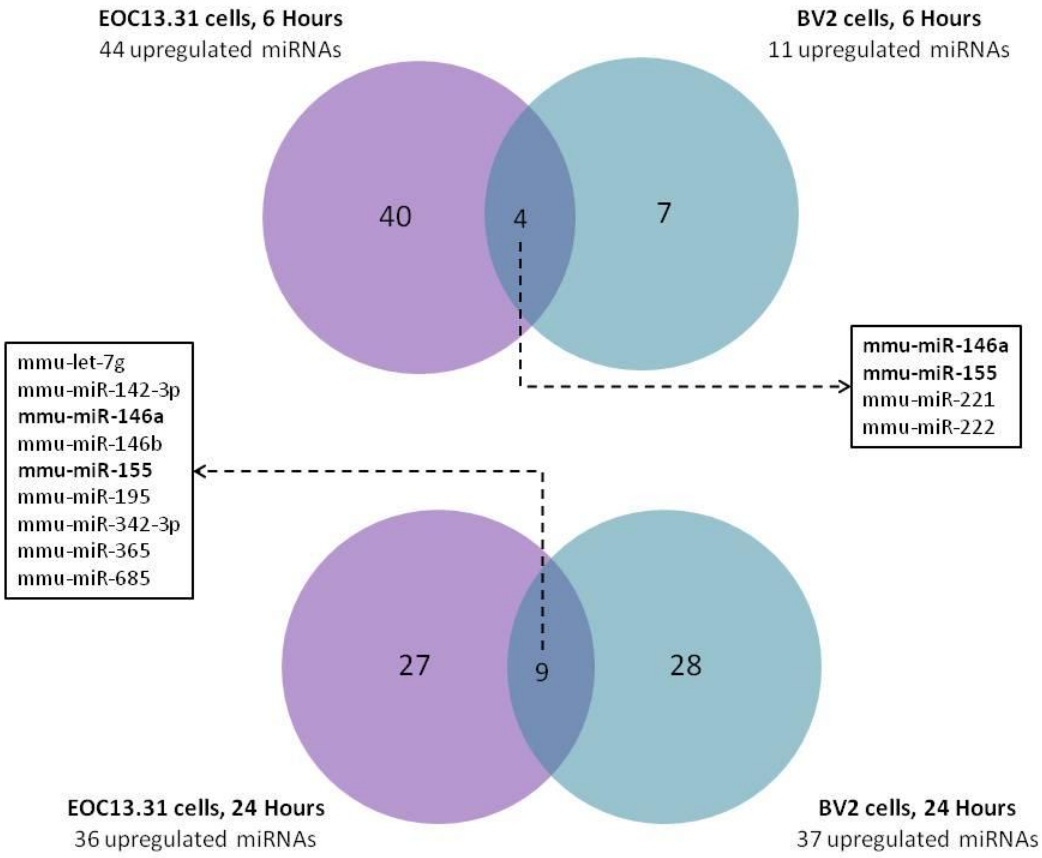

Figure 3.1 Comparison of significantly upregulated miRNAs in EOC13.31 cells and BV2 cells at similar timepoints upon stimulation with LPS and IFN- γ. Fold change > 1.4 and p-value < 0.05 were considered significant. MiRNAs found to be upregulated in the EOC13.31 and BV2 cells were then compared to one another at 6 and 24 hours. MiRNAs common to both cell lines at each timepoint are listed in boxes and those bolded are shared amongst both data sets.

Table 3.4 Fold changes of similar upregulated miRNAs in EOC 13.31 and BV2 cells upon stimulation with LPS and IFN- γ.

MiRNA	Fold Change	
	EOC 13.31 cells	BV2 cells
6 Hours		
mmu-miR-146a	6.5	2.4
mmu-miR-155	3.9	34.4
mmu-miR-221	2.3	2.5
mmu-miR-222	1.6	1.6
24 Hours		
mmu-let-7g	1.4	2.1
mmu-miR-142-3p	1.5	1.7
mmu-miR-146a	1.7	7.0
mmu-miR-146b	1.5	2.3
mmu-miR-155	3.2	142.8
mmu-miR-195	1.5	1.5
mmu-miR-342-3p	1.6	2.6
mmu-miR-365	2.2	1.5
mmu-miR-685	1.4	2.5

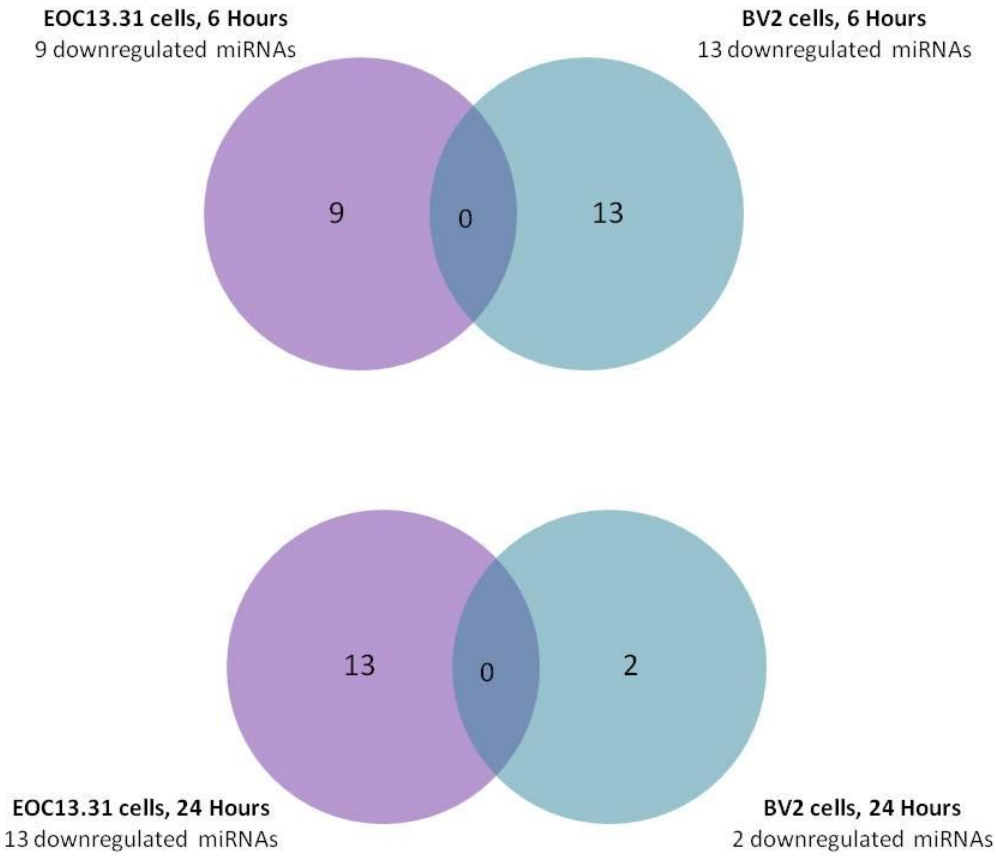

Figure 3.2 Comparison of significantly downregulated miRNAs in EOC 13.31 cells and BV2 cells at similar timepoints upon stimulation with LPS and IFN- γ. Fold change > 1.4 and p-value < 0.05 were considered significant. MiRNAs found to be downregulated in the EOC13.31 and BV2 cells were then compared to one another at 6 and 24 hours.

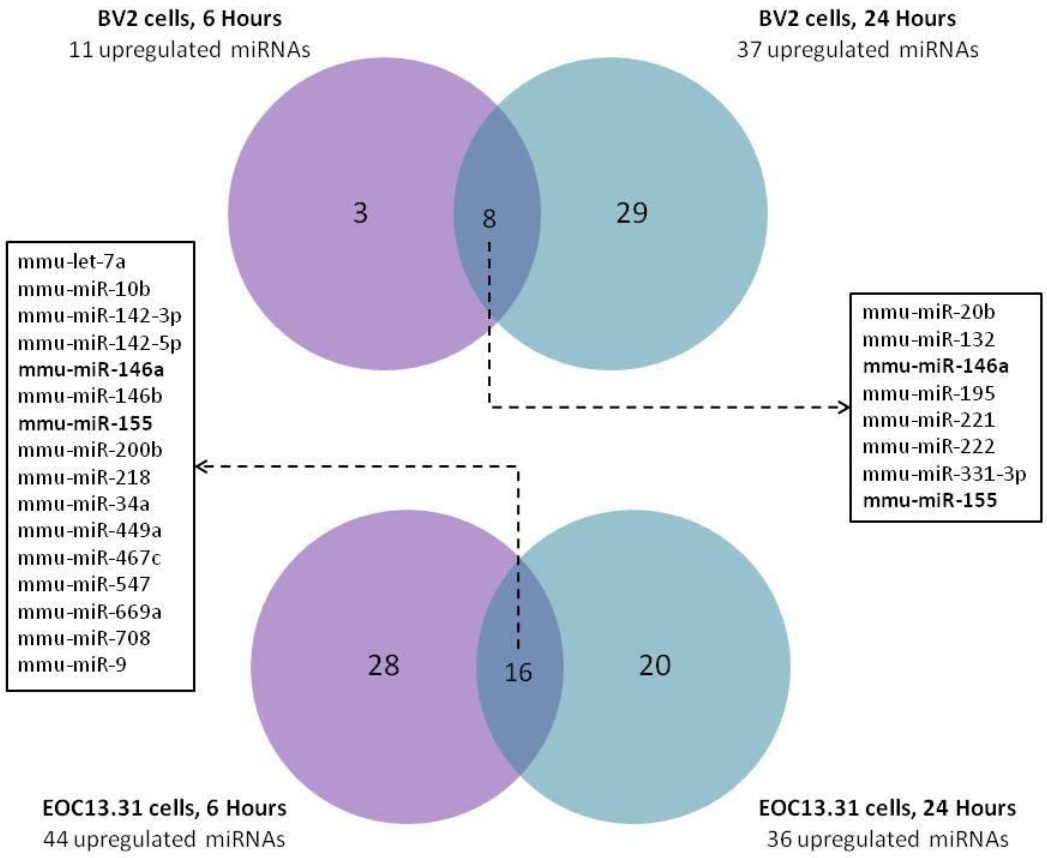

Figure 3.3 Comparison of miRNAs persistently upregulated over time in BV2 and EOC 13.31 cells upon stimulation with LPS and IFN- γ. Fold change > 1.4 and p-value < 0.05 were considered significant. MiRNAs found to be upregulated at both timepoints in individual cell lines were then compared to one another. MiRNAs common at 6 and 24 hours in each cell line are listed in boxes and those bolded are shared amongst both data sets.

Table 3.5 Fold changes of similar upregulated miRNAs at 6 and 24 hours in EOC 13.31 and BV2 cells upon stimulation with LPS and IFN- γ.

MiRNA	Fold Change	
	6 hours	24 hours
BV2 cells		
mmu-miR-20b	2.5	117.8
mmu-miR-132	1.5	2.7
mmu-miR-146a	2.4	7.0
mmu-miR-195	1.9	1.5
mmu-miR-221	2.5	4.1
mmu-miR-222	1.6	9.0
mmu-miR-331-3p	2.3	2.6
mmu-miR-155	34.4	142.8
EOC 13.31 cells		
mmu-let-7a	2.8	2.8
mmu-miR-10b	1.5	2.2
mmu-miR-142-3p	2.5	1.5
mmu-miR-142-5p	1.7	1.5
mmu-miR-146a	6.5	1.7
mmu-miR-146b	1.8	1.5
mmu-miR-155	3.9	3.2
mmu-miR-200b	1.5	1.5
mmu-miR-218	2.0	1.4
mmu-miR-34a	1.9	1.8
mmu-miR-449a	1.6	1.9
mmu-miR-467c	1.8	2.0
mmu-miR-547	1.4	2.0
mmu-miR-669a	1.8	1.5
mmu-miR-708	5.4	3.0
mmu-miR-9	2.2	1.5

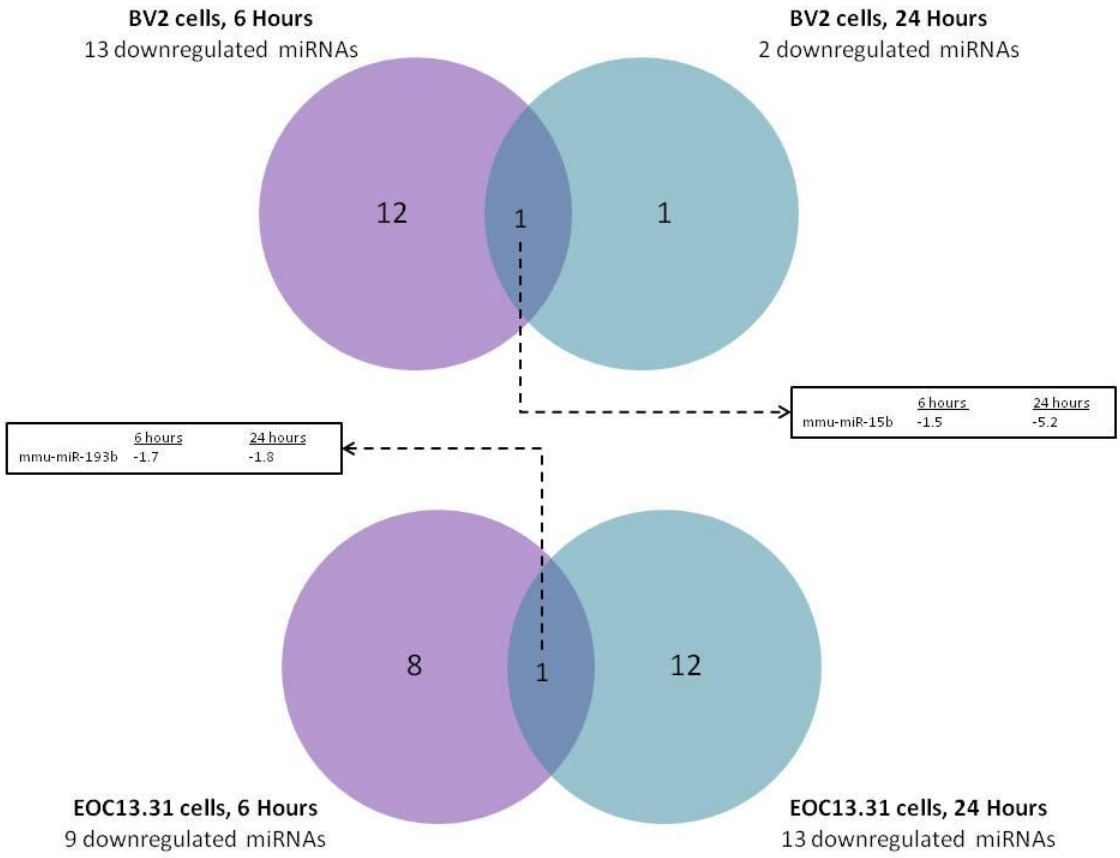

Figure 3.4 Comparison of miRNAs persistently downregulated over time in BV2 and EOC13.31 cells upon stimulation with LPS and IFN- γ**.** Fold change > 1.4 and p-value < 0.05 were considered significant. MiRNAs found to be downregulated at both timepoints in individual cell lines were then compared to one another. MiRNAs common at 6 and 24 hours in each cell line are indicated in the boxes. Also presented, is their respective fold changes.

3.1.2 MiRNA profiling in microglia cells activated with a TLR2 agonist

A second method of microglial activation was employed by treating the BV2 cells with a TLR2 agonist to induce a signalling cascade in BV2 cells, given that TLR2 has been reported to be significantly upregulated in mouse brain tissue during prion infection (Saba et al., 2012). The BV2 cells were stimulated with the TLR2 agonist HKLM over a course of 24 hours and miRNAs were profiled using the same microarray cards previously mentioned and compared to mock stimulated cells. Using a Ct threshold of > 20 and < 32, 70 miRNAs were selected for further analysis indicated in **Table 3.6**. Significant differential expression is also presented in this table. There were 9, 5 and 15 miRNAs found to be upregulated and 5, 5, and 0 miRNAs found to be downregulated at 8, 12 and 24 hours, respectively (**Table 3.7**).

The intersection between miRNAs deregulated over the 24 hour period were determined and are illustrated in **Figure 3.5** for upregulated miRNAs and **Figure 3.6** for downregulated miRNAs. While comparison of downregulated miRNAs did not elude to any one miRNA being persistently downregulated, 2 miRNAs were found to be downregulated at both 8 and 12 hours. On the other hand, comparison of upregulated miRNAs revealed 3 similar miRNAs at 8 and 12 hours, 2 similar miRNAs at 12 and 24 hours, and 4 similar miRNAs at 8 and 24 hours. Only two miRNAs, miR-146a and miR-155, were found to be upregulated across all three timepoints. Expression dynamics for both miR-146a and miR-155 were characterized by a gradual but steady increase over time. By 24 hours, miR-146a reached over 3-fold change and miR-155 reached over 5-fold change. Taken together with the previous study, it has become appreciated that miR-

155 and miR-146a are quite responsive to immune stimuli in a similar fashion to that observed in macrophages and play an integral role in microglial activation.

Table 3.6 Biologically relevant and deregulated miRNAs in BV2 cells upon activation by a TLR2 agonist. BV2 cells were stimulated with 10^8 cells/ml HKLM for 8, 12 and 24 hours and RNA was collected. MiRNAs were then profiled using the "Pool A" TaqMan Low Density Array (TLDA) from Applied Biosystems and compared to mock stimulated cells. Experiments were performed in triplicate and data was normalized to that of U6 levels. MiRNAs with Ct values > 20 and < 32 were considered biologically relevant. Fold changes > 1.4 and p-value < 0.05 were considered significant. Upregulated and downregulated miRNAs are denoted by the arrows ↑ and ↓, respectively.

MiRNA	8 hours	12 hours	24 hours
mmu-let-7c	↑		↑
mmu-let-7d		↓	↑
mmu-let-7e	↓		↑
mmu-let-7g			↑
mmu-let-7i			
mmu-miR-15b			
mmu-miR-16			
mmu-miR-18a			
mmu-miR-19a			
mmu-miR-19b			
mmu-miR-20a			
mmu-miR-21			↑
mmu-miR-24			
mmu-miR-25			↑
mmu-miR-26a			
mmu-miR-26b			
mmu-miR-27a			
mmu-miR-27b			
mmu-miR-28	↑	↑	
mmu-miR-29c			
mmu-miR-30b			↑
mmu-miR-30c			
mmu-miR-30d			↑

mmu-miR-93					
mmu-miR-103	↑				
mmu-miR-125b-5p	↓			↑	
mmu-miR-126-3p	↓		↓		
mmu-miR-130b					
mmu-miR-132					
mmu-miR-139-5p					
mmu-miR-140					
mmu-miR-142-3p					
snoRNA135					
mmu-miR-146a	↑		↑	↑	
mmu-miR-146b				↑	
mmu-miR-186					
mmu-miR-191					
mmu-miR-195					
snoRNA202					
mmu-miR-221	↑			↑	
mmu-miR-222				↑	
mmu-miR-223					
mmu-miR-301a					
mmu-miR-301b					
mmu-miR-320					
mmu-miR-328					
mmu-miR-331-3p					
U87	↓		↓		
mmu-miR-340					
mmu-miR-340-5p					
mmu-miR-342-3p					
mmu-miR-365			↑		
Y1	↑				
mmu-miR-467a	↑				
mmu-miR-484					
mmu-miR-532-3p	↓				
mmu-miR-532-5p					
mmu-miR-574-3p					
mmu-miR-744			↑		
mmu-miR-652					
mmu-miR-685					
mmu-let-7a	↑		↓		
mmu-miR-106b					
mmu-miR-155	↑		↑	↑	
mmu-miR-17					
mmu-miR-29a					

mmu-miR-30a	
mmu-miR-30e	
mmu-miR-92a	
mmu-miR-106a	↓

Table 3.7 Summary of the number of significantly deregulated miRNAs in BV2 cells upon stimulation with a TLR2 agonist.

Timepoint	Upregulated	Downregulated
8 hours	9	5
12 hours	5	5
24 hours	15	0

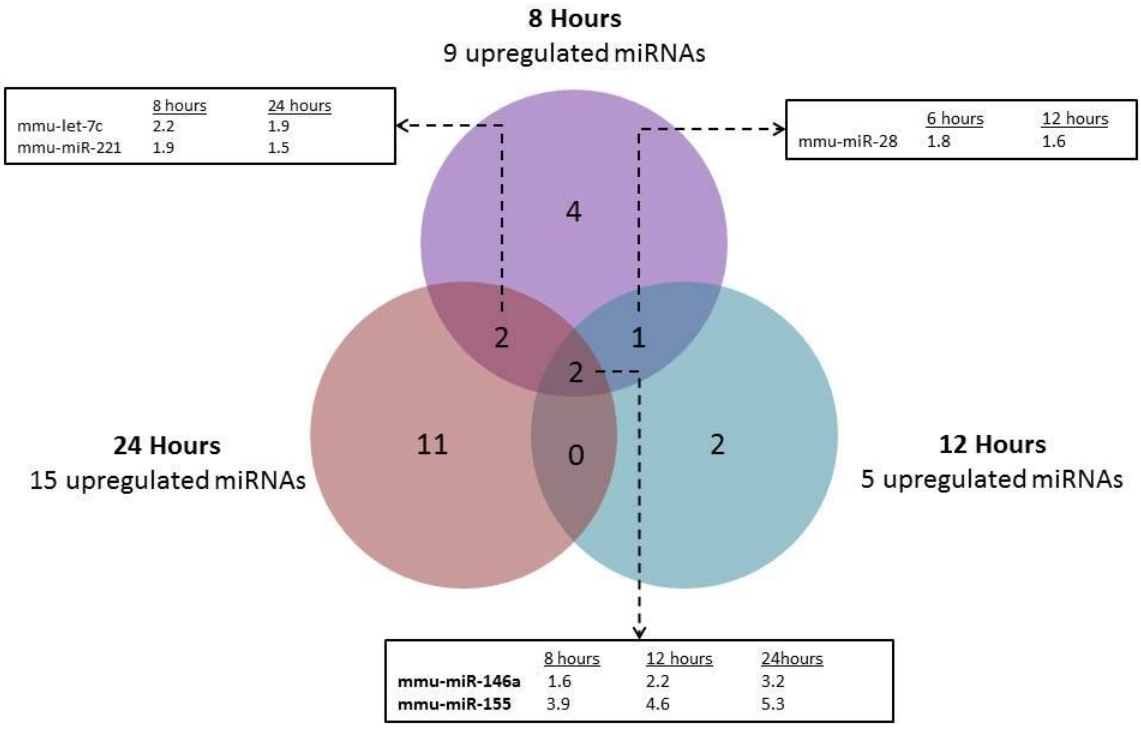

Figure 3.5 Venn diagram showing the intersection between miRNAs upregulated over a 24 hour period in BV2 cells stimulated with a TLR2 agonist. BV2 cells were stimulated over a course of 24 hours with 10^8 HKLM cells/ml and RNA was collected. MiRNAs were then profiled using the "Pool A" TaqMan Low Density Array (TLDA) from Applied Biosystems and compared to mock stimulated cells. The experiments were performed in triplicate and data was normalized to that of U6 levels. Fold change > 1.4 and p-value < 0.05 were considered significant. MiRNAs listed in white boxes represent the shared upregulated miRNAs amongst the indicated timepoints. Also indicated is fold change.

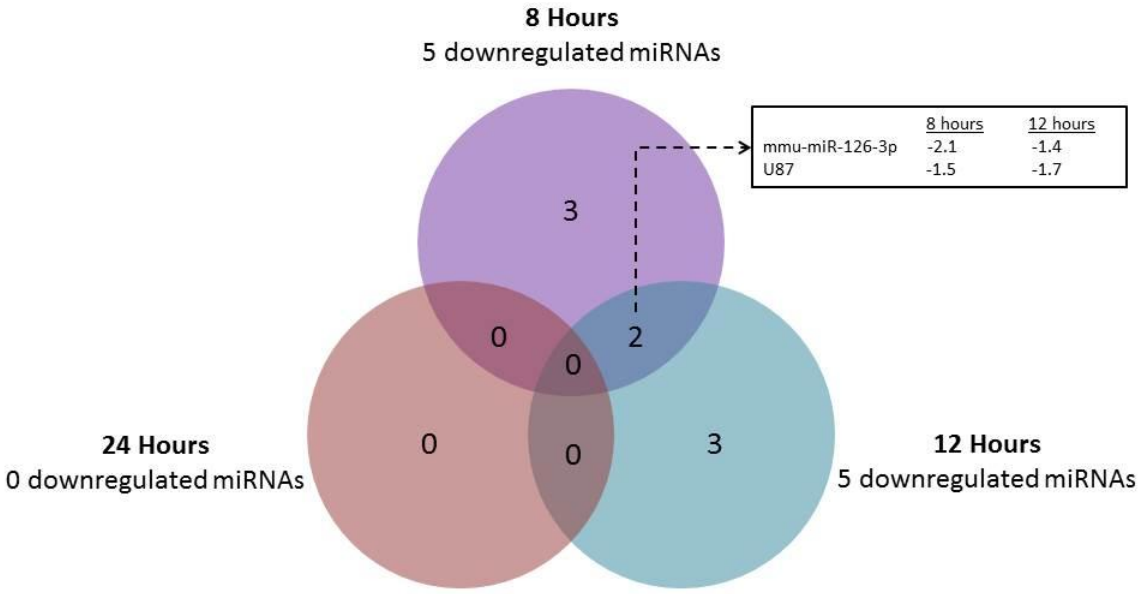

Figure 3.6 Venn diagram showing the intersection between miRNAs downregulated over a 24 hour period in BV2 cells stimulated with a TLR2 agonist**.** BV2 cells were stimulated over a course of 24 hours with 10^8 HKLM cells/ml and RNA was collected. MiRNAs were then profiled using the "Pool A" TaqMan Low Density Array (TLDA) from Applied Biosystems and compared to mock stimulated cells. The experiments were performed in triplicate and data was normalized to that of U6 levels. Fold change > 1.4 and p-value < 0.05 were considered significant. MiRNAs listed in the white box represent the shared downregulated miRNAs amongst 8 and 12 hours. Also indicated is fold change.

3.2 MiR-146a induction in microglia cells

Stimulation of microglia cells with inflammatory agonists resulted in numerous changes to the miRNA profile, however, the largest and most persistent changes were observed in the induction of miR-146a and miR-155. Both miRNAs were found to be significantly and consistently up-regulated upon microglial activation and interestingly, our lab found that miR-146a, and to a lesser extent miR-155, were amongst a select group of miRNAs up-regulated during prion disease (Saba et al., 2008). Saba et al (2012) also showed that expression of these miRNAs to be highly enriched in cells of microglial lineage.

3.2.1 MiR-146a response to PrP-beta

It is known that microglial activation occurs very early in the development of prion disease. Immunohistochemical staining for microglial markers and transcriptional profiling shows that microglial activation is concurrent with the earliest accumulation of proteinase K resistant PrP^{Sc}. At this stage of disease, well before halfway through the incubation period, no clinical symptoms are evident and neuronal cell death is not significant, although synaptic dysfunction and loss is apparent and reported by numerous pathophysiological studies. Given these factors it would seem that microglial activation is not triggered as a response to dead and dying cells but by prion replication or very early prion pathology. This activation could be by misfolded prion accumulation acting as a direct agonist for microglia or by indirect signaling from neurons or other cells in response to prion replication in the brain. It is very difficult to study these steps in microglial activation as an *in vitro* model that mirrors prion infection in the brain is not

available. As a first step toward a better understanding of the molecular mechanisms involved in miRNA induction in microglial cells activated during prion pathobiology, treatment with a PrP^{Sc} mimic, PrP-beta, and whether it was enough to induce the expression of miRNAs that are characteristic of microglial activation, were examined. PrP-beta is a synthetic analog of PrP^{Sc} produced by refolding of recombinant protein. It is identical in weight and amino acid sequence as the infectious form and shares similar biochemical properties including a heavily beta-pleated conformation, resistance to proteinase K, and the ability to form protein aggregates. It is believed to be similar in structure to infectious PrP^{Sc} and therefore used as a model by a number of researchers, including the immune activation (Kazlauskaite et al., 2005; Khalili-Shirazi, Quaratino et al., 2005; Khalili-Shirazi, Summers et al., 2005; Khalili-Shirazi et al., 2007). Upregulation of miR-146a was used as a marker for activation as it was shown previously to be consistently over expressed on treatment of BV2 cells with various innate immune agonists. In addition, it is the most highly and consistently induced miRNA in prion infected mouse brain based on previous studies from the Booth laboratory. However, stimulation of microglia cells with varying concentrations of PrP-beta for 6 and 24 hours failed to induce miR-146a expression as determined by TaqMan qRT-PCR specific for the miRNA **(Figure 3.7).** This result can be explained in a number of ways. It's possible that the PrP-beta was not in the appropriate disease-specific conformational or aggregation state necessary to bind to microglial receptors and trigger activation under the experimental conditions used here. Alternatively, microglia may require a signal other than misfolded PrP for activation in the brain such as a secondary trigger released by another cell type, or the microglial cell line BV2 may not behave in the same manner

as primary microglia in the brain. In any case, it was determined that treatment with PrP-beta could not be used to mimic disease *in vitro* as a consistent means to study miRNAs involved in microglial activation in further studies.

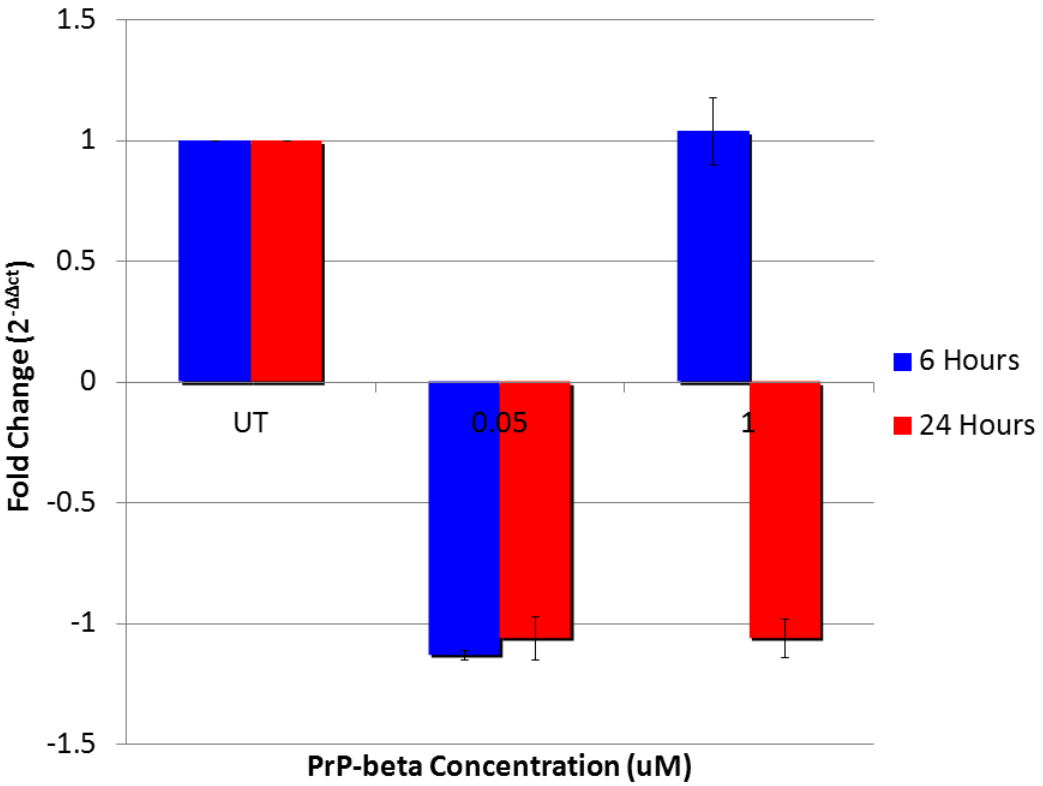

Figure 3.7 MiR-146a expression in microglia cells treated with a synthetic analog of PrP^{Sc} (PrP-beta). BV2 cells were treated for 6 and 24 hours with concentrations of PrP-beta as indicated and total RNA was collected. MiR-146a expression was determined by Taqman qRT-PCR relative to untreated cells (UT). The experiment was performed in triplicate and the average fold change ± SD is shown.

3.2.2 MiR-146a response to TLR agonists

Given the lack of prion-specific models for *in vitro* stimulation of cultured microglial cells, alternative agonists were explored. Studies in prion infected mice have shown the potential involvement of TLR2, TLR4 and TLR9 in the disease process (Sethi et al., 2002; Spinner et al., 2007; Spinner et al., 2008; Tal et al., 2003). Taganov et al (2006) reported significant upregulation of miR-146a in macrophages upon stimulation of TLR1, TLR2, TLR4 and TLR5 (Taganov et al., 2006). The expression of miR-146a during activation of microglia by specific agonists known to act upon these receptors was investigated to determine whether a similar response was induced in microglia-derived cell-lines. It was confirmed that all of these agonists induced the expression of miR-146a in microglia cells as outlined below.

3.2.2.1 TLR1/2 agonists

BV2 cells were incubated for 24 hours with 0.1-1 ug/ml of PAM3CSK4. PAM3CSK4 is a synthetic triacylated lipopeptide (LP) that mimics the acylated amino terminus of bacterial LPS that results in TLR1/2. Agonist treatment resulted in over a 5 fold increase in miR-146a expression relative to mock treated cells as determined by TaqMan qRT-PCR **(Figure 3.8).**

3.2.2.2 TLR2 agonist

Stimulation of the microglial TLR2 signalling cascade over a 72 hour period with heat killed *Listeria Monocytogenes* (HKLM) revealed a time-dependant increase in miR-146a expression as determined by qRT-PCR **(Figure 3.9)**. The BV2 cells showed a gradual rise in miR-146a expression that peaked at 48 hours followed by a decline at 72 hours. Similarly, we found EOC 13.31 cells to respond in the same manner when treated

with the HKLM. However, miR-146a expression was more pronounced in BV2 cells in comparison to the EOC13.31 cells.

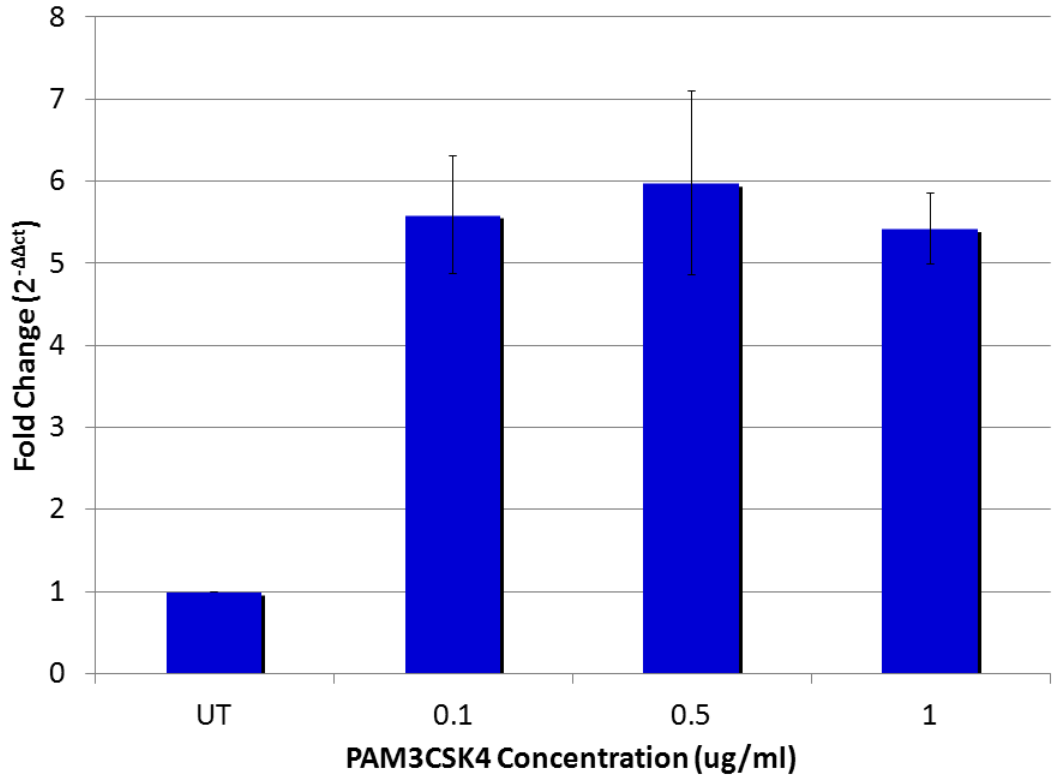

Figure 3.8 MiR-146a expression in microglia cells treated with a TLR1/2 agonist. BV2 cells were stimulated with 0.1, 0.5 and 1 μg/ml of PAM3CSK4 for 24 hours and total RNA was collected. MiR-146a expression was determined by TaqMan qRT-PCR relative to untreated cells (UT). The experiment was performed in triplicate and the average fold change ± SD is shown.

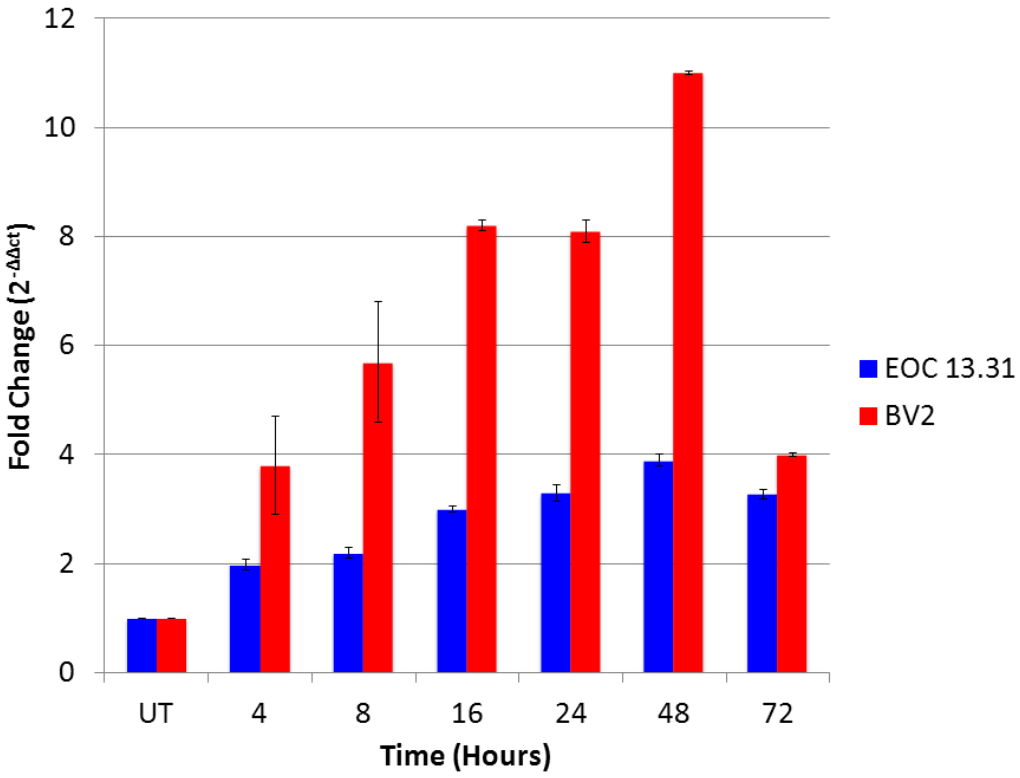

Figure 3.9 Expression of miR-146a in two microglial cell lines treated with a TLR2 agonist. BV2 and EOC 13.31 cells were treated with 10^8 HKLM cells/ml over a 72 hour period and RNA was collected. MiR-146a expression was determined by TaqMan qRT-PCR relative to untreated cells (UT). The experiment was performed in triplicate and the average fold change ± SD is shown.

3.2.2.3 TLR4 agonist

Stimulation of BV2 cells with 0.1-100 ng/ml lipopolysaccharide (LPS) for 8 hours resulted in a dose dependant response in miR-146a expression as determined by qRT-PCR **(Figure 3.10A)**. LPS is the major component of the outer membrane of Gram-negative bacteria and is specific to TLR4. The LPS used in these studies were derived from *Escherichia coli* 055:B5. MiR-146a levels reached more than a 12 fold increase in expression upon stimulation with 100 ng/ml LPS compared to control cells. Temporal changes in miR-146a expression were also observed in BV2 cells **(Figure 3.10B)**. Specifically, cells were stimulated using 100 ng/ml LPS over a 72 hour period and miR-146a expression was determined by qRT-PCR. Analysis revealed a time dependant response that followed a similar pattern of expression to microglia stimulated with the TLR2 agonist HKLM. Expression of miR-146a peaked at 48 hours reaching a fold increase of approximately 11, followed by a decline at 72 hours.

A

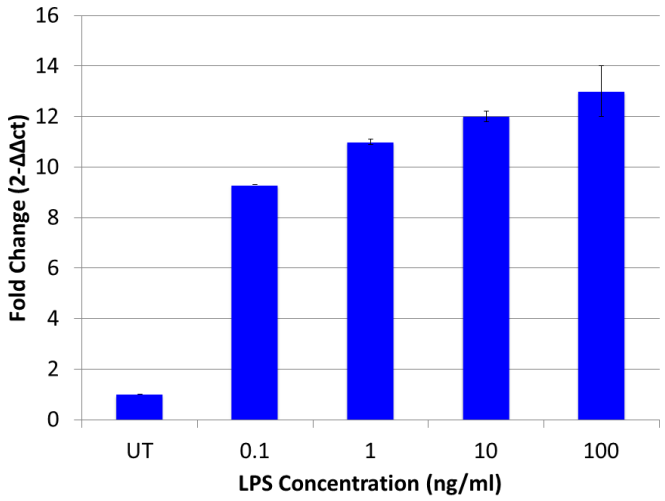

B

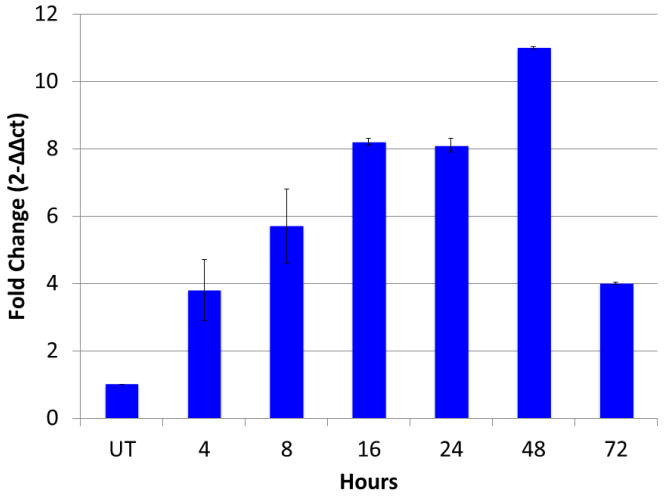

Figure 3.10 MiR-146a expression in microglia cells stimulated with a TLR4 agonist. **A.** BV2 cells were treated with LPS at concentration ranging from 0.1-100 ng/ml for 8 hours and RNA was collected. MiR-146a expression was determined by TaqMan qRT-PCR relative to untreated cells (UT). The experiment was performed in triplicate and the

average fold change ± SD is shown. **B.** BV2 cells were treated with 100 ng/ml LPS over a 72 hour period and RNA was collected. MiR-146a expression was determined by TaqMan qRT-PCR relative to untreated cells (UT). The experiment was performed in triplicate and the average fold change ± SD is shown.

3.2.2.3.1 Analysis of two TLR4 agonist preparations

LPS signalling is mediated by TLR4 since mutations or deletions of the TLR4 locus completely abolish LPS-mediated signalling (Coutinho & Meo, 1978; Poltorak et al., 1998). To show that miR-146a induction is specifically mediated by the LPS/TLR4 signalling pathway, the EOC13.31 cells were employed since they possess an inherent mutation in the TLR4 gene (Tlr4Lps-d) making them hyporesponsive to LPS (Walker, Gatewood, Olivas, Askew, & Havenith, 1995). Unexpectedly, significant up-regulation of miR-146a in EOC13.31 cells treated with LPS was observed. Although speculative, it was hypothesized that this response was due to the presence of a contaminant in the particular LPS preparation in use, an observation previously reported by others (Qin, Wilson, Lee, Zhao, & Benveniste, 2005). Stimulation with an ultrapure LPS preparation did not evoke miR-146a up-regulation in EOC 13.31 cells confirming this was the most likely explanation **(Figure 3.11A)**. Taganov et al (2006) previously showed that TLR2 stimulation by exposure to peptidoglycan and its synthetic analog, Pam3CSK4, produced an up-regulation of miR-146a in human monocytes in contrast to TLR3, TLR7 and TLR9 agonists (Taganov et al., 2006). To test whether the crude LPS preparation in the laboratory contained agonists capable of stimulating EOC 13.31 TLR2 receptors, cells were treated with an anti-TLR2 antibody for 30 minutes prior to treatment with LPS. This treatment, in turn, prevented the induction of miR-146a in EOC 13.31 cells stimulated via the crude LPS preparation, but not similarly treated BV-2 cells which have a functional TLR4 **(Figure 3.11B)**.

A

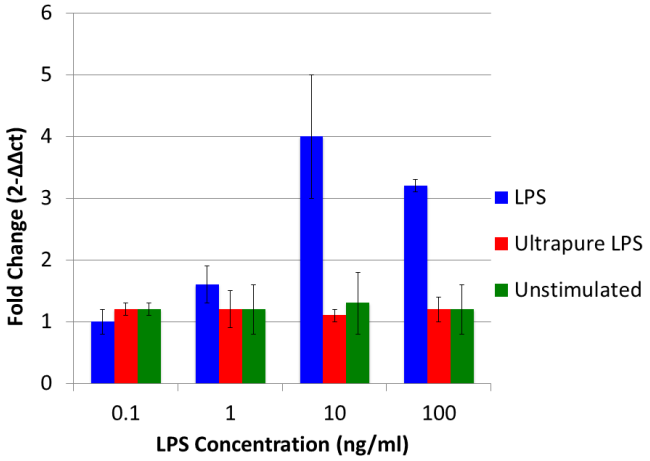

B

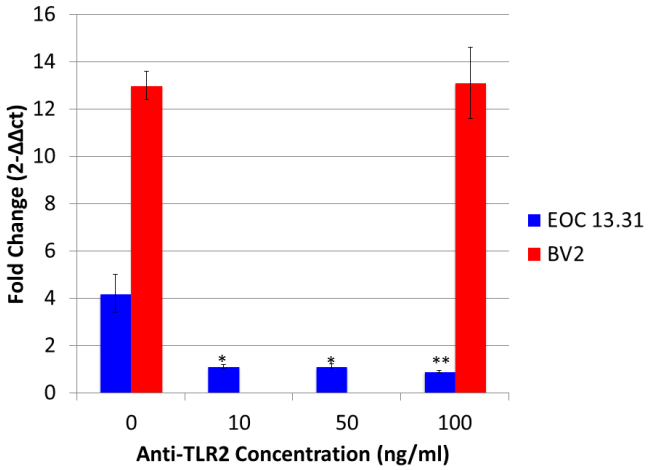

Figure 3.11 Analysis of two LPS preparations. **A.** EOC 13.31 cells were treated with increasing concentrations of semi-pure LPS and ultra-pure LPS. Total RNA was collected after 8 hours and miR-146a expression was measured by TaqMan qRT-PCR. Fold induction relative to untreated cells is shown. The experiment was performed in triplicate and the average fold change ± SD is shown. **B.** EOC 13.31 cells were incubated with

increasing concentrations of an anti-TLR2 antibody for 30 minutes prior to treatment with 100 ng/ml LPS. MiR-146a expression relative to mock-treated control cells was measured by TaqMan qRT-PCR. Inhibition of miR-146a expression following anti-TLR2 antibody treatment was significant at all concentrations; * $p < 0.01$, ** $p < 0.005$. Treatment of BV2 cells with 100 ng/ml anti-TLR2 antibody prior to LPS treatment failed to inhibit miR-146a induction. The experiment was performed in triplicate and the average fold change ± SD is shown.

3.2.2.4 TLR5 agonist

BV2 cells were treated for 24 hours with varying concentrations of flagellin isolated from *Salmonella typhimurium*, known as FLA-ST. Treatment with this TLR5 agonist resulted in a dose-dependent response in miR-146a expression where expression increased with increasing concentration (**Figure 3.12**). Expression of miR-146a peaked upon stimulation with 10 µg/ml FLA-ST to over a 4.5 fold increase compared to mock treated cells.

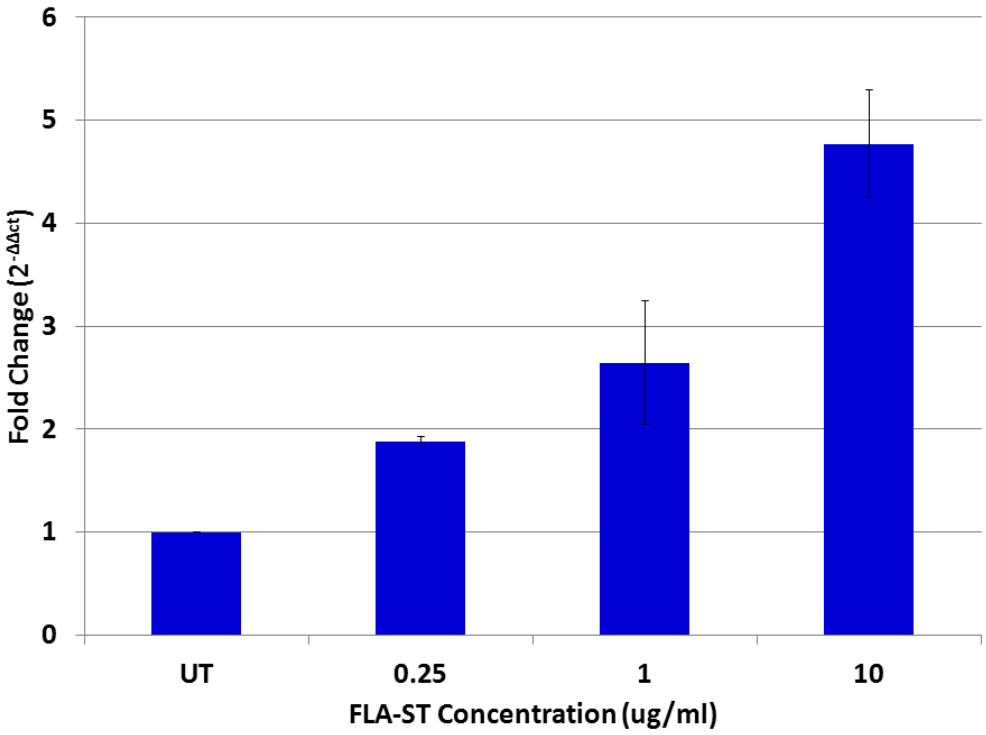

Figure 3.12 MiR-146a expression in microglia cells treated with a TLR5 agonist. BV2 cells were treated with 0.25, 1 and 10 µg/ml of FLA-ST for 24 hours and total RNA was collected. MiR-146a expression was determined by TaqMan qRT-PCR relative to untreated cells (UT). The experiment was performed in triplicate and the average fold change ± SD is shown.

3.3 Identification of miR-146a targets

Understanding the mechanism of action and identifying functionally important mRNA targets of miR-146a are essential to unravelling its biological function, role in prion disease, and for tapping its undoubted therapeutic potential. There are several approaches in identifying miRNA targets and the use of computational prediction programs and transcriptome profiling are presumably the most common. However, both approaches have inherent limitations that may be addressed with the use of proteomics. Therefore, with the aim of identifying genes under miR-146a control, a functional proteomic strategy was employed to determine the extent of proteomic changes modulated by miR-146a expression in microglia cells.

3.3.1 MiR-146a over-expression and knock-down in microglia cells

Over expression or knock-down of miR-146a was employed as a strategy to identify the proteins that are under the regulation of miR-146a. Over-expression of miR-146a was achieved by transiently transfecting BV2 cells with a synthetic miRNA precursor known as pre-miR-146a for 8, 24 and 48 hours. This precursor is processed by the cellular machinery, RISC complex, to produce the mature active form of miR-146a. The resulting levels of mature miR-146a in transfected cells was determined by qRT-PCR and subsequently compared to cells transfected with a scrambled pre-miR negative control. Transfection of pre-mir-146a for 8 hours resulted in approximately a 250,000 fold increase of miR-146a in comparison to negative control cells **(Figure 3.13A)**. Such a drastic increase is likely not an accurate measure of the actual levels of transfected miR-146a within the cells. The collective measurement of miR-146a within the cells and residual miR-146a left over from the transfection process is one possible explanation.

Increased levels of mature miR-146a were maintained over a period of 48 hours. Knockdown of miR-146a was attained by transfecting BV2 cells over a period of 48 hours with a miR-146a anti-miR, a modified anti-sense oligonucleotide that binds to the mature miR-146a sequence effectively blocking its activity. MiR-146a knock-down was found to be optimal between 16 and 48 hours post transfection compared to cells transfected with scrambled anti-miR negative control as determined by qRT-PCR **(Figure 3.13B)**.

A

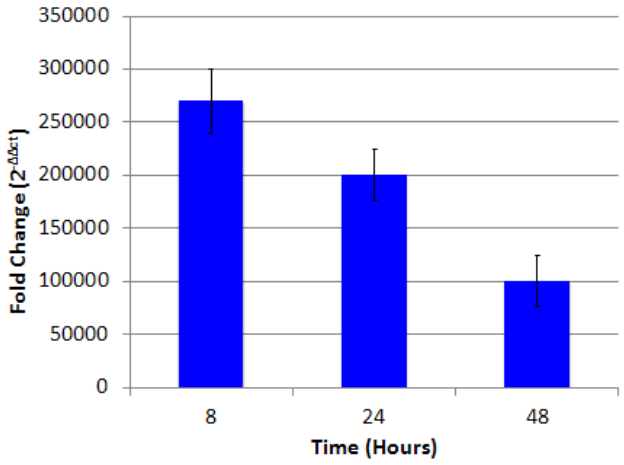

B

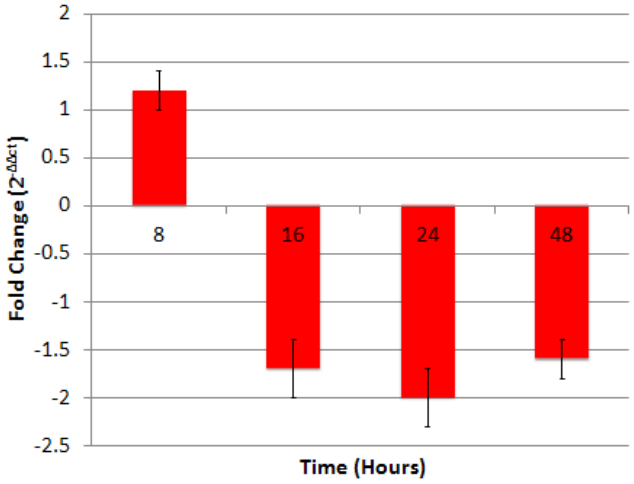

Figure 3.13 MiR-146a over-expression and knock-down in microglia cells. **A**. MiR-146a over-expression as measured by TaqMan qRT-PCR in BV2 cells after 8, 24, and 48 hours of treatment with 30 nM of transfected pre-miR-146a in comparison to 30 nM of transfected scrambled negative control miRNA. An average fold change ± SD were

measured from triplicate experiments. **B**. MiR-146a knock-down as measured by TaqMan qRT-PCR in BV2 cells after 8, 16, 24, and 48 hours of treatment with 50 nM of transfected anti-miR-146a in comparison to 50 nM of transfected scrambled negative control miRNA. An average fold change ± SD were measured from triplicate experiments.

3.3.2 Functional model of miR-146a

Based on previous studies, miR-146a has been shown to play an important role in the modulation of the innate immune response. MiR-146a can directly down-regulate the production of pro-inflammatory cytokines by acting as a negative feedback effector of the inflammatory signalling pathway initiated by NF-κB (Taganov et al., 2006). Given this fact, it was hypothesized that the majority of miR-146a targets would likely only be evident during conditions in which cells were stimulated by a ligand that leads to a downstream inflammation-related program of gene expression. To this end, BV2 cells were transfected with pre-miR-146a or anti-miR-146a prior to stimulation of TLR2. TLR2 was the most relevant receptor for study as it results in a significant level of miR-146a induction in BV2 cells, a very specific agonist HKLM is available, and was recently found to be the most significantly up-regulated TLR in prion infected mouse brain tissue (Saba et al., 2012). In addition, it has been shown to be a primary receptor for the amyloid β peptide that can trigger neuroinflammatory activation in Alzheimer's disease, a neurodegenerative disease similar to prion disease (S. Liu et al., 2012).

3.3.2.1 Validation of miR-146a functional model

To confirm the model was functional and provided a valid means to identify proteins that are either direct targets of miR-146a, or deregulated in consequence of being downstream of miR-146a targets, it was confirmed that cells transfected with miR-146a mimics expressed decreased levels of the pro-inflammatory cytokine IL6. MiR-146a has been previously shown to attenuate the expression of critical inflammatory cytokines, including IL6, in LPS-stimulated macrophages through a negative feedback regulation loop involving downregulation of IRAK1, TRAF6 and to a lesser extent, NOTCH1 (He

et al., 2014; Taganov et al., 2006). In this study, production of this cytokine was significantly reduced by miR-146a over-expression upon TLR2 stimulation of BV2 cells versus cells transfected with a scrambled control RNA **(Figure 3.14).** In addition, transfection of miR-146a anti-miR resulted in a small but significant up-regulation of IL-6.

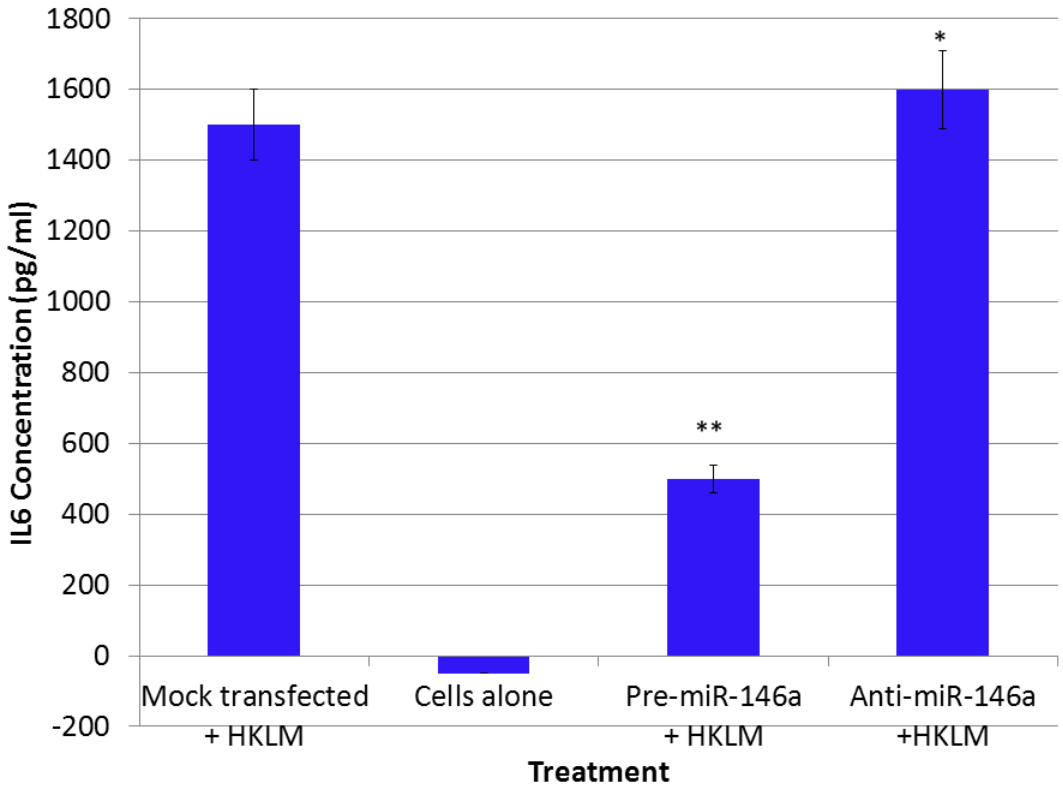

Figure 3.14 Analysis of IL6 levels by ELISA. BV2 cells were transfected with 30 nM of pre-miR-146a or 50 nM anti-mR-146a and 16 hours later stimulated with a TLR2 agonist. At 24 hours post stimulation, culture supernatant was collected and the levels of IL-6 were determined by ELISA; significance ** $p < 0.001$, * $p < 0.01$.

3.3.3 Proteomic analysis of miR-146a functional model

Unlike the miR-146a knock-out strategy, which ultimately depends upon changes in the pre-existing abundance of miR-146a, over-expression allows for greater manipulation of the cellular miR-146a content. Therefore, changes in the proteome following miR-146a overexpression under inflammatory conditions was best suited to shed light on the overall effect and biological role of this particular miRNA. It was known that proinflammatory cytokine expression is under regulation by miR-146a, probably via the known miR-146a targets IRAK1 and/or TRAF6. However, miRNAs can have multiple targets in a particular cell type and it was decided to test the use of a global approach to identify a complete profile of proteins and pathways under regulation by miR-146a. To this end, a relative quantitative proteomics approach using mass spectrometric analysis of TMT labelled peptides was implemented (**Figure 3.15**).

Briefly, microglia were transfected with pre-miR-146a prior to stimulation with a TLR2 agonist yielding an environment comparable to that observed during prion-induced neurodegeneration. Peptides of microglia overexpressing miR-146a or a scrambled sequence as control were TMT labelled and subsequently analyzed by mass spectrometry. In total, 3750 proteins were identified using an FDR of less than 2% at the protein level and at least two peptides per protein. Comparison of the protein maps revealed statistically significant differences between the two groups in the expression of 3290 proteins when applying a threshold of at least 1.1 fold change and q-value < 0.02. This fold change cutoff was implemented for two reasons. Firstly, miRNA induced proteomic changes have been shown to be extremely modest when experimentally tested (Baek et al., 2008; Bargaje et al., 2012). Secondly, the magnitude of the observed changes in

protein expression in this study was very small as illustrated in **Figure 3.16**. Whereas the 3118 upregulated proteins were most likely indirect targets, the 172 downregulated proteins may be inhibited by miR-146a either directly or indirectly.

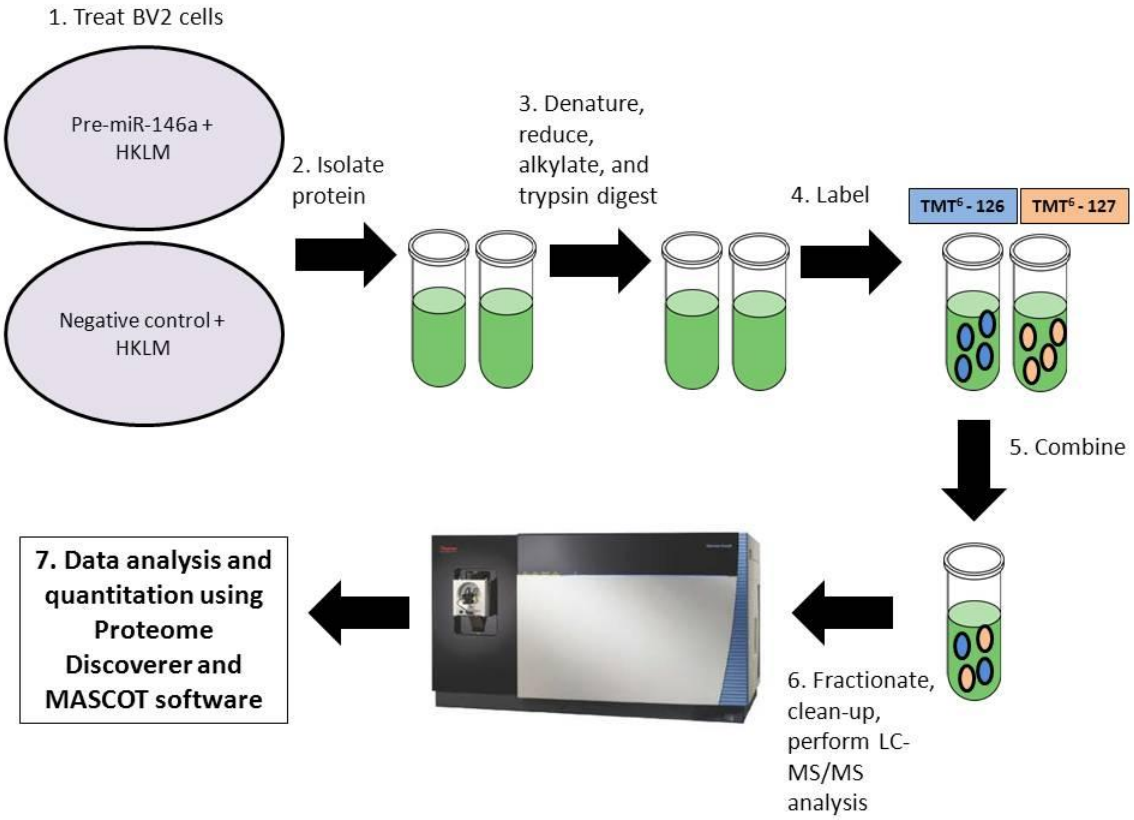

Figure 3.15 Experimental schema for miRNA-proteomics. Cells were transfected with either pre-miR-146a or scrambled negative control prior to stimulation with HKLM. Protein was isolated, digested into peptides and labelled with TMT reagents. Labelled samples were combined, fractionated and analyzed by high resolution Orbitrap LC-MS/MS before data analysis to identify peptides and quantify reporter ion relative abundance. The experiment was performed in triplicate and differential protein expression relative to scrambled negative control + HKLM were determined.

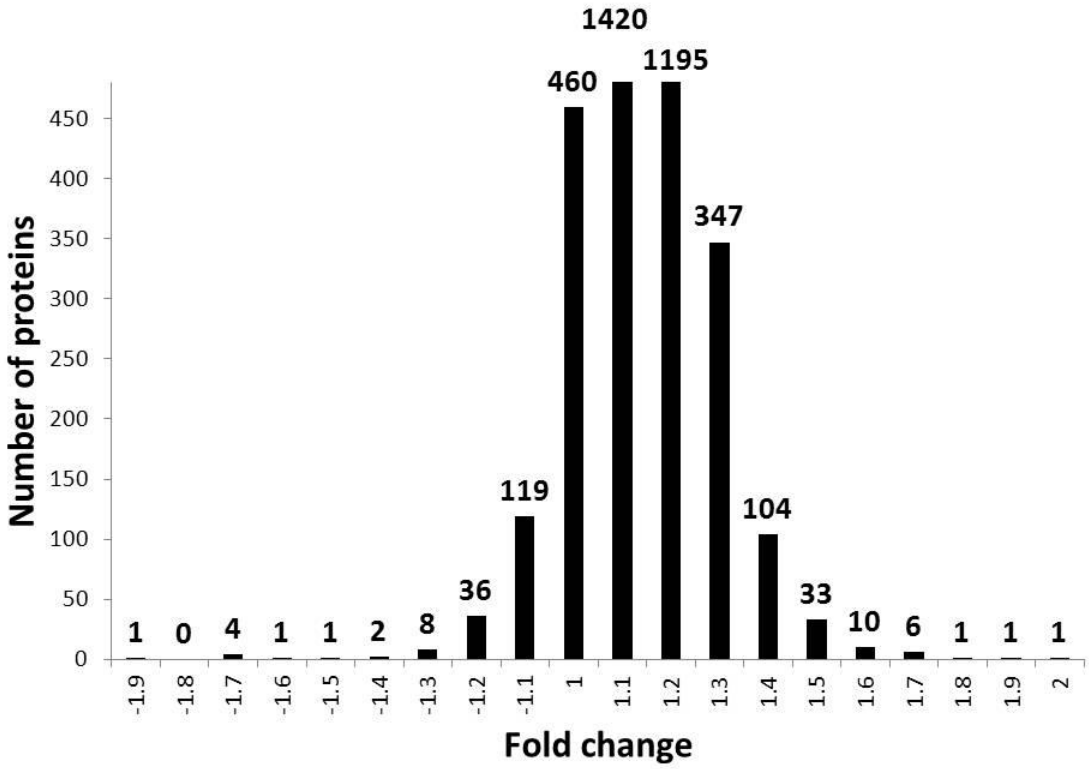

Figure 3.16 Histogram of differentially expressed proteins in microglia cells upon miR-146a overexpression. Distribution of fold changes of differentially expressed proteins in cells overexpressing miR-146a compared to negative control. The experiment was performed in triplicate and fold changes of at least 1.1 were considered significant.

3.3.3.1 Biological function of miR-146a regulated proteins in microglia

It was hypothesized that functionally important miR-146a targets would likely be those downregulated upon miR-146a over-expression in our proteomic study. To this end, the cellular processes affected by miR-146a, both directly or indirectly, according to gene ontology classification of downregulated proteins using the Ingenuity Pathway Knowledge Base (IPKB) were evaluated. IPKB contains information on human, mouse, and rat genes including annotations, synonyms, and over 1.4 million published biological interactions between genes, proteins, and drugs. The database is continually updated and supplemented with curated relationships taken from MEDLINE abstracts (each gene interaction held in the knowledge base is supported by published information). In general, IPKB provides a framework by which lists of genes identified by large scale genomic or proteomic studies can be annotated in terms of their functional and biological relationships, and those that have been shown to interact. IPKB identified key biological functions of the experimentally determined miR-146a regulated proteins, including molecular and cellular functions, diseases and disorders, and physiological system development and function. Representative biological functions which were over-represented (p-value < 0.05) in our study are provided in **Figures 3.17-19.** Notably, proteins under miR-146a regulation were found to be involved in cellular growth and proliferation, cellular movement, cell signalling, cell morphology, neurological disease, inflammatory response, immunological disease, infectious disease, inflammatory disease, psychological disorders, immune cell trafficking, and nervous system development and function.

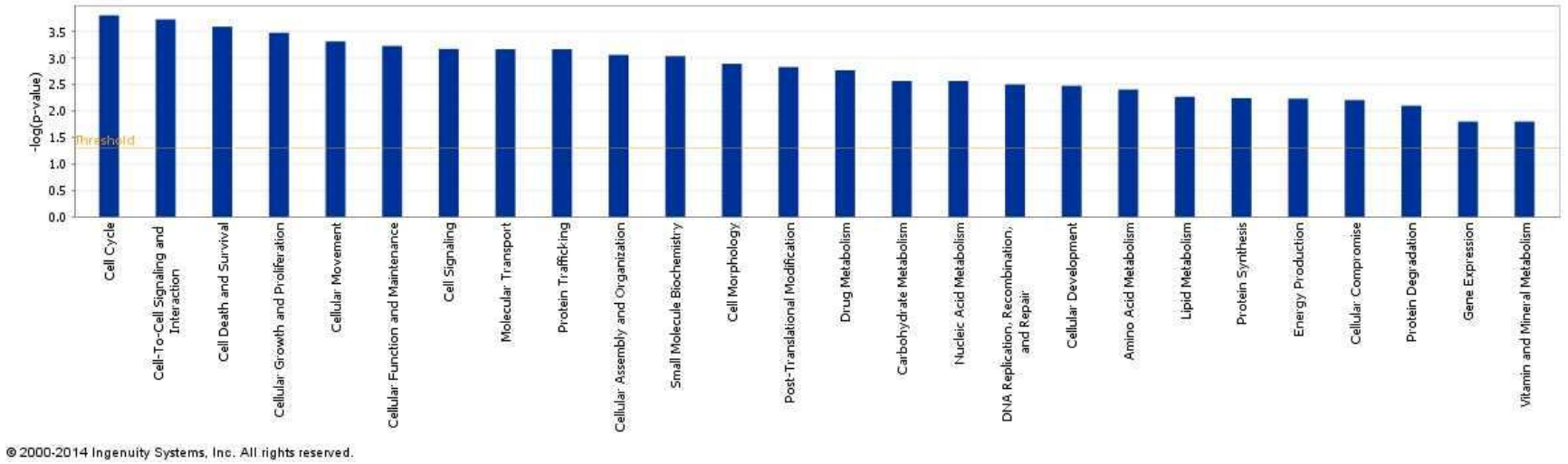

Figure 3.17 Significant molecular and cellular functions over-represented by the 172 experimentally determined miR-146 regulated proteins using the IKPB functional analysis tool

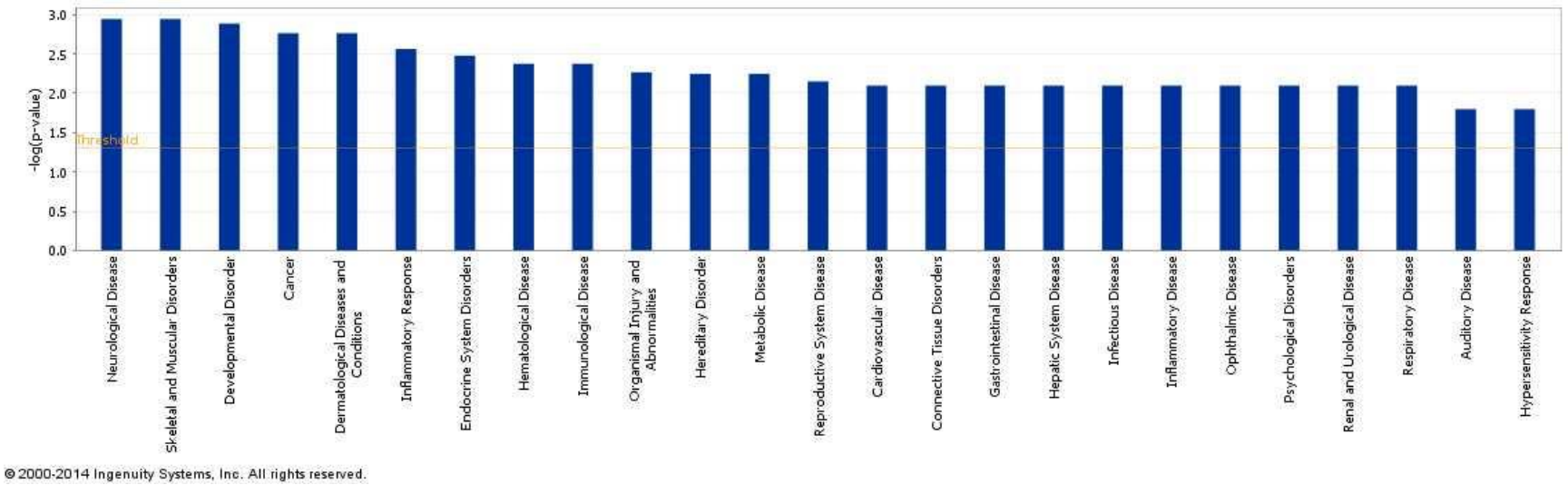

Figure 3.18 Significant diseases and disorders over-represented by the 172 experimentally determined miR-146 regulated proteins using the IKPB functional analysis tool.

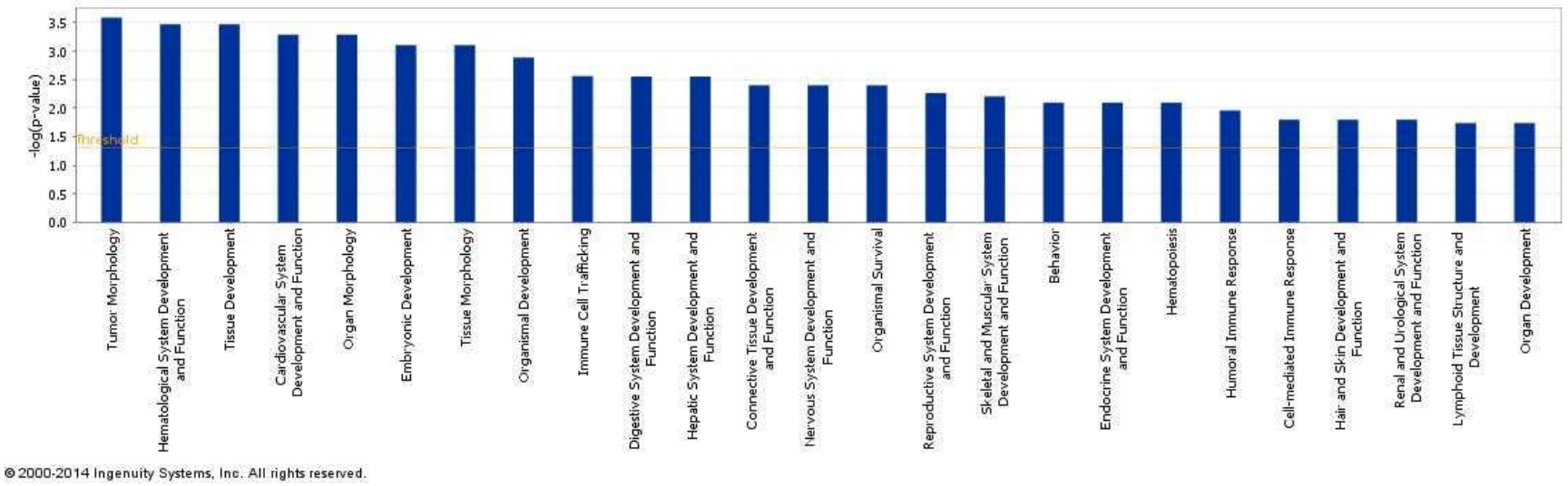

Figure 3.19 Significant physiological system development and functions over-represented by the 172 experimentally determined miR-146 regulated proteins using the IKPB functional analysis tool.

Individual regulated proteins may interact to have a coordinated role in specific pathways. Indeed, the identification of potential networks of related proteins is possible in IPKB. This methodology integrates data with mining techniques to predict protein networks that comprise protein-protein interactions and other functional linkages. Each potential network is given a score, which is a probabilistic fit between the networks, and a list of biological functions stored in the IPKB. The score takes into account the number of focus proteins in the network, and the size of the network, to approximate how relevant it is to the original list of proteins; these scores are used to rank the networks. IPKB revealed approximately 11 statistically significant networks (a network is often considered significant if the score is ≥ 3 (p-value = 0.001)). The proteins comprising these networks, the scores of these networks, and the top biological functions in which these networks most likely participate in are indicated in **Table 3.8.** Additionally, these networks of gene interactions are illustrated in **Figures 3.20-30**.

Table 3.8 MiR-146a regulated proteins involved in the composition of networks of related proteins

ID	Molecules in Network	Score	Focus Molecules	Top Diseases and Functions
1	**ABCB6**,**BID**,**BRD4**,**C1QBP**,Calcineurin protein(s),caspase,**CCNT1**,**CHTF18**,**CLPX**,**CYC1**,Cytochrome bc1,cytochrome C,cytochrome-c oxidase,**DDX11**,**DFFA**,ERK1/2,**FKBP1A**,Holo RNA polymerase II,**HUS1**,KRT17,MAP2K1/2,Mitochondrial complex 1,**MKNK1**,**MRPS10**,**NDUFA8**,**NDUFB4**,**NELFE**,**POLR2B**,**RAD17**,RNA polymerase II,RPA,**RPS27L**,**SIRT1**,**UBA5**,**UGDH**	38	24	Cell Cycle, DNA Replication, Recombination, and Repair, Tissue Morphology
2	**AIMP2**,Alp,Alpha catenin,**ANP32E**,Ap1,**ARF6**,**CCDC47**,**CHMP2B**,F Actin,**FAF2**,**GMPPA**,**GNA13**,**GRHPR**,Hsp70,**KRAS**,**Map4k4**,NADPH oxidase,**NDRG1**,NFkB (complex),Pdgf (complex),PDGF BB,Phosphatidylinositol4,5 kinase,Pld,**PNPLA2**,**RHOA**,**RNF25**,Rock,**RPL12**,Sapk,**SQSTM1**,**STXBP1**,Tgf beta,**TLK2**,**TRAF2**,**UBQLN1**	38	21	Cellular Function and Maintenance, Molecular Transport, Protein Trafficking
3	CDK5RAP1,**CRELD2**,CSPG5,**EXOSC1**,**EXOSC4**,**EXOSC5**,FAHD1,**GNG12**,**GNS**,**GOPC**,**HERC2**,**LSM2**,LSM14B,**MINK1**,**MYO1D**,NDUFB11,NT5C1B,PRPF18,**RDH11**,RDH14,**RPL29**,RPL39,RPL3L,RPRD1B,SDR16C5,SDSL,**SEH1L**,SNRNP25,SNRNP48,**SUMF1**,SUMF2,**TUBGCP4**,UBC,**YME1L1**,ZCRB1	29	17	Visual System Development and Function, Developmental Disorder, Hereditary Disorder
4	**CCDC132**,**DHRS13**,ETS1,**FAM206A**,**HEATR6**,HECW2,IFT88,KMT2D,**KTI12**,LSM1,**LYRM4**,MAGEB2,MEPCE,**MFSD10**,**NDUFAF7**,NFS1,NPM1,**NUDCD1**,PRKAA1,PTPN11,PVRL2,**RABL5**,RAN,**RANGRF**,**SDE2**,**SERHL2**,**SZRD1**,**TM9SF3**,**TMEM214**,TNFRSF1B,TOP3A,UBC,UNC93B1,USP36,VCP	27	16	Molecular Transport, Cell-To-Cell Signaling and Interaction, Hematological System Development and Function
5	C10orf35,**CBWD1**,**CMSS1**,CNIH4,**COMMD5**,**CTC1**,**EIF1AD**,**EMC4**,EXOC1,GYG1,**JAGN1**,**LACTB**,METAP1,**MFSD5**,NUP88,OBFC1,PEX19,PIN4,POMP,**PSMG2**,**RRP1**,**SFR1**,SLC35F6,**SLC39A11**,**SLTM**,SPRTN,SSR4,TRAPPC3,TRAPPC8,TRAPPC11,**TRAPPC13**,TRAPPC2L,UBC,ZBTB39,**ZDHHC13**	27	16	Cardiovascular Disease, Hereditary Disorder, Neurological Disease
6	AP1S1,APIP,**ARMC6**,**ASB6**,**C1orf35**,CACHD1,CEP152,CHMP6,CHMP1B,**COG1**,COG2,COG4,COG5,COG7,COG8,**FAM175B**,**HEBP1**,**KNSTRN**,MAN1B1,**NOB1**,**RANBP10**,**RPIA**,**SAAL1**,SNF8,**STAMBPL1**,STK36,THAP5,**TXNDC9**,TXNL4B,UBC,**UTP18**,**VPS25**,VPS36,XRCC3,**ZNHIT3**	27	16	Developmental Disorder, Hereditary Disorder, Metabolic Disease
7	26s Proteasome,Akt,BCR (complex),**CD86**,Cyclin A,Cyclin E,**DAXX**,**DHPS**,E2f,**HLA-B**,**IFI35**,Ifn,IFN alpha/beta,IFN Beta,Ifnar,IgG1,Igm,IL12 (complex),IL12 (family),Immunoglobulin,Interferon alpha,**MLST8**,**NEK6**,**NSMCE1**,p70 S6k,**PLEKHA2**,**PPT1**,**PSMD10**,**RBL1**,**S100A10**,thymidine kinase,Tlr,**Tlr13**,Ubiquitin,**UXS1**	25	15	Neurological Disease, Skeletal and Muscular Disorders, Cellular Function and Maintenance
8	**AGFG2**,**ANKZF1**,APC,APP,ATL3,C2orf57,**CCDC25**,COMMD2,COMMD7,DNAAF2,**ECHDC1**,FAM90A1,GIMAP6,**GMEB2**,HMCES,**ISOC2**,KIAA0513,**LRRC25**,**NAGPA**,NAT2,NFKB1,NLN,**NOA1**,PLEKHO2,**PNISR**,**RASAL3**,**SPR**,superoxide,THSD4,tretinoin,**VPS45**,VSIG4,YWHAZ,**ZFYVE16**,ZNF839	21	14	Cellular Compromise, Cell-To-Cell Signaling and Interaction, Molecular Transport
9	Actin,calpain,CD3,**CEBPZ**,Collagen(s),**COMT**,ERK,Focal adhesion kinase,Growth hormone,hemoglobin,Hsp27,IL1,Integrin,**ITGA4**,Mapk,**MARCKS**,Mek,**NIP7**,P38 MAPK,p85 (pik3r),PI3K (complex),Pkc(s),**RAB5C**,**RANBP9**,Ras,**RPP30**,**SF1**,Sos,**SPP1**,STAT5a/b,TCR,**TES**,Tnf (family),**TSTA3**,Vegf	18	12	Cancer, Cell Morphology, Cardiovascular System Development and Function
10	ACBD6,**ADAT1**,ARHGAP11A,**ASUN**,ATAD5,C21orf59,**CHORDC1**,**CRELD1**,**CROT**,FAM50B,HNF4A,IFT122,INTS4,IQCB1,**Krt42**,LARP4,**MEAF6**,MIS18BP1,MRPS15,NAP1L1,OGFR,PARP4,**RAVER1**,RBM6,SH3BGRL2,SLC5A3,SUMO2,TMEM43,TRMT1L,**TTLL10**,UTP11L,WBSCR22,**ZCCHC9**,**ZNF326**,ZNF644	16	11	Hereditary Disorder, Nephrosis, Ophthalmic Disease
11	AHSP,ARHGAP22,Brdt,Cg,Ck2,Cpe,CRTC3,ELP4,ELP6,FAM3D,FSH,**GGCT**,Gsk3,Hdac,**HIRIP3**,HISTONE,Histone h3,Histone h4,Insulin,Jnk,**MAX**,miR-9-3p (and other miRNAs w/seed UAAAGCU),MTORC1,PADI3,**PCCB**,Pka,PSG5,RNU7-1,**SLC38A2**,SLC52A2,SLITRK1,**SON**,**TELO2**,vitamin K1,**YWHAB**	10	8	Auditory Disease, Hereditary Disorder, Neurological Disease

a. The genes in bold are the experimentally determined miR-146a regulated proteins of miR-146a. Other proteins were included in the network by IPKB to generate a network of related proteins.
b. The scores are a function of the total number of input proteins per a network; a network is often considered significant if the score is ≥ 3 ($p = 0.001$).
c. Focus molecules refers to the input proteins (experimentally determined miR-146a regulated proteins).

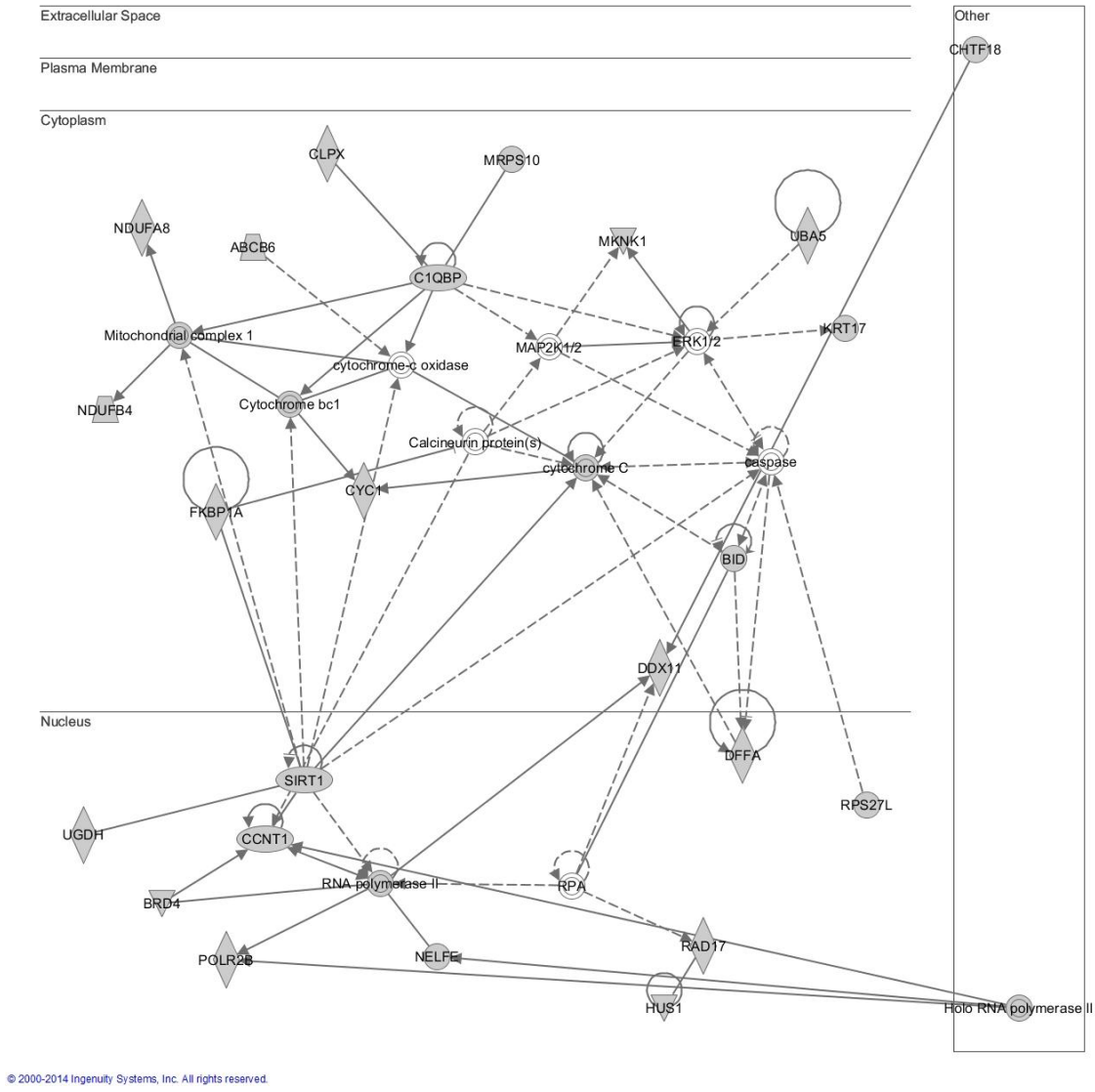

Figure 3.20 IPKB network analysis showing the interactions between several experimentally determined miR-146a regulated proteins. This network is composed of 24 focus molecules. The top functions of this network of proteins is cell cycle, DNA replication, recombination and repair, and tissue morphology. Shaded proteins are the experimentally determined miR-146a regulated proteins and uncolored proteins were proteins introduced by IPKB to form the network.

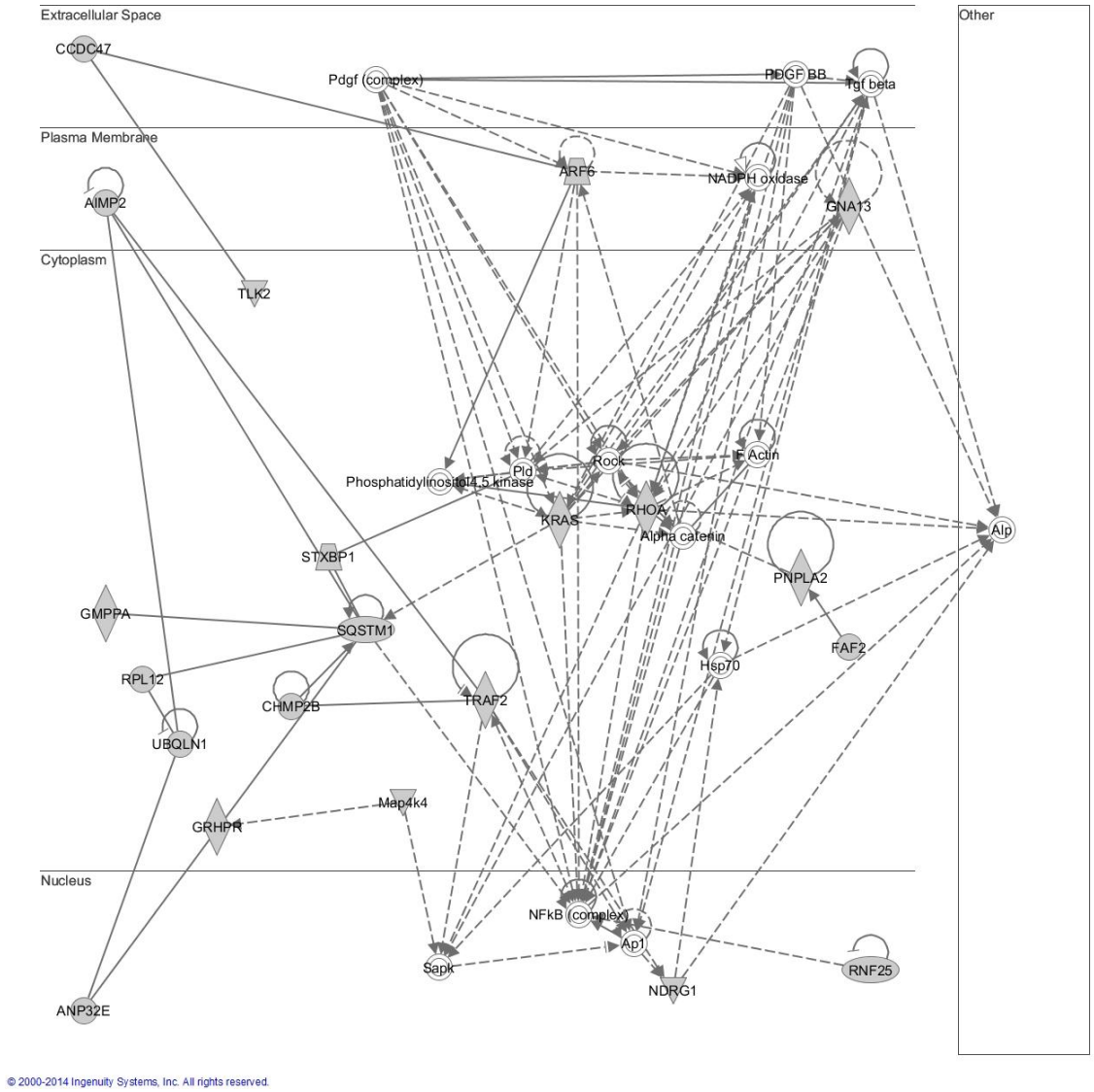

Figure 3.21 IPKB network analysis showing the interactions between several experimentally determined miR-146a regulated proteins. This network is composed of 21 focus molecules. The top functions of this network of proteins is cellular function and maintenance, molecular transport, and protein trafficking. Shaded proteins are the experimentally determined miR-146a regulated proteins and uncolored proteins were proteins introduced by IPKB to form the network.

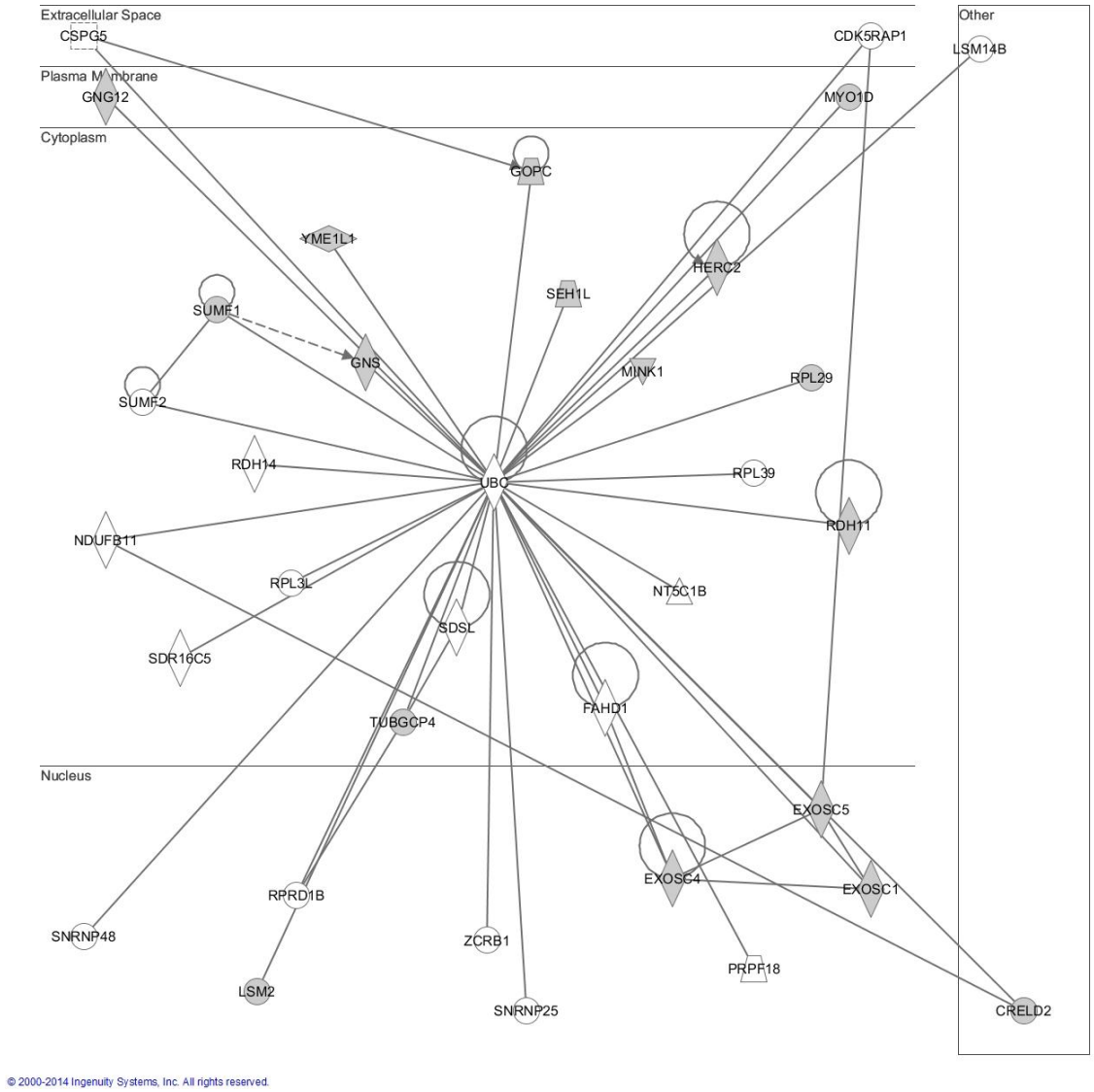

Figure 3.22 IPKB network analysis showing the interactions between several experimentally determined miR-146a regulated proteins. This network is composed of 17 focus molecules. The top functions of this network of proteins is visual system development and function, developmental disorder, and hereditory disorder. Shaded proteins are the experimentally determined miR-146a regulated proteins and uncolored proteins were proteins introduced by IPKB to form the network.

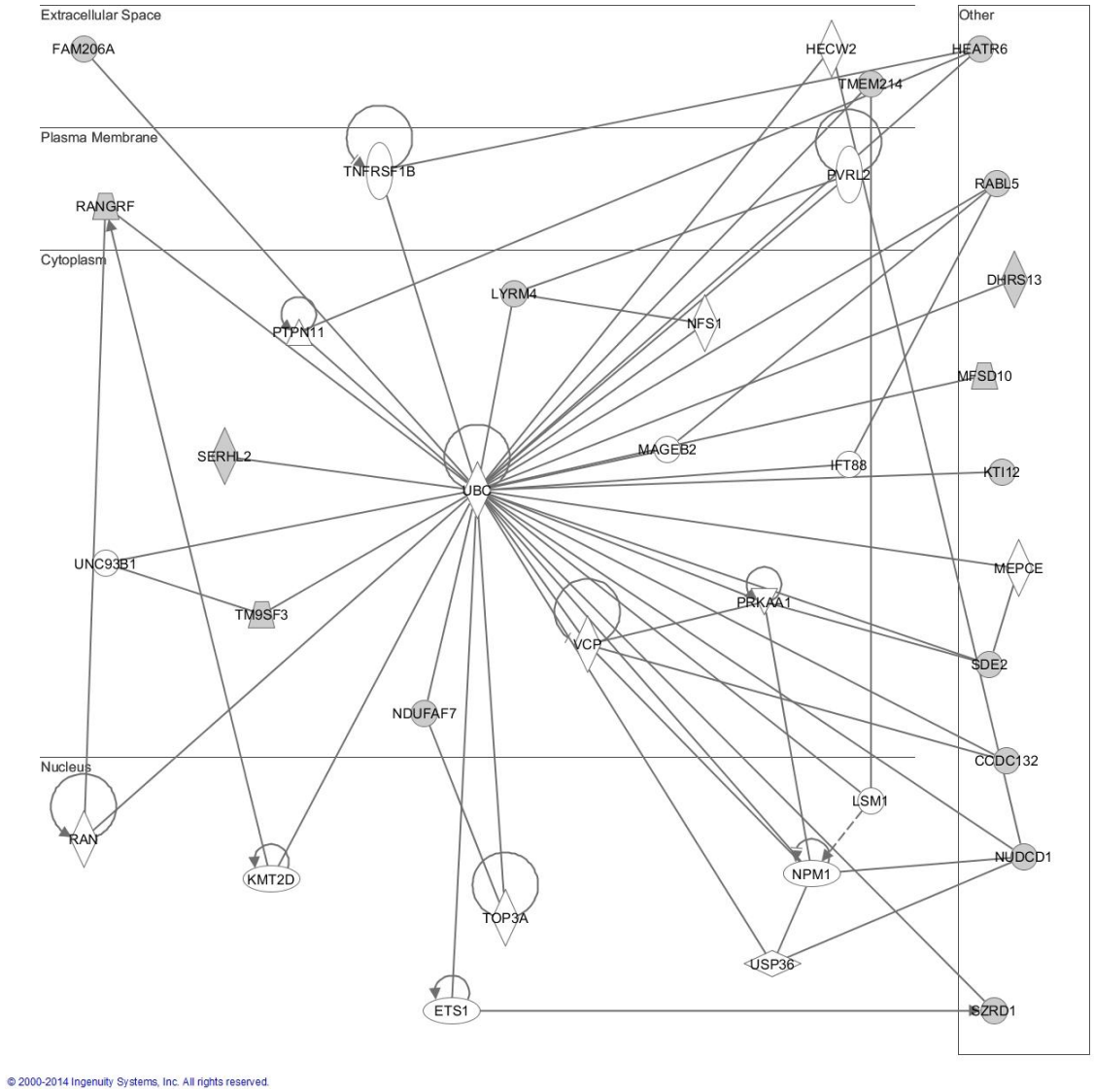

Figure 3.23 IPKB network analysis showing the interactions between several experimentally determined miR-146a regulated proteins. This network is composed of 16 focus molecules. The top functions of this network of proteins is molecular transport, cell to cell signaling and interaction, and hematological system development and function. Shaded proteins are the experimentally determined miR-146a regulated proteins and uncolored proteins were proteins introduced by IPKB to form the network.

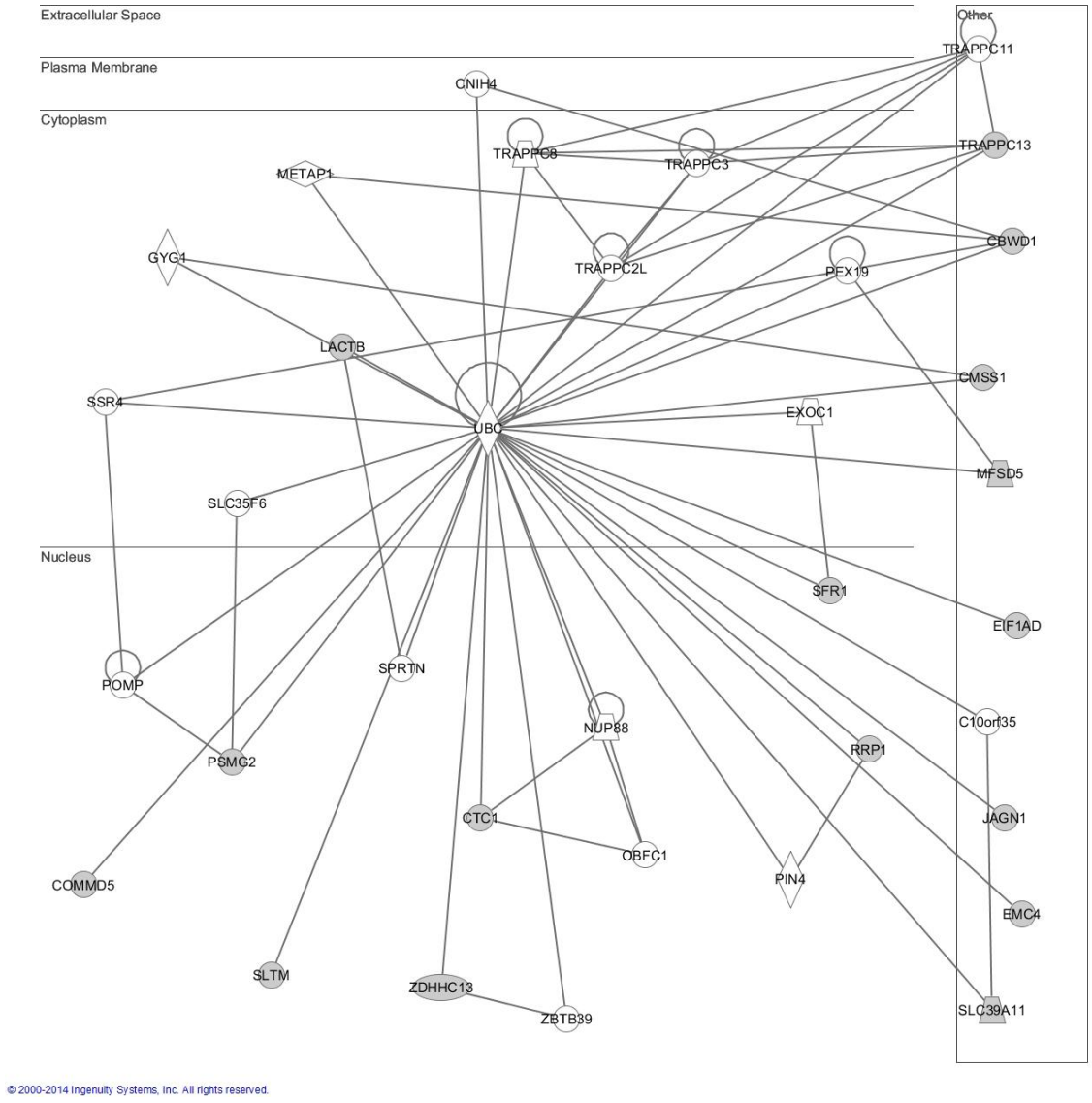

Figure 3.24 IPKB network analysis showing the interactions between several experimentally determined miR-146a regulated proteins. This network is composed of 16 focus molecules. The top functions of this network of proteins is cardiovasular disease, hereditory disorder, and neurological disease. Shaded proteins are the experimentally determined miR-146a regulated proteins and uncolored proteins were proteins introduced by IPKB to form the network.

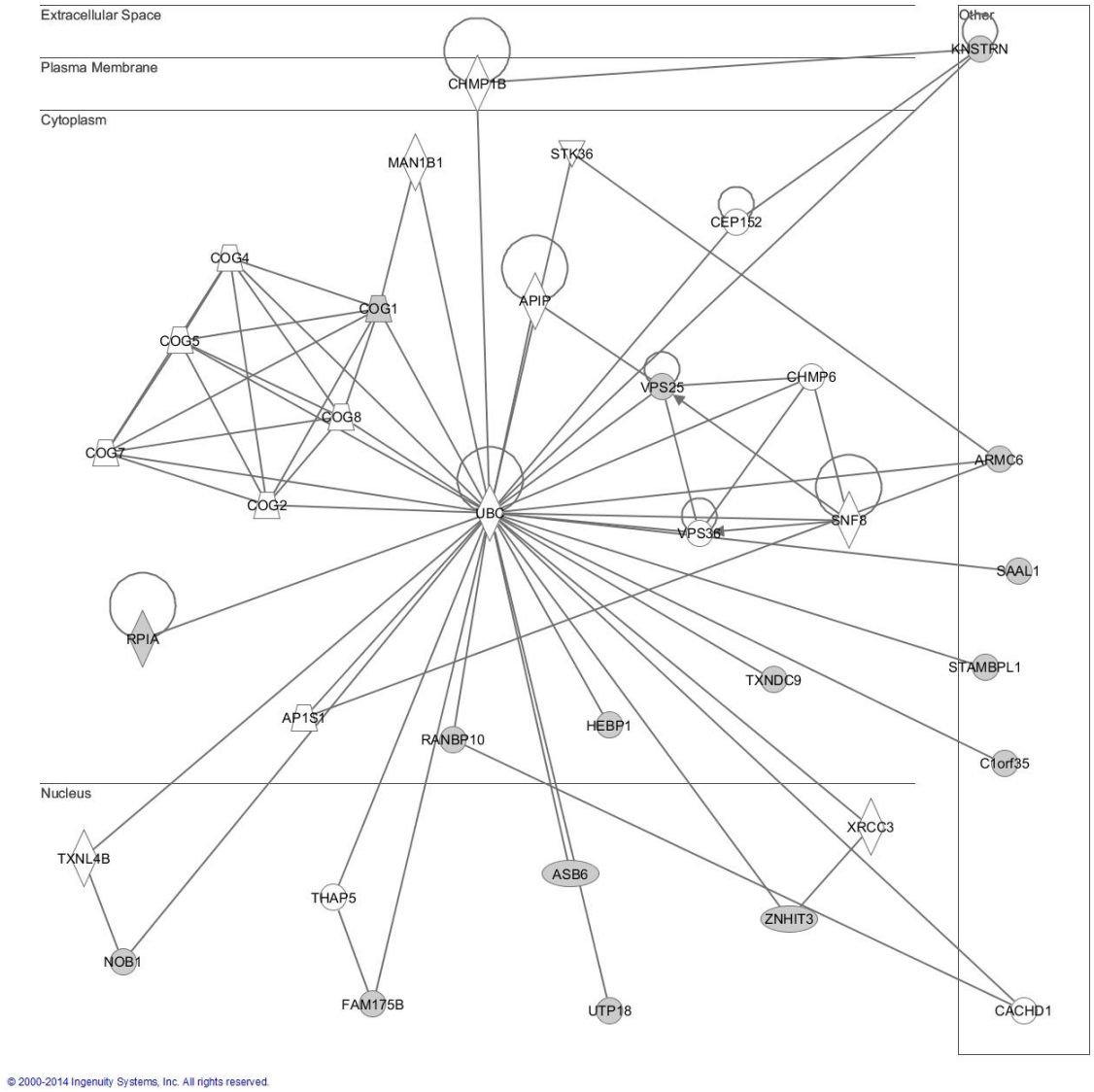

Figure 3.25 IPKB network analysis showing the interactions between several experimentally determined miR-146a regulated proteins. This network is composed of 16 focus molecules. The top functions of this network of proteins isdevelopmental disorder, hereditory disease, and metabolic disease. Shaded proteins are the experimentally determined miR-146a regulated proteins and uncolored proteins were proteins introduced by IPKB to form the network.

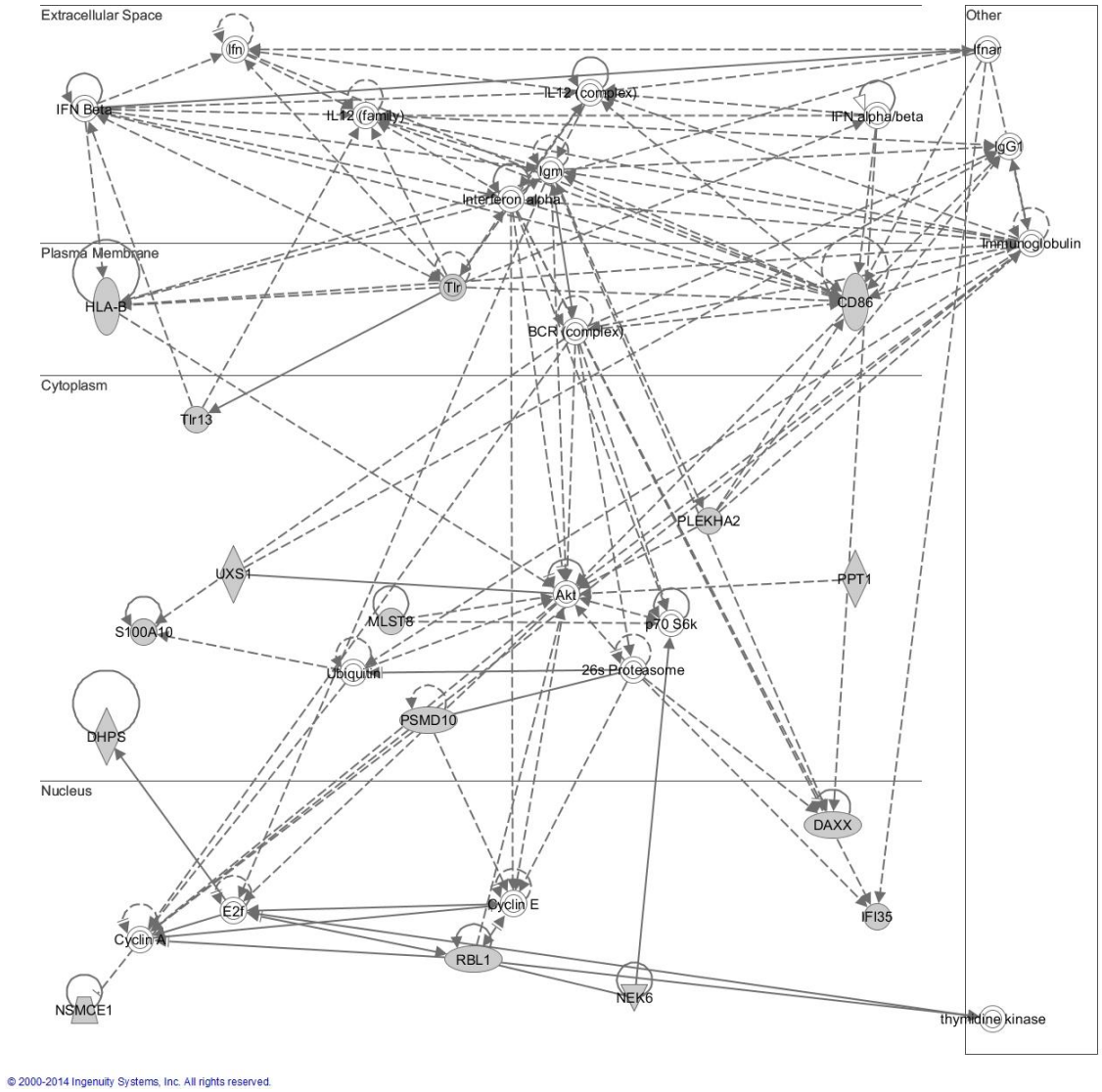

Figure 3.26 IPKB network analysis showing the interactions between several experimentally determined miR-146a regulated proteins. This network is composed of 15 focus molecules. The top functions of this network of proteins is neurological disease, skeletal and muscular disorders, and cellular function and maintenance. Shaded proteins are the experimentally determined miR-146a regulated proteins and uncolored proteins were proteins introduced by IPKB to form the network.

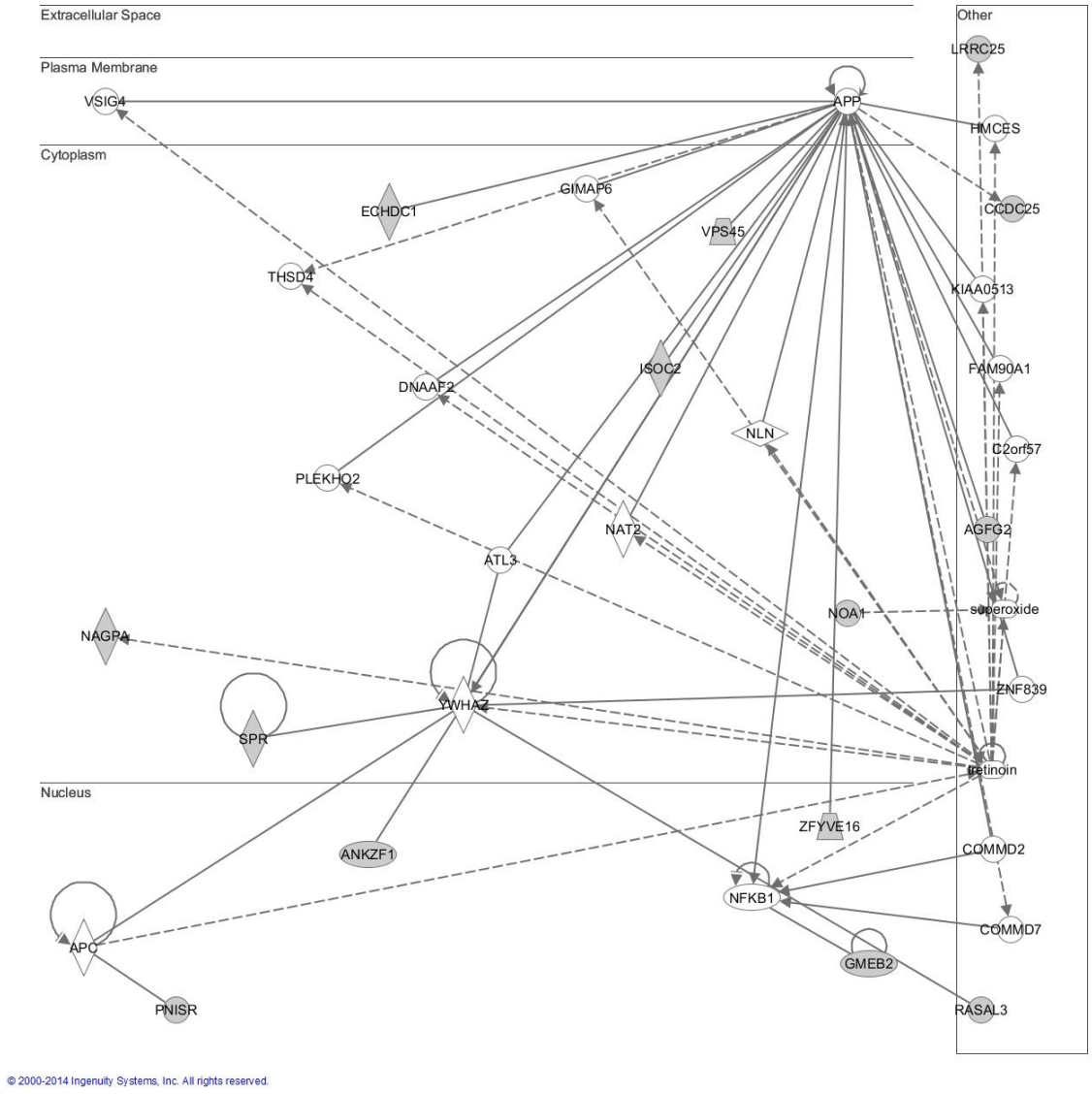

Figure 3.27 IPKB network analysis showing the interactions between several experimentally determined miR-146a regulated proteins. This network is composed of 14 focus molecules. The top functions of this network of proteins is cellular compromise, cell to cell signaling and interaction, and molecular transport. Shaded proteins are the experimentally determined miR-146a regulated proteins and uncolored proteins were proteins introduced by IPKB to form the network.

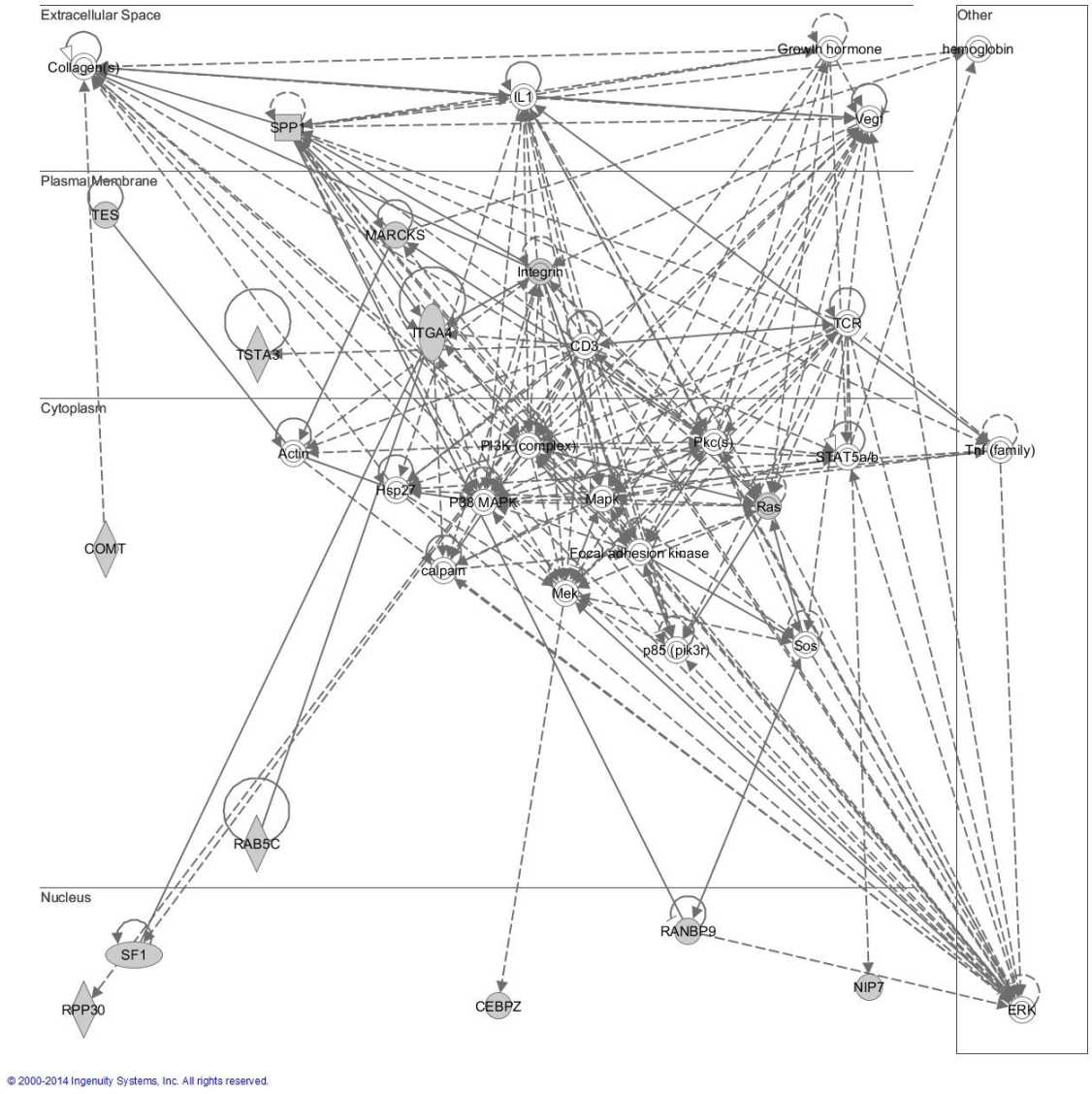

Figure 3.28 IPKB network analysis showing the interactions between several experimentally determined miR-146a regulated proteins. This network is composed of 12 focus molecules. The top functions of this network of proteins is cancer, cell morphology, and cardiovascular system development and function. Shaded proteins are the experimentally determined miR-146a regulated proteins and uncolored proteins were proteins introduced by IPKB to form the network.

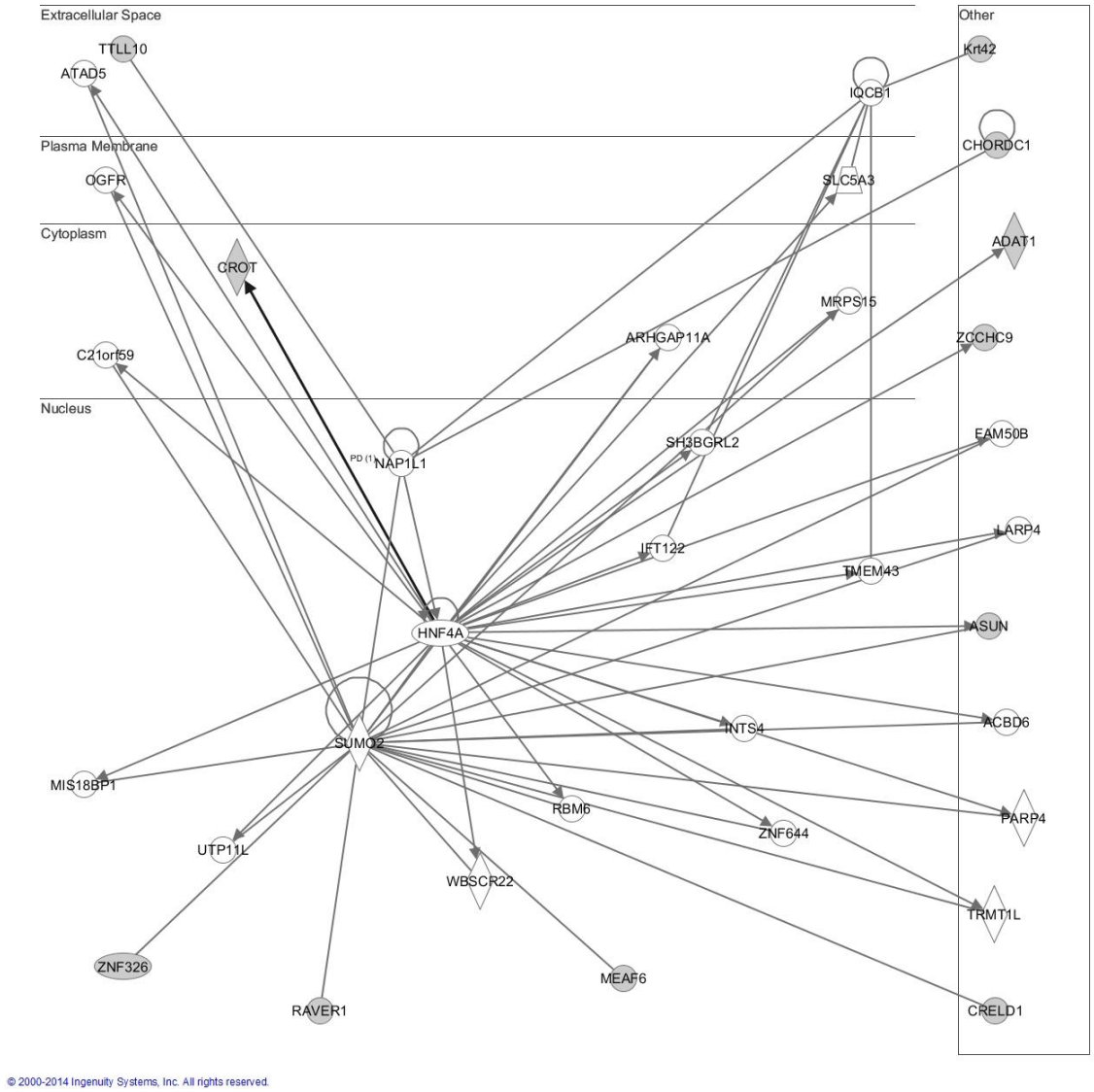

Figure 3.29 IPKB network analysis showing the interactions between several experimentally determined miR-146a regulated proteins. This network is composed of 11 focus molecules. The top functions of this network of proteins is hereditory disorder, nephrosis, and ophthalmic disease. Shaded proteins are the experimentally determined miR-146a regulated proteins and uncolored proteins were proteins introduced by IPKB to form the network.

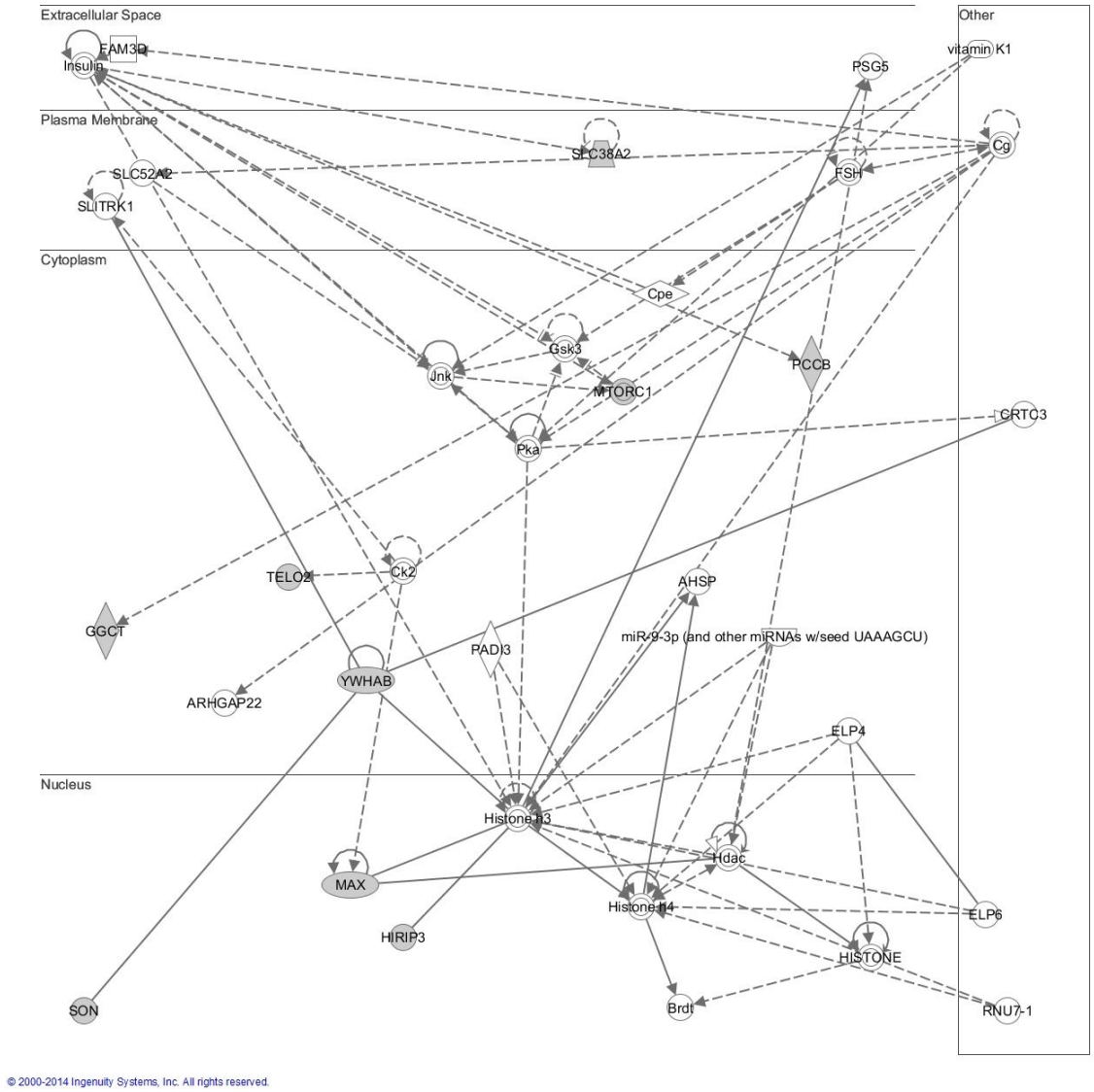

Figure 3.30 IPKB network analysis showing the interactions between several experimentally determined miR-146a regulated proteins. This network is composed of 8 focus molecules. The top functions of this network of proteins is auditory disease, hereditory disorder, and neurological disaese. Shaded proteins are the experimentally determined miR-146a regulated proteins and uncolored proteins were proteins introduced by IPKB to form the network.

Taken together, IPKB analysis of miR-146a regulated proteins appear to be relevant within the context of the biological role of microglial cells as the resident immune cells of the CNS. Microglia cells, upon activation, are known to undergo cellular proliferation and differentiation, characterized by morphological alterations that result in the cell changing from a ramified morphology to a more rounded morphology (Aloisi, 2001; Davis, Foster, & Thomas, 1994; Garden & Moller, 2006; Hanisch & Kettenmann, 2007; Vilhardt, 2005). Since miRNAs are negative regulators of gene expression and miR-146a has been previously implicated in dampening the innate immune response, then it is possible that one of the roles of miR-146a during prion infection may be to restrain the activation of microglia in response to the chronic accumulation of PrP^{Sc}. Possibly, in an effort to curb an unrestrained immune response by the cell. An *in vivo* unrestrained microglial immune response to the accumulating PrP^{Sc} may damage neighboring neuronal cells and lead to an exacerbation of the disease. MiR-146a may mediate this restrain by negatively regulating the most basic response mechanism of a microglial cell to a pathogen, the cellular transformation process from an inactive state with the latter state being the catalyst for generating an immune response (Aloisi, 2001; Davis et al., 1994; Garden & Moller, 2006; Hanisch & Kettenmann, 2007; Vilhardt, 2005)

3.3.4 Identifying candidate miR-146a direct targets

The key to understanding the role of miR-146a in prion-induced microglial immune activation lies in the proficient identification of target genes directly under its regulation. To discriminate between direct and indirect miR-146a targets among proteins found to be downregulated in miR-146a overexpressing microglia cells, the miRNA Target Filter application in IPA was employed. IPA's microRNA Target Filter and analytics enable bench scientists to use biological annotation in combination with experimental data to identify high priority mRNA targets, and rapidly refine an initial large list of targets to a set of biologically compelling, high quality microRNA and mRNA worthy of further investigation. It incorporates experimentally demonstrated and predicted microRNA-mRNA interactions from the databases TarBase, miRecords, and TargetScan, as well as from peer-reviewed microRNA original research articles as the content base for the microRNA Target Filter. IPA's ability to prioritize microRNA and mRNA hits based on biological context is key to overcoming the inherent complexity in microRNA data analysis and allows for a focused data analysis. In total, IPA recognized 650 genes as being potential targets of miR-146a. When the miR-146a target filter was applied to the experimentally determined miR-146a regulated proteins, 4 proteins were identified as being candidate direct miR-146a targets. They were: ARF6, RhoA, FAF2 and ZDHHC13 (**Figure 3.31)**. While it is clear from the literature that both ARF6 and RhoA play important biological roles in immune activation of microglia especially with regard to phagocytic capabilities, there is no role ascribed to FAF2 and ZDHHC13 in the activation state of microglia (Aflaki et al., 2011; Balana et al., 2005; Fan et al., 2011; J.

G. Kim et al., 2012; Tzircotis, Braga, & Caron, 2011; Van Acker et al., 2014; Q. Zhang, Cox, Tseng, Donaldson, & Greenberg, 1998)

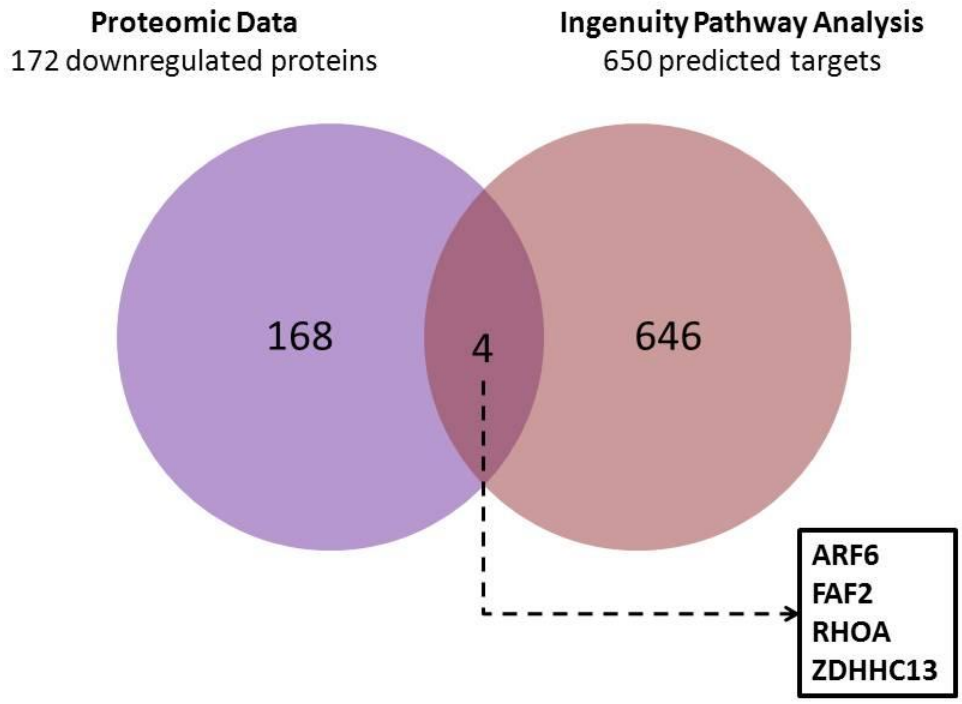

Figure 3.31 Identification of candidate direct miR-146a targets. Venn diagram to show the intersection of experimentally determined miR-146a regulated proteins and those predicted by IPA software. Candidate direct miR-146a targets are presented in the box.

3.4 MiR-146a target gene validation

Using an integrative approach that utilized proteomic data and IPA software, 4 candidate direct miR-146a targets were identified. Of the four, 2 were further investigated. They were; ARF6 and RhoA, molecules that play important roles in microglial phagocytosis. NOS2 was also investigated as it is induced by activation of TLR receptors and is involved in the oxidative burst, important during phagocytosis. Although it could not be detected at the proteomic level, its regulation by miR-146a has been shown at the genomic level in microglia cells treated in a similar fashion to this proteomic study (Saba et al., 2012). In addition, NOS2 is one of the 650 predicted miR-146a targets identified in IPA.

3.4.1 Luciferase assay analysis

Luciferase reporter assays were used to experimentally validate if these genes were indeed miR-146a targets. Briefly, the 3'UTR's were cloned into the dual luciferase reporter vector and co-transfected into primary mouse hippocampal neurons with increasing concentrations of pre-miR-146a or scrambled negative control. Luciferase activity was then measured and normalized to that of *Renilla*. When the vector is transfected into cells expressing the targeting miRNA, luciferase activity should be lower than luciferase activity in cells expressing the scrambled negative control if direct miRNA:mRNA binding is occurring. Transfection of the ARF6 and RhoA constructs resulted in no significant difference in luciferase activity between transfection with pre-miR-146a and the negative control **(Figure 3.32 and 3.33)**. However, miR-146a was shown to significantly repress the reporter plasmid containing NOS2 **(Figure 3.34)**.

Interestingly, it appeared to be more effective between 10 nM and 50 nM of exogenous miRNA tested. Nonetheless, NOS2 was further validated at the proteomic level.

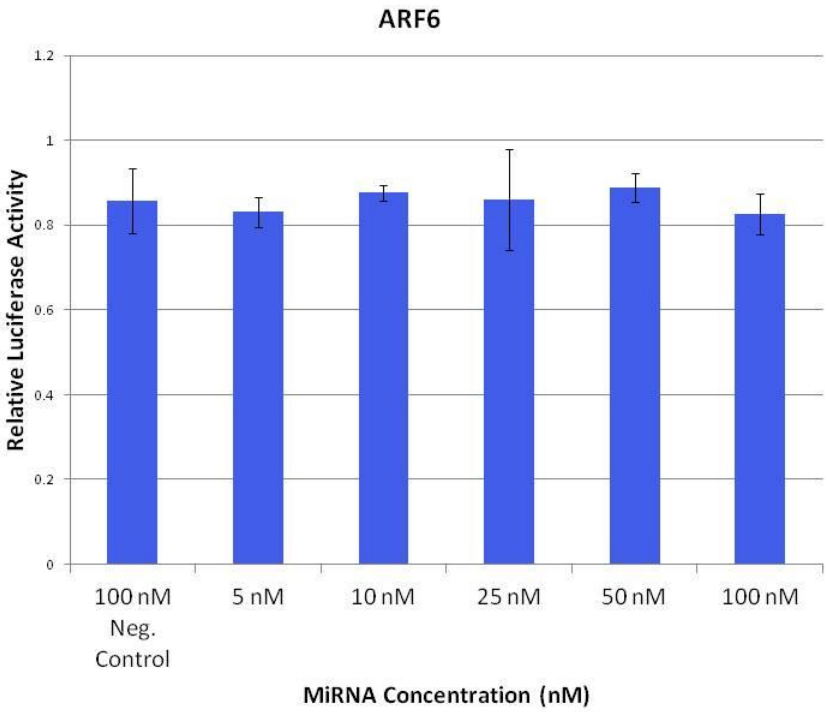

Figure 3.32 MiR-146a target gene validation of ARF6 using luciferase reporter gene assay. Primary mouse hippocampal neurons were co-transfected with concentrations of pre-miR-146a or scrambled negative control as indicated above and 200 ng of the ARF6 3'UTR dual luciferase reporter construct. After 24 hours incubation, luciferase activity was measured and normalised to that of *Renilla* activity. The average relative luciferase activity ± SD were measured from triplicate experiments.

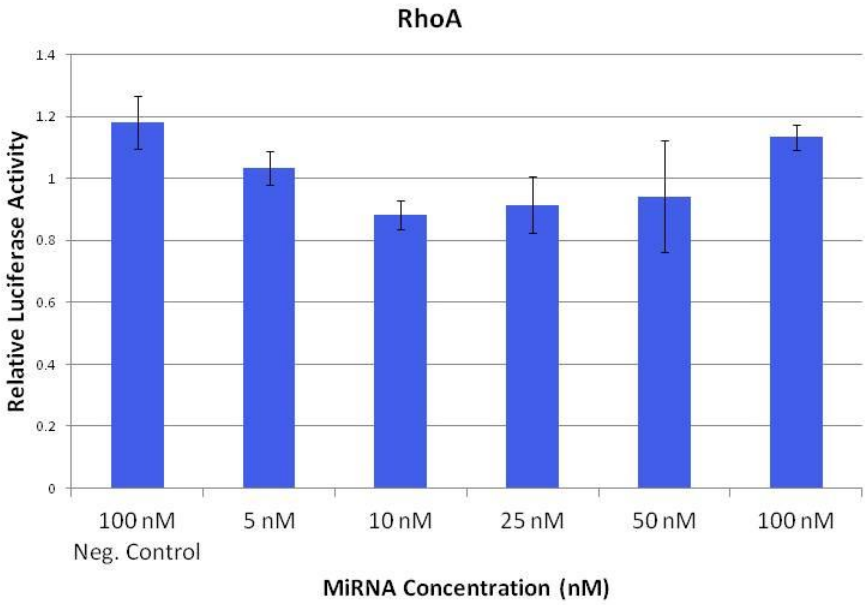

Figure 3.33 MiR-146a target gene validation of RhoA using luciferase reporter gene assay. Primary mouse hippocampal neurons were co-transfected with concentrations of pre-miR-146a or scrambled negative control as indicated above and 200 ng of the RhoA 3'UTR dual luciferase reporter construct. After 24 hours incubation, luciferase activity was measured and normalised to that of *Renilla* activity. The average relative luciferase activity ± SD were measured from triplicate experiments.

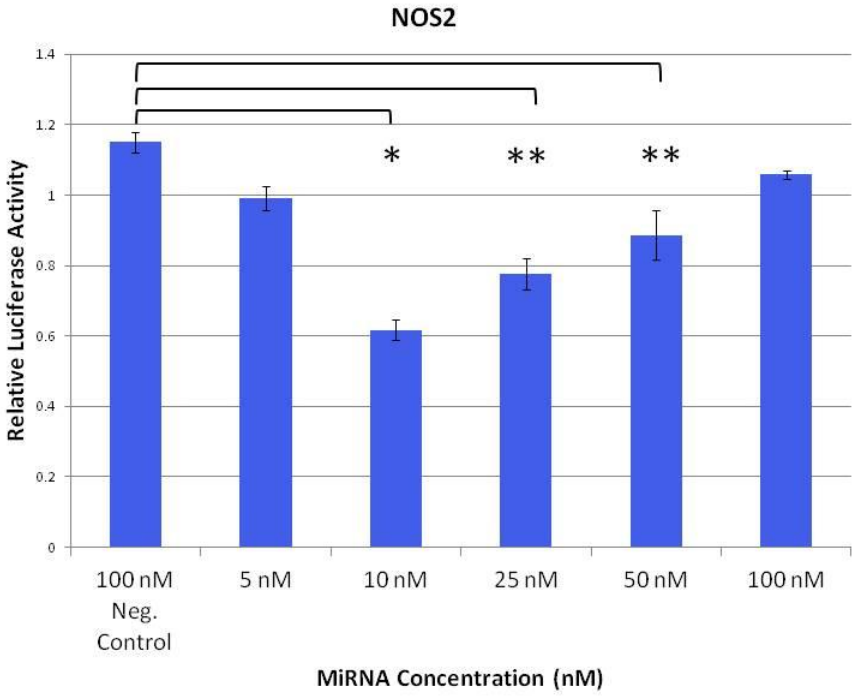

Figure 3.34 MiR-146a target gene validation of NOS2 using luciferase reporter gene assay. Primary mouse hippocampal neurons were co-transfected with concentrations of pre-miR-146a or scrambled negative control as indicated above and 200 ng of the NOS2 3'UTR dual luciferase reporter construct. After 24 hours incubation, luciferase activity was measured and normalised to that of *Renilla* activity. The average relative luciferase activity ± SD were measured from triplicate experiments; significance * $p < 0.001$, ** $p < 0.01$.

3.4.2 Western blot analysis

To further validate the finding that miR-146a targets the 3'UTR of NOS2, protein expression levels of NOS2 were analysed by western blot. BV2 cells overexpressing miR-146a and treated with the TLR2 agonist HKLM resulted in approximately a 50% decrease in NOS2 protein expression when compared to negative control cells (scrambled sequence followed by treatment with HKLM)**(Figure 3.35)**. In addition, upon knockout of miR-146a and treatment with HKLM, NOS2 levels slightly increased in relation to negative control cells. Based on the inverse relationship between miR-146a expression and NOS2 protein expression and the results of the luciferase assay, NOS2 appears to be a direct miR-146a target.

A

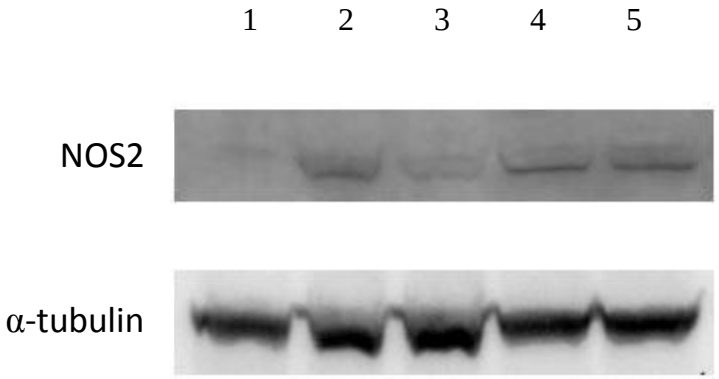

B

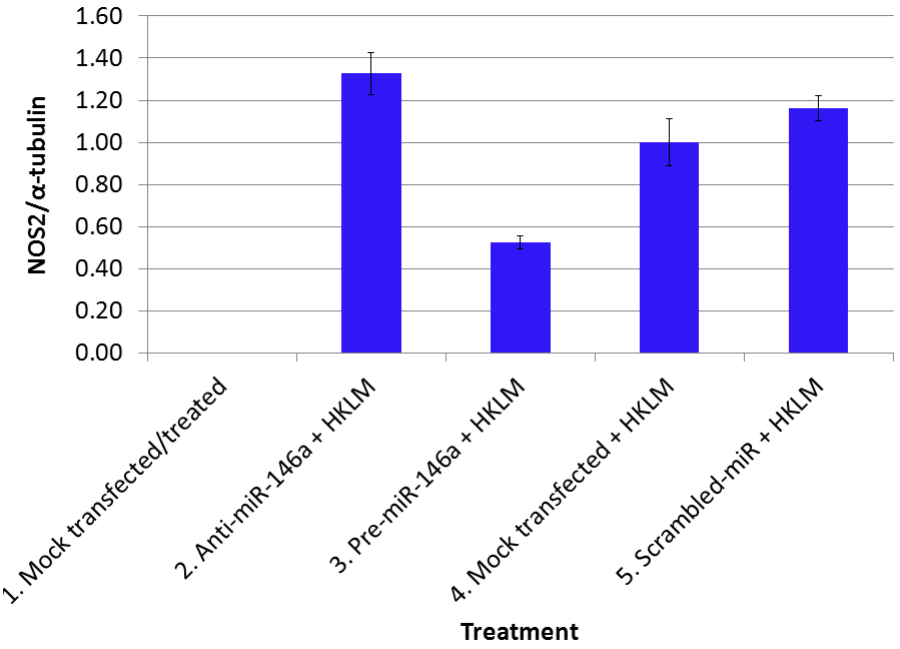

Figure 3.35 MiR-146a target gene validation of NOS2 using western blot analysis. **A.** BV2 cells were transfected with 30nM of pre-miR-146a, 30nM of scrambled-miR or 50nM anti-miR-146a and 8 hours later stimulated with the TLR2 agonist HKLM. At 24 hours post stimulation, protein was extracted and a western blot was performed. Lanes 1-

5 represent sample treatment indicated in part B. **B.** Densitometric analysis of immunoblot band intensities was performed and NOS2 was normalized to α-tubulin. Values represent the average of three independent experiments and standard deviation is shown.

4. Discussion

4.1 De-regulation of miRNA expression during microglial activation

A distinctive pathological feature of prion pathogenesis is microglial activation, which in some instances precedes other signs of neurodegeneration such a spongiosis and neuronal cell death (Giese et al., 1998). Microglial activation in the CNS is the major driving force of the neuroinflammatory response and the process of wound healing. While it may be useful to determine all those genes that are potentially involved in microglial activation, it is especially important to identify the key regulators of these processes and pathways. These may include transcription factors, regulatory kinases and miRNAs, a potent new class of regulatory molecules. Analysis of the miRNA profile in activated macrophages has been extensively studied. However, significantly less attention has been paid to that of microglia. Therefore, the primary aim of this study was to examine miRNAs expressed in microglia cells that contribute to immune function in the brain. The second objective was to identify those miRNAs implicated in the inflammatory response initiated during the prion disease process.

First, highly expressed miRNAs were determined in two microglial cell lines. Using extremely stringent criteria which included Ct values between 20 and 32 in all replicates and treatment groups, 119 and 56 miRNAs were scored as present in the EOC 13.31 and BV2 cells, respectively (Table 3.1 and 3.2). These results correspond well with a recent study that confirmed the consistent expression of 74 miRNAs in human primary macrophages using two miRNA microarray techniques (Luers, Loudig, & Berman, 2010). Of the 74 miRNAs detected in the primary macrophages, 58 were also found to be expressed in the EOC 13.31 cells and 41 in the BV2 cells. While there seems to be general consensus in the miRNAs expressed, microglial cells indeed differentiate from

peripheral macrophages in several ways. For example, it was found that activated microglia produce a lower level of superoxide dismutase (SOD) and a very low level of NO during neuroinflammation when compared with peripheral macrophages (Enose et al., 2005; Ponomarev, Maresz, Tan, & Dittel, 2007). Furthermore, in the CNS of mice with experimental autoimmune encephalitis (EAE), activated microglia were found to express lower levels of the markers CD45, MHC class II, CD40, CD86, and CD11c compared to peripheral macrophages (Ponomarev, Novikova, Maresz, Shriver, & Dittel, 2005; Ponomarev, Shriver, & Dittel, 2006). These observations lead to the conclusion that while macrophages and microglia may behave qualitatively the same, they differ quantitatively, due in part to the expression of specific miRNAs. Expression of one such miRNA is the CNS specific miR-124 which is expressed in EAE activated microglia but absent or expressed at low levels in peripheral macrophages (Ponomarev, Veremeyko, Barteneva, Krichevsky, & Weiner, 2011). MiR-124 functions to maintain the quiescent state of microglia and promote differentiation under physiological conditions in the CNS microenvironment through targeting of the transcription factor CEBPα and the cyclins CDK4 and CDK6 (Ponomarev et al., 2011). Notably, miR-124 was not included in this study as it failed to meet the stringent cutoff criteria. Perhaps loosening the criteria would have resulted in the inclusion of this important miRNA and others that may be important to the innate immune functioning of microglia. This also illustrates the fact that the absence of a particular miRNA in this study does not mean it is biologically irrelevant.

Activation of macrophages have long been known to be induced by microbial stimuli alone, leading to TLR signaling, or in combination with the Th1cytokine IFN-γ and several studies have indicated that TLR signals can modulate miRNA expression by

various techniques such as microarray and deep sequencing (Y. Zhang et al., 2013). Although miRNA expression after TLR stimulation have been found to be relatively subtle, a subset of strong miRNA targets of TLR signaling has emerged, especially miR-146a, miR-155 and miR-21. All three miRNAs have been shown to be potent regulators of the innate immune response but function in a slightly different way. While, in general, miR-146a and miR-21 appear to negatively regulate inflammation, miR-155 serves to enhance this response (Androulidaki et al., 2009; Nahid, Satoh, & Chan, 2011; O'Connell, Taganov, Boldin, Cheng, & Baltimore, 2007; O'Connell, Chaudhuri, Rao, & Baltimore, 2009; Sheedy et al., 2010; Taganov et al., 2006). Similar to other TLR-induced genes, this miRNA subset can be further classified as early or late response miRNAs, according to the response speed following TLR ligand stimulation (O'Neill, Sheedy, & McCoy, 2011). Specifically, miR-146a and miR-155 are highly induced within 2 hours after TLR treatment, and thus belong to the early response miRNAs; however, miR-21 belongs to the late response miRNAs (Nahid et al., 2011; Sheedy et al., 2010; Taganov et al., 2006). Similar expression dynamics of these miRNAs were observed in this study whereby microglia cells were activated using the TLR4 agonist, LPS, in conjunction with IFN-γ, and the TLR2 agonist, HKLM, alone. High-throughput miRNA microarray analysis of microglia cells activated upon application of the agonists mentioned above relative to those in a resting phenotype, revealed prominent and persistent upregulation of miR-146a and miR-155 as early as 6 hours and across all timepoints, while miR-21 was found only to be induced at 24 hours post stimulation. While analysis of the expression of key miRNAs in microglia cells in an activated state closely resembled that of activated macrophages described in the literature, there exists

subtle nuances in miRNA expression profiles stratified by the TLR ligand used, stimulation time, and specific cell types and lines.

Interestingly, the first TLR-induced miRNA expression profiling was performed in human macrophages treated with LPS (Taganov et al., 2006). In this seminal research, miR-146a, miR-155 and miR-132 were found to be upregulated. Similarly, when treated with LPS and IFN-γ, there was marked upregulation of miR-146a and miR-155 in both cell lines employed in this study. MiR-132 was also persistently upregulated in response to treatment with LPS and IFN-γ; however, this was only observed in the BV2 cells. Furthemore, upregulation of miR-9 and miR-210 were only observed in the EOC 13.31 cells when treated in this manner and not the BV2 cells. Both miR-9 and miR-210 have been found to be induced in response to LPS in macrophages and negatively regulate the innate immune response by direct targeting of NF-κB (Bazzoni et al., 2009; Qi et al., 2012). Although the EOC 13.31 and BV2 cells are both mouse microglial cells and generally correspond in function and response to immune stimuli, their independant method of derivation likely contribute to the observed discrepancies. BV2 cells are derived from microglia immortalized after infection with a v-raf/v-myc recombinant retrovirus whereas EOC 13.31 cells are spontaneously immortalized (Stansley, Post, & Hensley, 2012). Moreover, contrary to the BV2 cells, the mice from which the EOC 13.31 cells originate, lack TLR4 signalling making them hyporesponsive to LPS (Walker et al., 1995). This provides a likely explanation as to why the upregulation of miR-146a and miR-155 were more pronounced using this method of activation in the BV2 cells compared to the EOC 13.31 cells.

With regard to treatment of cells with LPS and IFN-γ, there is also the notion of downregulated miRNAs. While little is known about how TLR signals decrease miRNA expression, lines of evidence suggest it occurs through transcriptional repression or post-transcriptional destabilization of miRNA (O'Neill et al., 2011). Notably, fewer significantly downregulated miRNAs were detected in both cell lines activated in this manner compared to those resting. To establish profound downregulation of miRNAs, longer timepoints may need to be explored. However, downregulation of miR-125b and miR-98 at 6 hours in the BV2 cells were observed. Both miRNAs have been found to be decreased in macrophages treated with LPS. Reduced expression of miR-125b has been associated with enhanced immune responses while reduced expression of miR-98 has been associated with enhanced levels of the anti-inflammatory cytokine IL-10, closely involved in endotoxin tolerance (Y. Liu et al., 2011; Tili et al., 2007).

The second method of microglial activation in this study employed the TLR2 agonist HKLM given that this TLR was reported to be significantly upregulated in mouse brain tissue during prion infection (Saba et al., 2012). Interestingly, this resulted in upregulation of miR-28 at 8 and 12 hours but not at 24 hours. A recent study profiling miRNA expression in macrophages infected with the intracellular parasite *Leishmania* also found this miRNA to be upregulated at early timepoints but not at later timepoints (Lemaire et al., 2013). While the entry mechanism of *Leishmania* is not fully elucidated, several TLRs including TLR2 have been implicated (Lemaire et al., 2013). Furthermore, little information is available regarding the function of this particular miRNA, especially as it relates to the immune activities of microglia. Several other miRNAs were also induced in response to TLR2 signaling, but similar to microglial activation via LPS and

IFN-γ, the most apparent and persistent were observed in expression of miR-146a and miR-155.

Taken together, although significant perturbations to the miRNA profile were observed in microglia cells in response to inflammatory challenge, the main finding affirmed that both miR-146a and miR-155 play integral roles in the proper functioning of these highly plastic cells of the CNS. Specifically, they appear to serve as key regulators of the activation state and inflammatory response to pathogens and/or tissue insult. Recently, the Booth Lab confirmed miR-146a, and to a lesser extent miR-155, to be upregulated in the brains of prion infected mice (Saba et al., 2008; Saba et al., 2012). MiR-146a has also been implicated in several other protein misfolding disorders such as AD and ALS. Given its relevance to neurodegenerative diseases as a whole and the immunomodulatrory role ascribed in macrophages, upregulation of miR-146a within the context of prion disease warranted further investigation.

4.2 MiR-146a induction in microglia

Very little is known about the molecular pathways triggered during prion-induced neurodegeneration leading to damage and the ultimate death of neurons. What is known, is that miR-146a is significantly upregulated in the brains of mice during scrapie infection and its expression appears to be enriched in cells of microglial origin (Saba et al., 2008; Saba et al., 2012). Moreover, miR-146a has been associated with regulating the activation state and immune response of microglia, a distinct pathological feature of prion disease. At present, it is somewhat controversial whether the prolonged activation of microglial cells in the brain is beneficial or harmful in the overall pathobiology of the disease as sustained secretion of inflammatory and immunomodulatory mediators can be detrimental and lead to the subsequent damage of neighboring cells including neurons (D. R. Brown, Schmidt, & Kretzschmar, 1996; Castelnau, Campbell, & Powell, 1997; Fabrizi et al., 2001; Liberski, Yanagihara, Nerurkar, & Gajdusek, 1994; Muhleisen, Gehrmann, & Meyermann, 1995). Therefore, determining the mechanism of miR-146a induction in microglia is a priority as it may potentially lead to the development of treatments for this invariably fatal disorder.

Given that microglial activation is apparent well before halfway through the incubation period no clinical symptoms are evident, and neuronal cell death is not significant, it would appear that it is not triggered as a response to dead or dying cells. Rather, activation may reflect a response to the prion agent directly or other cells in response to prion replication in the brain. As a synthetic analog of PrP^{Sc} exists and has been cited in the literature as having identical weight and amino acid structure, and similar biochemical properties to that of the infectious form, it was decided to examine

whether treatment with this recombinant protein was enough induce expression of miR-146a in microglia. However, stimulation with varying concentrations of the PrP^{Sc} mimic resulted in little to no activation of this miRNA. There are several possible explanations. Perhaps the PrP mimic was not in the appropriate disease specific conformational or aggregational state necessary to bind microglial receptors. Secondly, microglia may require a signal other than misfolded PrP for activation in the brain such as a secondary trigger released by another cell type. Lastly, despite a number of publications suggesting BV2 cells are a sufficient substitute to primary microglia, it's possible they may not behave in the same manner (Henn et al., 2009; Hickman, Allison, & El Khoury, 2008).

There is evidence of the involvement of TLRs in the regulation of the microglial response in prion disease. For example, mice defective in TLR4 signaling, making them hyporesponsive to LPS, exhibit an accelerated rate of prion disease (Spinner et al., 2008). This implies a protective role for TLR stimulation of microglia during disease. In AD, a pathology in which an oligomeric form of beta amyloid (Aβ) builds up in a similar fashion to PrP^{Sc} in prion disease, phagocytosis of Aβ by activated microglia is significantly increased in the presence of ligands that activate TLRs (K. Chen et al., 2006; Iribarren et al., 2005; Kakimura et al., 2002). Landreth and Reed-Geagham (2009) have also shown that the response of microglia to fibrillar Aβ is reliant upon the expression of TLR4, TLR2 and the co-receptor CD14 to activate intracellular signaling (Landreth & Reed-Geaghan, 2009). Cells lacking these receptors could not initiate a Src-Vav-Rac signaling cascade required to stimulate phagoctyosis of Aβ (Landreth & Reed-Geaghan, 2009). Interestingly, TLRs have also been associated with miR-146a expression. Taganov and colleagues were the first to report significant upregulation of

miR-146a upon stimulation of TLRs 1, 2, 4 and 5 (Taganov et al., 2006). Several other studies have corroborated this finding (Brudecki, Ferguson, McCall, & El Gazzar, 2013; Nahid et al., 2011; M. M. Perry et al., 2008a; Quinn, Wang, O'Callaghan, & Redmond, 2013; Schnitger et al., 2011). In this study, microglia treated with the agonists known to activate these receptors did indeed induce miR-146a expression. Notably, only TLR2 and TLR4 have been found to be increased in prion diseased brains suggesting that potentially one or both of these molecules are responsible for the over-expression of miR-146a during prion pathogenesis (Saba et al., 2012).

TLR4 stimulation of the BV2 cells resulted in the activation and transcription of miR-146a, as did stimulation with the TLR2 agonist, HKLM. Agonist treatment uniformly resulted in the induction of miR-146a expression that increased over time to a maximum at 48 hours post-stimulation, but still elevated even at 72 hours post stimulation in both instances. This observation was in contrast to the generally rapid induction of cytokine expression following LPS treatment. Expression of cytokines IL6, GM-CSF and TNF-α were found to peak well before 24 hours post-stimulation and had all returned to basal levels by 48 hours (Saba et al., 2012). Our data suggest that induction of miR-146a may be secondary to the initial response triggered by the TLR agonist. This has been previously described in macrophages where miR-146a expression was found to be capable of dampening the immediate innate immune response mediated by TLR2 and TLR4 (Nahid et al., 2011; M. M. Perry, Moschos, Williams, Shepherd, Larner-Svensson, & Lindsay, 2008b; Taganov et al., 2006). Recently, the contribution of miR-146a to the establishment of a macrophage state primed in some way for response to repeated

exposure to immune activators has also been suggested (Nahid et al., 2011). A similar role in microglia is likely.

In conclusion, while miR-146a was not induced by treatment with a PrP-mimic in microglia, activation of TLR1, 2, 4, and 5 resulted in its over-expression similar to what has been previously observed in macrophages. Furthermore, in contrast to the rapid and transient induction of transcription of inflammatory mediators, miR-146a follows alternate kinetics functioning to prolong dampening of the innate immune response following activation via TLR4 and TLR2.

4.3 Identification of miR-146a targets

There is substantial evidence linking the development of disease with the conformational conversion of PrP^{C} into the infectious form, PrP^{Sc}. In contrast, there is a dearth of knowledge regarding the molecular pathways triggered by these agents that lead to the damage, and ultimate death of neurons. While the molecular events leading to prion induced neurodegeneration are poorly characterized, efforts have been made to identify genes involved in the disease process. In an early study by Xiang *et al.* (2004), differential expression of genes encoding proteins involved in proteolysis, protease inhibition, cell growth and maintenance, the immune response, signal transduction, cell adhesion and molecular metabolism were reported (Xiang et al., 2004). The differential expression in this study was related temporally to both the accumulation of PrP^{Sc} and the activation of glial cells (Xiang et al., 2004). Evaluation of prion infected whole brains by Brown *et al.* (2004) showed differential expression of a limited number of genes but, nevertheless, their work pointed towards the involvement of primarily glial-associated genes in the disease process (A. R. Brown, Webb, Rebus, Williams, & Fazakerley, 2004). Indeed, when gene expression profiles were performed specifically on microglia cells during prion disease, differential expression of approximately 30 genes, with 6 genes being specific to microglia, were reported (Baker & Manuelidis, 2003). Subsets of the genes identified were found to be involved in inflammation, cytoskeleton organization and signal transduction (Baker & Manuelidis, 2003). The significant upregulation of miR-146a during prion disease and its role in the regulation of the immune activities of microglia, make it possible to ascribe some of these alterations in gene expression to the post-

transcriptional silencing roles played by this particular miRNA. Hence, with this goal in mind, a search for target genes of miR-146a was initiated. Since proteins are the major executors of life processes, it was decided to test the use of a global quantitative proteomic approach.

The experimental approach used to identify miR-146a target genes first involved perturbing the abundance of miR-146a in microglial cells. Experimentally, miRNA abundance is typically perturbed by employing either miRNA overexpression strategies or knockdown strategies. Indeed, transfection of microglia with pre-miR-146a (miR-146a mimics) and anti-miR-146a (miR-146a inhibitors) resulted in significant up- and down-regulation of this miRNA, respectively (Figure 3.13). However, unlike the knockout strategy which ultimately depends on pre-existing abundance of this miRNA, over-expression allowed for a greater manipulation of the cellular miR-146a content. For this reason, it was decided to measure the effect of an overexpressed miRNA on the proteome to uncover its potential targets. One consideration, however, is the potential for bias and off target effects caused by supraphysiological levels of miRNA content. To ameliorate this tendency, only 30nM of pre-miR were employed in these studies. Nevertheless, one of the first published reports using quantitative proteomics to identify miRNA targets employed this very strategy. Overexpression of miR-1 resulted in repression of 12 proteins, from a set of 504 detected proteins, in HeLa cells (Vinther, Hedegaard, Gardner, Andersen, & Arctander, 2006). This repressed set of genes significantly overlapped with miR-1 regulated genes that had been identified previously (Vinther et al., 2006). Moreover, they found that the 3'UTR for the repressed set were enriched in miR-1

complementary sites (Vinther et al., 2006). Overexpression continues to be the most common method of miRNA manipulation.

It was hypothesized that the majority of miR-146a targets, important to the microglial immune response, would likely only be evident during conditions in which cells were stimulated by a ligand. In addition, it was thought that induction of miR-146a by overexpression followed by treatment with a TLR2 agonist would lead to a more robust detection of potential miR-146a targets. To determine if this model was capable of downregulating immune effectors at the protein level, production of the cytokine IL6 was evaluated. IL6 production has been shown to be attenuated by miR-146a through direct targeting of IRAK1, TRAF6 and to a lesser extent, NOTCH1 (He et al., 2014; Taganov et al., 2006). In our study, production of this cytokine was significantly reduced upon overexpression of miR-146a within an inflammatory milieu versus cells transfected with a negative control confirming the validity of the model in identifying miR-146a regulated genes.

Using a functional proteomic approach, a total of 172 proteins were identified as being regulated by miR-146a. This may very well be the first study to employ tandem mass tags (TMT) for quantitative proteomic analysis with the aim of identifying miRNA targets. A few other studies have previously tried to use proteomics to identify the effects of miRNAs. Notably, stable isotope labelling by amino acids in cell culture (SILAC) technology allowed for the first large scale, high-throughput miRNA target verification studies. In fact, Vinther *et al*. (2006) was the very first to use SILAC to study the effect of miR-21on the proteome in HeLa cells (Vinther et al., 2006). Subsequently, SILAC was applied to capture the effects of miR-124, miR-1

and miR-181 in HeLa cells and miR-223 in knock-out mice neutrophils (Baek et al., 2008). MiR-29a targets were also recently identified by SILAC technology (Bargaje et al., 2012). Pulsed SILAC was used to study the effect of miR-1, miR-155, miR-16, miR-30a and let-7b in HeLa cells (Selbach et al., 2008). The effect of miR-21 and miR-143 was also studied by miRNA-proteomics using isobaric tags for relative and absolute quantification (iTRAQ) and SILAC, respectively (Yang, Chaerkady, Beer, Mendell, & Pandey, 2009; Yang et al., 2010). In contrast to iTRAQ and TMT labeling, as employed in this study, where protein extraction occurs prior to labeling, SILAC is characterized by the isotopic labeling of proteins *in vivo*. To date, there is little information available regarding which method is a more powerful or effective quantitative proteomic tool. Selected reason monitoring (SRM), a mass spectrometry based method, has also been used to validate computationally predicted targets in C. Elegans. Each of the previous reports independently concluded that while proteomic technology enables the assaying of the ultimate phenotypic effect of a given miRNA, the effects of miRNAs on the proteome are mild both in terms of differentially expressed proteins and fold changes in target expression. Furthermore, since many miRNAs show only 30-60% reduction of target expression in reporter-UTR assays, prevalent thresholds (like fold change greater than 2) in proteomic and genomic studies are not suitable for miRNA-proteomic studies. For example, two studies noted that few proteins change by more than 2 fold, while there are hardly any proteins changing by greater than 4 fold (Baek et al., 2008; Selbach et al., 2008). The results of this study correspond with this phenomenom resulting in much looser inclusion criteria compared to those routinely employed in comparative transcriptomic profiling

studies. Therefore, the major limitation of comparative proteomics remains the inability to reliably detect modest effects. This finding also implies that miRNAs fine tune gene expression rather than induce dramatic changes.

Microglial activation has been recognised for quite some time encompassing morphological changes, proliferation, chemotaxis and the production of numerous cytokines and chemokines involved in inflammatory and immunomodulatory responses. Interestingly, gene ontology assignments and network analysis performed on the 172 experimentally determined miR-146a regulated genes suggested an over-representation of genes that are involved in cell dynamics such as cell differentiation and proliferation, cell growth and morphology, and cellular movement. Conceivably, many of these functions can have profound consequences on the ability of microglial cells to become activated and to produce an immune response to prion infection. As a result, it is possible that one of the roles for miR-146a induction in micorglial cells during the course of prion disease may be to repress some of the aforementioned functions, in effect diminishing the overall degree of activation of microglial cells. Activation of these cells has been said to act as a double edged sword. While initially serving to protect and defend CNS homeostasis, chronic activation can actually exacerbate the disease process through the release of cytotoxic mediators such as free radicals, proteinases, cytokines, and NO having damaging effects on neighboring cells such as neurons (Muhleisen et al., 1995). Therefore, the upregulation of miR-146a during prion disease may actually function to subdue microglial activation and circumvent bystander damage that would inevitable develop by prolonged activation of microglia. Interestingly, the role of miR-146a as a negative regulator of cellular

events such as cell differentiation, cell morphology and cell movement has been previously demonstrated in various cancers such as gastric, pancreatic, breast and prostate cancer whereby tumor suppressor activity has been postulated (Bhaumik et al., 2008; Hurst et al., 2009; Kogo et al., 2011; Kuang et al., 2009; Lin et al., 2008; Mei et al., 2011). For example, Bhaumik *et al* (2008) found that in a highly metastatic breast cancer cell line, miR-146a functioned as a downstream mediator of metastasis suppression by direct targeting of epidermal growth factor receptor and inhibition of invasion and migration (Bhaumik et al., 2008). Similar results were also observed by Lin and colleagues (2008) who showed that expression of miR-146a resulted in reduced proliferation by direct targeting of ROCK1 (Lin et al., 2008). Additionally, Kuang *et al* (2009) reported an inhibitory role for miR-146a in the differentiation of a myoblast cell line to muscle cells upon silencing of the NOTCH signaling molecule NUMB (Kuang et al., 2009).

One clear limitation inherent to quantitative proteomics, is the inability to distinguish between direct and indirect targets. With this in mind, the proteomic list was filtered to include only those predicted to be direct miR-146a targets by IPA analysis. This list reduced considerably and identified 4 potential direct targets: ARF6, RhoA, FAF2 and ZDHHC13. However, it is imperative to recognize key candidate genes from this list for further experimental validation. Therefore, given that ARF6 and RhoA play important roles in microglial phagocytosis and have been shown previously to be miR-146a regulated at the genomic level when treated in a similar fashion, they were selected for further experimental validation (Saba et al., 2012). Notably absent from the proteomic dataset was expression of NOS2 whose

regulation by miR-146a has been shown at the genomic level in addition to the bioinformatic level. This is likely due to the limitation of quantitative proteomics in identifying low abundance proteins. Nevertheless, NOS2, an important component of the oxidative burst in microglia, was also selected for further validation.

The data in this work suggests a model whereby miR-146a induction in microglia during prion disease may play a central role in the attempt of the host to halt the ensuing pathobiology. The induction of miR-146a appears to regulate genes that play important roles in determining the degree of activation of microglia. Moreover, the potential direct targets identified in this study suggest miR-146a is capable of altering the phagocytic potential of microglia important in clearance of toxic protein inclusions.

4.4 Validation of direct miR-146a targets

Identifying direct targets of a particular miRNA is essential to uncovering its biological function. It becomes especially important when a particular miRNA has been found to be deregulated in a diseased state as in the case of miR-146a in prion disease and other neurodegenerative disorders. MiR-146a has been shown to be involved in innate immunity, the inflammatory response, development of cancer, and antiviral pathways. Although miR-146a is clearly an important miRNA, only a handful of targets have been identified thus far.

From these studies, three putative direct miR-146a targets in microglia were identified as being worthy of further investigation. ARF6 was selected as it has been found to affect endocytosis, phagocytosis, receptor recycling and the formation of actin-rich protrusions and ruffles (D'Souza-Schorey, Li, Colombo, & Stahl, 1995; D'Souza-Schorey et al., 1998; Galas et al., 1997; Radhakrishna & Donaldson, 1997) . One particular study showed that activation of ARF6 enhances pathogen constituent uptake (CpG ODN) in macrophages (Q. Zhang et al., 1998). Conversely, ARF6 inactivation resulted in impaired microbial uptake (Q. Zhang et al., 1998). A study by Balana and colleagues (2005) actually showed that ARF6 controls uptake and invasion of Chlamydia through extensive actin reorganization (Balana et al., 2005). Furthermore, ARF6 is reportedly a requirement for Fc-γ receptor-mediated phagocytosis and is an important mediator of cytoskeletal alterations after Fc-γ activation (Wu & Kuo, 2012). Therefore, miR-146a mediated downregulation of ARF6 could lead to impaired phagocytosis, which has been identified as a prominent clearing mechanism of PrP^{Sc} by activated microglia (Beringue et al., 2000; Luhr et al., 2004; McHattie et al., 1999).

The second molecule investigated, RhoA, is also central to the phagocytic potential of microglia and has been associated with regulating several aspects of cell physiology including morphology, rearrangement of cytoskeletal proteins, and migration. RhoA has been well studied in the regulation of stress fiber formation and focal adhesion (Van Aelst & D'Souza-Schorey, 1997). One particular study found RhoA to be essential for CR3-mediated phagocytosis in macrophages (Caron & Hall, 1998). Another study showed that β2-interin is engaged in binding of microglia cells to Aβ peptide and that inhibition of RhoA enhanced binding to Aβ peptide thereby promoting phagocytosis (Jeon et al., 2008). Regulation of superoxide production by RhoA was shown in a study by Kim et al. (2004) to be associated with macrophage engulfment of IgG-opsonized zymosan and serum-opsonized zymosan particles (J. S. Kim et al., 2004). Superoxide regulation by RhoA has also been observed in microglia in response to Aβ peptide through an unknown mechanism. The involvement of miRNAs in regulating this process cannot be ruled out.

Despite the fact that miR-146a regulation of ARF6 and RhoA would tie in nicely with the overall role of this miRNA in altering microglial functionality, it appears neither are direct miR-146a targets. A common tool used to affirm direct mRNA targeting is by employing luciferase assays. Briefly, cells are co-transfected with the reporter plasmid containing the 3'UTR of the candidate mRNA target and the miRNA. The binding, or lack of binding, of the miRNA to the cloned construct should either repress or have no significant effect on the expression of the upstream reporter luciferase gene, respectively. Luciferase analysis of ARF6 and RhoA resulted in no changes in luciferase activity. Therefore, it was concluded that both molecules are likely indirect miR-146a targets. It

would be interesting to determine which upstream molecules are being targeted by miR-146a, ultimately resulting in reduced ARF6 and RhoA expression.

The third protein evaluated for miR-146a targeting was NOS2. NOS2 is released by activated microglia and play a crucial role in mediating the interactions between microglia and other cells present in the nervous system, as it is known to regulate inflammation, immune functions, blood vessel dilation, neurotransmission and neural cell survival (Bruhwyler, Chleide, Liegeois, & Carreer, 1993; Nathan, 1992). On one hand, NOS2 production can be viewed as cytoprotective and neuroprotective, but on the other, it can also be cytotoxic, particularly at high levels, as shown with oligodendricytes in culture and studies of direct effects on blood brain barrier permeability (Cho & Gauld, 2005; C. A. Colton, 1995; Merrill, Ignarro, Sherman, Melinek, & Lane, 1993; Thiel & Audus, 2001). NOS2 induction can also inhibit neuronal respiration, causing depolarization, glutamate release from neurons and astrocytes, and inhibition of cytochrome oxidase, eventually leading to excitotoxicity (Bal-Price & Brown, 2001; G. C. Brown, 2007; C. Colton & Wilcock, 2010). In recent years, much attention has been focused on the role played by NOS2 in the establishment and/ or prevention of brain damage. Not surprising, microglia-produced NOS2 have been suggested to mediate neuronal cell death in various neurodegenerative disorders. For example, in various PD-like insults, NOS2 is firmly implicated in the progression of neuropathology (Broom et al., 2011). Expression of NOS2 has also been reported in prion infected brains and the authors suggest it play a role in the neurodegenerative process of disease (Ju et al., 1998). Interestingly, luciferase analysis and western blot confirmed that NOS2 was in fact a direct target of miR-146a. Western blot also served to confirm the low abundance of this

particular protein as an excessive amount of protein, 70ug, was loaded for detection. This was in agreement with the comparative proteomics section of the study where expression of NOS2 was below the threshold level of detection. Therefore, upregulation of miR-146a during prion disease may in fact be providing protection from potentially harmful immune mediators as these results show direct targeting of miR-146a to one such molecule, NOS2.

Microglia are particularly sensitive to even subtle disturbances in CNS homeostasis and initiate an innate immune response when threatened by pathogens or exposure to toxins. Microglia alter from a resting state to an activated one triggering the expression pro-inflammatory mediators such as NOS2. Prolonged expression of these factors results in severe cerebral inflammation and can lead to acute neuronal death. A powerful way to restore normal tissue homeostasis after injury or foreign insult and to control the "killing" phase of the innate immune response induced by activated microglia, is to change the activation state by switching from a pro-inflammatory gene profile to one that supports repair and tissue reconstruction. Indeed, in prion disease, an anti-inflammatory profile has been observed and molecules such as TGF-β, prostaglandin E_2 and IL-10 have often been shown to suppress pro-inflammatory mediators, thus protecting neurons from bystander damage (Cunningham et al., 2003; V. H. Perry et al., 2002). It is clear that the balance between pro- and anti- inflammatory mediators in the CNS is under tight regulation. The lack of appropriate regulation during prion disease may have the potential to accelerate the appearance of pathological conditions and symptoms. Based on the results of this study, it appears that miR-146a functions to fine tune the immune response during prion pathogenesis by regulating genes that play

important roles in determining the activation state and phagocytic potential of microglia. Moreover, it was found that miR-146a directly targets NOS2, a potentially neurotoxic mediator, thereby protecting neighboring cells from the ensuing pathobiology that would inevitably occur upon sustained expression of this molecule.

5. Future Directions

Although this study provided some key insight into the role of miR-146a in microglia during a prion-induced immune response, there is still much to uncover. Determining the exact sphere of influence miR-146a has on gene networks and on microglial functionality may be essential to the development of potential therapies.

It is known that miR-146a is upregulated in various prion disease models. For example, increased expression of miR-146a has been observed in the brain tissue of humans with sCJD and GSS and in mice infected with various strains of mouse-adapted scrapie and BSE (Lukiw, Dua, Pogue, Eicken, & Hill, 2011; Saba et al., 2008). A study by Montag *et al.* (2009) also found that macaques infected with BSE resulted in increased expression of this particular miRNA (Montag et al., 2009). Since CWD is epidemic is deer populations in North America and there is the concern of transmissibility to humans, it would be worth noting if miR-146a expression is also induced in this model of prion disease.

Interestingly, expression of miR-146a may be a feature of other neurodegenerative diseases as it has been found to be upregulated in human Alzheimer diseased brains and stressed primary culture mixture of neuronal and microglial cells (Lukiw, Zhao, & Cui, 2008). Therefore, in order to make such a broad claim, it is imperative to investigate the expression of miR-146a in other models of neurodegeneration such as PD, HD, ALS, HIV-associated dementia, and herpes simplex virus encephalitis, where microglia activation may exacerbate the disease process.

Given that TLR2 induces miR-146a expression and is extremely abundant and highly upregulated upon prion infection, we hypothesize that signaling through this TLR

play a role in disease. MyD88 is the main adaptor protein implicated in TLR signaling and is considered essential for the induction of inflammatory cytokines triggered by most TLRs, including TLR2. Nevertheless, the study determined by Prinz *et al*. (2003) showed that MyD88 knock-out mice were readily infectable with scrapie and did not show any significant alteration in the time-course or pathology of the disease (Prinz et al., 2003). This data implies that TLR2-signaling is not essential to the disease process and that our model may not mimic processes that occur during disease. However, effector molecules downstream of multiple cell surface receptors, including TLR2 (and TLR4) signals, are similar and the action of miR-146a to modulate the innate immune response and microglial activation in these model systems is likely to be indicative, despite the original upstream signal. In addition, recent studies have shown that TLR2 stimulation is indeed capable of eliciting a MyD88- and TRIF-independent inflammatory cytokine response (Takeda & Akira, 2004). Some evidence also exists suggesting that this response is independent of phagocytic clearance pathways that appear to be MyD88 dependent (Henneke et al., 2002). Interestingly, in a mouse model of Alzheimer's disease, MyD88 deficient and APP over-expressing mice had an accelerated disease process pointing to a role for MyD88 in clearance of amyloid (Michaud, Richard, & Rivest, 2011). It has also been reported by others that TLR 2, 4, and 9 signaling modulates phagocytosis and clearance of neurotoxic amyloid deposition in neurodegenerative diseases, perhaps by MyD88 independent signaling pathways (Iribarren et al., 2005; Tahara et al., 2006). Those genes that are involved in phagocytosis and morphological changes that are altered in response to miR-146a over-expression may therefore be important to these processes. Studies also link a reduction in TLR2 expression with an increase in phagocytosis,

implying an inverse relation between TLR2 expression and phagocytic activity. In terms of prion disease this suggests the considerable increase in expression of TLR2 observed at clinical stages of prion disease could be indicative of the accumulation of microglia that are not in an activation state that is optimal for phagocytosis. This could therefore contribute to defective clearing of debris and prion accumulation during later stages of disease. Investigation into whether TLR2 signaling is indeed important in prion disease pathology, and the identification of signaling pathways important in microglial activation independent of MyD88, warrants further investigation.

One of the more interesting findings upon the identification of miR-146a regulated targets in microglia cells was the over-representation of genes involved in cell differentiation and proliferation, cell growth and morphology, and cellular movement. It is conceivable, that in prion disease, the down-regulation of this subset of genes may lead to a less aggressive microglial phenotype. In prion disease, an activated phenotype may exacerbate the prion disease process by damaging neighboring cells through release of pro-inflammatory mediators. Therefore, next steps could include high-throughput profiling of the cytokine repertoire of microglial cells over-expressing miR-146a to observe if there is a reduction in cytokine output.

Activated microglia undergo numerous morphological alterations as they change from ramified cells to amoeboid cells; the latter form of cells possessing the ability to migrate to a site of infection and to initiate an immune response. As an area of future study, it would be interesting to perform migration assays on miR-146a over-expressing microglia to demonstrate if there is an effect on the ability of these cells to migrate. Another worthy assay would be a phagocytosis assay. Of the genes found to be miR-146a

regulated, there was significant enrichment for those capable of altering the phagocytic capacity of microglia.

6. Limitations

It was decided to use an *in vitro* model for these studies for ease of culturing, time and cost effectiveness, and because many microglial cell lines were readily available. However, *in vivo* modeling would have been more biologically relevant. Some argue that the results obtained from *in vitro* work are merely speculative and cannot be used to draw any concrete conclusions. In their natural setting, microglia associate with and respond to other cells and biological factors within the brain. This is certainly lacking in *in vitro* systems. Perhaps using a mixed culture would help strengthen *in vitro* results obtained from microglia cells in the event that *in vivo* work is not a possibility.

Another limitation of this research is that immortalized cell lines, and not primary cells, were employed. In this study, cells were manipulated in some fashion or another to ensure constant growth and proliferation which bring into question how similarly they behave to primary cells isolated directly from fresh brain tissue. However, there are numerous publications supporting the use of the cell line employed in this study, BV2 cells, for the analysis of neurodegenerative diseases and as a suitable substitute for primary cells.

The last major limitation of this particular study was the fact that very subtle proteomic changes in response to miRNA overexpression or knock-down were observed. The changes observed made it difficult to reach significance with regard to miR-146a regulated proteins. This is a general limitation of the use of a quantitative proteomic approach to detect modulations in target protein levels and has been described by others concomitantly with the progress of this study. The lack of sensitivity of comparative proteomic approaches due to limitations in the current methodologies also means that many putative miRNA targets are not even detectable. Therefore, at present, proteomic

data alone is not enough to identify miRNA targets and it is imperative to employ other complimentary approaches in the area of miRNA target identification. Perhaps with time, proteomic technologies will evolve in sensitivity and have the ability to readily detect low abundance proteins. The current state of proteomics is simply not there yet and caution should be exercised when considering its use for miRNA target research.

7. Summary and Significance

Innate immune regulating miRNAs have been extensively studied in macrophages. However, markedly less attention has been paid to those expressed in microglia, probably due to technical challenges in isolating primary microglia and limited cell culture models. This study confirmed that the miRNA profile in a microglial cell line activated by TLR stimulation, is indeed similar to that of macrophages. The consistent and dramatic expression of miR-146a by TLR4 and TLR2 stimulation was also noted, confirming a central role in innate immunity. This provided initial support for the study hypothesis that miR-146a is capable of regulating microglial functionality during the chronic immune response that is apparent in the brain during prion disease.

Significantly, this may be the first study to develop an *in vitro* model and employ quantitative proteomics with the aim of identifying miR-146a regulated proteins in microglia cells. Additionally, it was found that of the 172 miR-146a regulated proteins identified, there was an over-representation of proteins involved in important cellular functions pertaining to the phagocytic, migratory and proliferative capabilities of microglia cells, having direct implications on the activation state of these highly plastic cells. Furthermore, recognizing that proteomics alone would not be sufficient to discriminate direct from indirect miR-146a targets, an integrative approach was employed. Bioinformatic and genomic data complemented the proteomic data in this study resulting in the successful identification of NOS2 as a true miR-146a direct target. Interestingly, inhibition of this neuroinflammatory signal has been shown to delay the progress of neurodegeneration, positioning the upregulation of miR-146a during prion disease as a benefit to the host.

Taken together, these results progress the current state of miR-146a knowledge and confirm that, indeed, miR-146a is capable of altering microglial functionality during prion disease by specifically dampening the innate immune response. Therefore, manipulation of its control over the immune pathways involved in prion disease and other neurodegenerative processes as a whole may be an avenue to design new therapeutics.

8. References

Abid, K., & Soto, C. (2006). The intriguing prion disorders. *Cellular and Molecular Life Sciences : CMLS, 63*(19-20), 2342-2351. doi:10.1007/s00018-006-6140-5

Aflaki, E., Balenga, N. A., Luschnig-Schratl, P., Wolinski, H., Povoden, S., Chandak, P. G., . . . Kratky, D. (2011). Impaired rho GTPase activation abrogates cell polarization and migration in macrophages with defective lipolysis. *Cellular and Molecular Life Sciences : CMLS, 68*(23), 3933-3947. doi:10.1007/s00018-011-0688-4; 10.1007/s00018-011-0688-4

Aloisi, F. (2001). Immune function of microglia. *Glia, 36*(2), 165-179.

Androulidaki, A., Iliopoulos, D., Arranz, A., Doxaki, C., Schworer, S., Zacharioudaki, V., . . . Tsatsanis, C. (2009). The kinase Akt1 controls macrophage response to lipopolysaccharide by regulating microRNAs. *Immunity, 31*(2), 220-231. doi:10.1016/j.immuni.2009.06.024; 10.1016/j.immuni.2009.06.024

Baek, D., Villen, J., Shin, C., Camargo, F. D., Gygi, S. P., & Bartel, D. P. (2008). The impact of microRNAs on protein output. *Nature, 455*(7209), 64-71. doi:10.1038/nature07242; 10.1038/nature07242

Bailly, Y., Haeberle, A. M., Blanquet-Grossard, F., Chasserot-Golaz, S., Grant, N., Schulze, T., . . . Lemaire-Vieille, C. (2004). Prion protein (PrPc) immunocytochemistry and expression of the green fluorescent protein reporter gene under control of the bovine PrP gene promoter in the mouse brain. *The Journal of Comparative Neurology, 473*(2), 244-269. doi:10.1002/cne.20117

Baker, C. A., & Manuelidis, L. (2003). Unique inflammatory RNA profiles of microglia in creutzfeldt-jakob disease. *Proceedings of the National Academy of Sciences of the United States of America, 100*(2), 675-679. doi:10.1073/pnas.0237313100

Balana, M. E., Niedergang, F., Subtil, A., Alcover, A., Chavrier, P., & Dautry-Varsat, A. (2005). ARF6 GTPase controls bacterial invasion by actin remodelling. *Journal of Cell Science, 118*(Pt 10), 2201-2210. doi:10.1242/jcs.02351

Bal-Price, A., & Brown, G. C. (2001). Inflammatory neurodegeneration mediated by nitric oxide from activated glia-inhibiting neuronal respiration, causing glutamate release and excitotoxicity. *The Journal of Neuroscience : The Official Journal of the Society for Neuroscience, 21*(17), 6480-6491.

Bargaje, R., Gupta, S., Sarkeshik, A., Park, R., Xu, T., Sarkar, M., . . . Pillai, B. (2012). Identification of novel targets for miR-29a using miRNA proteomics. *PloS One, 7*(8), e43243. doi:10.1371/journal.pone.0043243; 10.1371/journal.pone.0043243

Bartel, D. P. (2004). MicroRNAs: Genomics, biogenesis, mechanism, and function. *Cell, 116*(2), 281-297.

Basyuk, E., Suavet, F., Doglio, A., Bordonne, R., & Bertrand, E. (2003). Human let-7 stem-loop precursors harbor features of RNase III cleavage products. *Nucleic Acids Research, 31*(22), 6593-6597.

Bazzoni, F., Rossato, M., Fabbri, M., Gaudiosi, D., Mirolo, M., Mori, L., . . . Locati, M. (2009). Induction and regulatory function of miR-9 in human monocytes and neutrophils exposed to proinflammatory signals. *Proceedings of the National*

Academy of Sciences of the United States of America, 106(13), 5282-5287. doi:10.1073/pnas.0810909106; 10.1073/pnas.0810909106

Belay, E. D., Maddox, R. A., Williams, E. S., Miller, M. W., Gambetti, P., & Schonberger, L. B. (2004). Chronic wasting disease and potential transmission to humans. *Emerging Infectious Diseases, 10*(6), 977-984. doi:10.3201/eid0905.020577

Beringue, V., Demoy, M., Lasmezas, C. I., Gouritin, B., Weingarten, C., Deslys, J. P., . . . Dormont, D. (2000). Role of spleen macrophages in the clearance of scrapie agent early in pathogenesis. *The Journal of Pathology, 190*(4), 495-502. doi:2-T

Bernstein, E., Kim, S. Y., Carmell, M. A., Murchison, E. P., Alcorn, H., Li, M. Z., . . . Hannon, G. J. (2003). Dicer is essential for mouse development. *Nature Genetics, 35*(3), 215-217. doi:10.1038/ng1253

Bhaumik, D., Scott, G. K., Schokrpur, S., Patil, C. K., Campisi, J., & Benz, C. C. (2008). Expression of microRNA-146 suppresses NF-kappaB activity with reduction of metastatic potential in breast cancer cells. *Oncogene, 27*(42), 5643-5647. doi:10.1038/onc.2008.171; 10.1038/onc.2008.171

Brandner, S., Isenmann, S., Raeber, A., Fischer, M., Sailer, A., Kobayashi, Y., . . . Aguzzi, A. (1996). Normal host prion protein necessary for scrapie-induced neurotoxicity. *Nature, 379*(6563), 339-343. doi:10.1038/379339a0

Broom, L., Marinova-Mutafchieva, L., Sadeghian, M., Davis, J. B., Medhurst, A. D., & Dexter, D. T. (2011). Neuroprotection by the selective iNOS inhibitor GW274150 in

a model of parkinson disease. *Free Radical Biology & Medicine, 50*(5), 633-640. doi:10.1016/j.freeradbiomed.2010.12.026; 10.1016/j.freeradbiomed.2010.12.026

Brown, A. R., Webb, J., Rebus, S., Williams, A., & Fazakerley, J. K. (2004). Identification of up-regulated genes by array analysis in scrapie-infected mouse brains. *Neuropathology and Applied Neurobiology, 30*(5), 555-567. doi:10.1111/j.1365-2990.2004.00565.x

Brown, D. R. (2001). Microglia and prion disease. *Microscopy Research and Technique, 54*(2), 71-80. doi:10.1002/jemt.1122

Brown, D. R. (2002). Copper and prion diseases. *Biochemical Society Transactions, 30*(4), 742-745. doi:10.1042/

Brown, D. R., Schmidt, B., & Kretzschmar, H. A. (1996). Role of microglia and host prion protein in neurotoxicity of a prion protein fragment. *Nature, 380*(6572), 345-347. doi:10.1038/380345a0

Brown, G. C. (2007). Mechanisms of inflammatory neurodegeneration: iNOS and NADPH oxidase. *Biochemical Society Transactions, 35*(Pt 5), 1119-1121. doi:10.1042/BST0351119

Brudecki, L., Ferguson, D. A., McCall, C. E., & El Gazzar, M. (2013). MicroRNA-146a and RBM4 form a negative feed-forward loop that disrupts cytokine mRNA translation following TLR4 responses in human THP-1 monocytes. *Immunology and Cell Biology, 91*(8), 532-540. doi:10.1038/icb.2013.37; 10.1038/icb.2013.37

Bruhwyler, J., Chleide, E., Liegeois, J. F., & Carreer, F. (1993). Nitric oxide: A new messenger in the brain. *Neuroscience and Biobehavioral Reviews, 17*(4), 373-384.

Bueler, H., Fischer, M., Lang, Y., Bluethmann, H., Lipp, H. P., DeArmond, S. J., . . . Weissmann, C. (1992). Normal development and behaviour of mice lacking the neuronal cell-surface PrP protein. *Nature, 356*(6370), 577-582. doi:10.1038/356577a0

Cai, X., Hagedorn, C. H., & Cullen, B. R. (2004). Human microRNAs are processed from capped, polyadenylated transcripts that can also function as mRNAs. *RNA (New York, N.Y.), 10*(12), 1957-1966. doi:10.1261/rna.7135204

Canadian Blood Services. (2005). vCJD travel deferral. Retrieved April 15, 2014, from http://www.blood.ca/centreapps/internet/uw_v502_mainengine.nsf/page/vCJD%20An%20Introduction

Canadian Food Inspection Agency of Canada. (2012). Chronic wasting disease (CWD) - fact sheet. Retrieved April 15, 2014, from http://www.inspection.gc.ca/animals/terrestrial-animals/diseases/reportable/cwd/fact-sheet/eng/1330189947852/1330190096558

Capellari, S., Cardone, F., Notari, S., Schinina, M. E., Maras, B., Sita, D., . . . Parchi, P. (2005). Creutzfeldt-jakob disease associated with the R208H mutation in the prion protein gene. *Neurology, 64*(5), 905-907. doi:10.1212/01.WNL.0000152837.82388.DE

Caron, E., & Hall, A. (1998). Identification of two distinct mechanisms of phagocytosis controlled by different rho GTPases. *Science (New York, N.Y.), 282*(5394), 1717-1721.

Cashman, N. R., Loertscher, R., Nalbantoglu, J., Shaw, I., Kascsak, R. J., Bolton, D. C., & Bendheim, P. E. (1990). Cellular isoform of the scrapie agent protein participates in lymphocyte activation. *Cell, 61*(1), 185-192.

Castelnau, P. A., Campbell, I. L., & Powell, H. C. (1997). Prion protein (PrP) is not involved in the pathogenesis of spongiform encephalopathy in transgenic mice expressing interleukin-6 in the brain. *Neuroscience Letters, 234*(1), 15-18.

Caughey, B. (2003). Prion protein conversions: Insight into mechanisms, TSE transmission barriers and strains. *British Medical Bulletin, 66*, 109-120.

Chen, C. Z., Li, L., Lodish, H. F., & Bartel, D. P. (2004). MicroRNAs modulate hematopoietic lineage differentiation. *Science (New York, N.Y.), 303*(5654), 83-86. doi:10.1126/science.1091903

Chen, K., Iribarren, P., Hu, J., Chen, J., Gong, W., Cho, E. H., . . . Wang, J. M. (2006). Activation of toll-like receptor 2 on microglia promotes cell uptake of alzheimer disease-associated amyloid beta peptide. *The Journal of Biological Chemistry, 281*(6), 3651-3659. doi:10.1074/jbc.M508125200

Chiarini, L. B., Freitas, A. R., Zanata, S. M., Brentani, R. R., Martins, V. R., & Linden, R. (2002). Cellular prion protein transduces neuroprotective signals. *The EMBO Journal, 21*(13), 3317-3326. doi:10.1093/emboj/cdf324

Cho, K. B., & Gauld, J. W. (2005). Second half-reaction of nitric oxide synthase: Computational insights into the initial step and key proposed intermediate. *The Journal of Physical Chemistry.B, 109*(49), 23706-23714. doi:10.1021/jp054864o

Cohen, F. E., & Prusiner, S. B. (1998). Pathologic conformations of prion proteins. *Annual Review of Biochemistry, 67*, 793-819. doi:10.1146/annurev.biochem.67.1.793

Colton, C., & Wilcock, D. M. (2010). Assessing activation states in microglia. *CNS & Neurological Disorders Drug Targets, 9*(2), 174-191.

Colton, C. A. (1995). Induction of nitric oxide in cultured microglia: Evidence for a cytoprotective role. *Advances in Neuroimmunology, 5*(4), 491-503.

Coutinho, A., & Meo, T. (1978). Genetic basis for unresponsiveness to lipopolysaccharide in C57BL/10Cr mice. *Immunogenetics, 7*(1), 17-24. doi:10.1007/BF01843983; 10.1007/BF01843983

Cunningham, C., Campion, S., Lunnon, K., Murray, C. L., Woods, J. F., Deacon, R. M., . . . Perry, V. H. (2009). Systemic inflammation induces acute behavioral and cognitive changes and accelerates neurodegenerative disease. *Biological Psychiatry, 65*(4), 304-312. doi:10.1016/j.biopsych.2008.07.024; 10.1016/j.biopsych.2008.07.024

Cunningham, C., Deacon, R., Wells, H., Boche, D., Waters, S., Diniz, C. P., . . . Perry, V. H. (2003). Synaptic changes characterize early behavioural signs in the ME7 model of murine prion disease. *The European Journal of Neuroscience, 17*(10), 2147-2155.

Curtale, G., Citarella, F., Carissimi, C., Goldoni, M., Carucci, N., Fulci, V., . . . Macino, G. (2010). An emerging player in the adaptive immune response: microRNA-146a is a modulator of IL-2 expression and activation-induced cell death in T lymphocytes. *Blood, 115*(2), 265-273. doi:10.1182/blood-2009-06-225987; 10.1182/blood-2009-06-225987

Davis, E. J., Foster, T. D., & Thomas, W. E. (1994). Cellular forms and functions of brain microglia. *Brain Research Bulletin, 34*(1), 73-78.

Deleault, N. R., Harris, B. T., Rees, J. R., & Supattapone, S. (2007). Formation of native prions from minimal components in vitro. *Proceedings of the National Academy of Sciences of the United States of America, 104*(23), 9741-9746. doi:10.1073/pnas.0702662104

Doench, J. G., Petersen, C. P., & Sharp, P. A. (2003). siRNAs can function as miRNAs. *Genes & Development, 17*(4), 438-442. doi:10.1101/gad.1064703

D'Souza-Schorey, C., Li, G., Colombo, M. I., & Stahl, P. D. (1995). A regulatory role for ARF6 in receptor-mediated endocytosis. *Science (New York, N.Y.), 267*(5201), 1175-1178.

D'Souza-Schorey, C., van Donselaar, E., Hsu, V. W., Yang, C., Stahl, P. D., & Peters, P. J. (1998). ARF6 targets recycling vesicles to the plasma membrane: Insights from an ultrastructural investigation. *The Journal of Cell Biology, 140*(3), 603-616.

Duffy, P., Wolf, J., Collins, G., DeVoe, A. G., Streeten, B., & Cowen, D. (1974). Letter: Possible person-to-person transmission of creutzfeldt-jakob disease. *The New England Journal of Medicine, 290*(12), 692-693.

El-Agnaf, O. M., Jakes, R., Curran, M. D., Middleton, D., Ingenito, R., Bianchi, E., . . . Wallace, A. (1998). Aggregates from mutant and wild-type alpha-synuclein proteins and NAC peptide induce apoptotic cell death in human neuroblastoma cells by formation of beta-sheet and amyloid-like filaments. *FEBS Letters, 440*(1-2), 71-75.

Enose, Y., Destache, C. J., Mack, A. L., Anderson, J. R., Ullrich, F., Ciborowski, P. S., & Gendelman, H. E. (2005). Proteomic fingerprints distinguish microglia, bone marrow, and spleen macrophage populations. *Glia, 51*(3), 161-172. doi:10.1002/glia.20193

Fabrizi, C., Silei, V., Menegazzi, M., Salmona, M., Bugiani, O., Tagliavini, F., . . . Lauro, G. M. (2001). The stimulation of inducible nitric-oxide synthase by the prion protein fragment 106--126 in human microglia is tumor necrosis factor-alpha-dependent and involves p38 mitogen-activated protein kinase. *The Journal of Biological Chemistry, 276*(28), 25692-25696. doi:10.1074/jbc.M100133200

Fadok, V. A., McDonald, P. P., Bratton, D. L., & Henson, P. M. (1998). Regulation of macrophage cytokine production by phagocytosis of apoptotic and post-apoptotic cells. *Biochemical Society Transactions, 26*(4), 653-656.

Fan, H., Hall, P., Santos, L. L., Gregory, J. L., Fingerle-Rowson, G., Bucala, R., . . . Hickey, M. J. (2011). Macrophage migration inhibitory factor and CD74 regulate macrophage chemotactic responses via MAPK and rho GTPase. *Journal of*

Immunology (Baltimore, Md.: 1950), 186(8), 4915-4924. doi:10.4049/jimmunol.1003713; 10.4049/jimmunol.1003713

Fischer, M., Rulicke, T., Raeber, A., Sailer, A., Moser, M., Oesch, B., . . . Weissmann, C. (1996). Prion protein (PrP) with amino-proximal deletions restoring susceptibility of PrP knockout mice to scrapie. *The EMBO Journal, 15*(6), 1255-1264.

Ford, M. J., Burton, L. J., Morris, R. J., & Hall, S. M. (2002). Selective expression of prion protein in peripheral tissues of the adult mouse. *Neuroscience, 113*(1), 177-192.

Forloni, G., Angeretti, N., Chiesa, R., Monzani, E., Salmona, M., Bugiani, O., & Tagliavini, F. (1993). Neurotoxicity of a prion protein fragment. *Nature, 362*(6420), 543-546. doi:10.1038/362543a0

Galas, M. C., Helms, J. B., Vitale, N., Thierse, D., Aunis, D., & Bader, M. F. (1997). Regulated exocytosis in chromaffin cells. A potential role for a secretory granule-associated ARF6 protein. *The Journal of Biological Chemistry, 272*(5), 2788-2793.

Garden, G. A., & Moller, T. (2006). Microglia biology in health and disease. *Journal of Neuroimmune Pharmacology : The Official Journal of the Society on NeuroImmune Pharmacology, 1*(2), 127-137. doi:10.1007/s11481-006-9015-5

Ghoshal, A., Das, S., Ghosh, S., Mishra, M. K., Sharma, V., Koli, P., . . . Basu, A. (2007). Proinflammatory mediators released by activated microglia induces neuronal death in japanese encephalitis. *Glia, 55*(5), 483-496. doi:10.1002/glia.20474

Giese, A., Brown, D. R., Groschup, M. H., Feldmann, C., Haist, I., & Kretzschmar, H. A. (1998). Role of microglia in neuronal cell death in prion disease. *Brain Pathology (Zurich, Switzerland), 8*(3), 449-457.

Goldfarb, L. G., Petersen, R. B., Tabaton, M., Brown, P., LeBlanc, A. C., Montagna, P., . . . Pendelbury, W. W. (1992). Fatal familial insomnia and familial creutzfeldt-jakob disease: Disease phenotype determined by a DNA polymorphism. *Science (New York, N.Y.), 258*(5083), 806-808.

Grimson, A., Farh, K. K., Johnston, W. K., Garrett-Engele, P., Lim, L. P., & Bartel, D. P. (2007). MicroRNA targeting specificity in mammals: Determinants beyond seed pairing. *Molecular Cell, 27*(1), 91-105. doi:10.1016/j.molcel.2007.06.017

Hanisch, U. K., & Kettenmann, H. (2007). Microglia: Active sensor and versatile effector cells in the normal and pathologic brain. *Nature Neuroscience, 10*(11), 1387-1394. doi:10.1038/nn1997

Harris, D. A., Huber, M. T., van Dijken, P., Shyng, S. L., Chait, B. T., & Wang, R. (1993). Processing of a cellular prion protein: Identification of N- and C-terminal cleavage sites. *Biochemistry, 32*(4), 1009-1016.

He, Y., Sun, X., Huang, C., Long, X. R., Lin, X., Zhang, L., . . . Li, J. (2014). MiR-146a regulates IL-6 production in lipopolysaccharide-induced RAW264.7 macrophage cells by inhibiting Notch1. *Inflammation, 37*(1), 71-82. doi:10.1007/s10753-013-9713-0; 10.1007/s10753-013-9713-0

Henn, A., Lund, S., Hedtjarn, M., Schrattenholz, A., Porzgen, P., & Leist, M. (2009). The suitability of BV2 cells as alternative model system for primary microglia cultures or for animal experiments examining brain inflammation. *Altex, 26*(2), 83-94.

Henneke, P., Takeuchi, O., Malley, R., Lien, E., Ingalls, R. R., Freeman, M. W., . . . Golenbock, D. T. (2002). Cellular activation, phagocytosis, and bactericidal activity against group B streptococcus involve parallel myeloid differentiation factor 88-dependent and independent signaling pathways. *Journal of Immunology (Baltimore, Md.: 1950), 169*(7), 3970-3977.

Hickman, S. E., Allison, E. K., & El Khoury, J. (2008). Microglial dysfunction and defective beta-amyloid clearance pathways in aging alzheimer's disease mice. *The Journal of Neuroscience : The Official Journal of the Society for Neuroscience, 28*(33), 8354-8360. doi:10.1523/JNEUROSCI.0616-08.2008; 10.1523/JNEUROSCI.0616-08.2008

Horie, T., Ono, K., Nishi, H., Nagao, K., Kinoshita, M., Watanabe, S., . . . Kimura, T. (2010). Acute doxorubicin cardiotoxicity is associated with miR-146a-induced inhibition of the neuregulin-ErbB pathway. *Cardiovascular Research, 87*(4), 656-664. doi:10.1093/cvr/cvq148; 10.1093/cvr/cvq148

Hurst, D. R., Edmonds, M. D., Scott, G. K., Benz, C. C., Vaidya, K. S., & Welch, D. R. (2009). Breast cancer metastasis suppressor 1 up-regulates miR-146, which suppresses breast cancer metastasis. *Cancer Research, 69*(4), 1279-1283. doi:10.1158/0008-5472.CAN-08-3559; 10.1158/0008-5472.CAN-08-3559

Iribarren, P., Chen, K., Hu, J., Gong, W., Cho, E. H., Lockett, S., . . . Wang, J. M. (2005). CpG-containing oligodeoxynucleotide promotes microglial cell uptake of amyloid beta 1-42 peptide by up-regulating the expression of the G-protein- coupled receptor mFPR2. *FASEB Journal : Official Publication of the Federation of American Societies for Experimental Biology*, *19*(14), 2032-2034. doi:10.1096/fj.05-4578fje

Ishibashi, D., Atarashi, R., & Nishida, N. (2012). Protective role of MyD88-independent innate immune responses against prion infection. *Prion, 6*(5), 443-446. doi:10.4161/pri.22579; 10.4161/pri.22579

Jarrett, J. T., & Lansbury, P. T.,Jr. (1993). Seeding "one-dimensional crystallization" of amyloid: A pathogenic mechanism in alzheimer's disease and scrapie? *Cell, 73*(6), 1055-1058.

Jeon, Y. J., Won, H. Y., Moon, M. Y., Choi, W. H., Chang, C. H., Lee, J. Y., . . . Park, J. B. (2008). Interaction of microglia and amyloid-beta through beta2-integrin is regulated by RhoA. *Neuroreport*, *19*(17), 1661-1665. doi:10.1097/WNR.0b013e3283140f10; 10.1097/WNR.0b013e3283140f10

Johnson, R., Zuccato, C., Belyaev, N. D., Guest, D. J., Cattaneo, E., & Buckley, N. J. (2008). A microRNA-based gene dysregulation pathway in huntington's disease. *Neurobiology of Disease, 29*(3), 438-445. doi:10.1016/j.nbd.2007.11.001

Johnson, R. T. (2005). Prion diseases. *Lancet Neurology, 4*(10), 635-642. doi:10.1016/S1474-4422(05)70192-7

Johnson, S. M., Lin, S. Y., & Slack, F. J. (2003). The time of appearance of the C. elegans let-7 microRNA is transcriptionally controlled utilizing a temporal regulatory element in its promoter. *Developmental Biology, 259*(2), 364-379.

Johnston, R. J., & Hobert, O. (2003). A microRNA controlling left/right neuronal asymmetry in caenorhabditis elegans. *Nature, 426*(6968), 845-849. doi:10.1038/nature02255

Ju, W. K., Park, K. J., Choi, E. K., Kim, J., Carp, R. I., Wisniewski, H. M., & Kim, Y. S. (1998). Expression of inducible nitric oxide synthase in the brains of scrapie-infected mice. *Journal of Neurovirology*, *4*(4), 445-450.

Kakimura, J., Kitamura, Y., Takata, K., Umeki, M., Suzuki, S., Shibagaki, K., . . . Shimohama, S. (2002). Microglial activation and amyloid-beta clearance induced by exogenous heat-shock proteins. *FASEB Journal : Official Publication of the Federation of American Societies for Experimental Biology, 16*(6), 601-603.

Kazlauskaite, J., Young, A., Gardner, C. E., Macpherson, J. V., Venien-Bryan, C., & Pinheiro, T. J. (2005). An unusual soluble beta-turn-rich conformation of prion is involved in fibril formation and toxic to neuronal cells. *Biochemical and Biophysical Research Communications, 328*(1), 292-305. doi:10.1016/j.bbrc.2004.12.172

Kertesz, M., Iovino, N., Unnerstall, U., Gaul, U., & Segal, E. (2007). The role of site accessibility in microRNA target recognition. *Nature Genetics, 39*(10), 1278-1284. doi:10.1038/ng2135

Khalili-Shirazi, A., Kaisar, M., Mallinson, G., Jones, S., Bhelt, D., Fraser, C., . . . Collinge, J. (2007). Beta-PrP form of human prion protein stimulates production of monoclonal antibodies to epitope 91-110 that recognise native PrPSc. *Biochimica Et Biophysica Acta, 1774*(11), 1438-1450. doi:10.1016/j.bbapap.2007.08.028

Khalili-Shirazi, A., Quaratino, S., Londei, M., Summers, L., Tayebi, M., Clarke, A. R., . . . Collinge, J. (2005). Protein conformation significantly influences immune responses to prion protein. *Journal of Immunology (Baltimore, Md.: 1950), 174*(6), 3256-3263.

Khalili-Shirazi, A., Summers, L., Linehan, J., Mallinson, G., Anstee, D., Hawke, S., . . . Collinge, J. (2005). PrP glycoforms are associated in a strain-specific ratio in native PrPSc. *The Journal of General Virology, 86*(Pt 9), 2635-2644. doi:10.1099/vir.0.80375-0

Khvorova, A., Reynolds, A., & Jayasena, S. D. (2003). Functional siRNAs and miRNAs exhibit strand bias. *Cell, 115*(2), 209-216.

Kim, J. G., Moon, M. Y., Kim, H. J., Li, Y., Song, D. K., Kim, J. S., . . . Park, J. B. (2012). Ras-related GTPases Rap1 and RhoA collectively induce the phagocytosis of serum-opsonized zymosan particles in macrophages. *The Journal of Biological Chemistry, 287*(7), 5145-5155. doi:10.1074/jbc.M111.257634; 10.1074/jbc.M111.257634

Kim, J. S., Diebold, B. A., Kim, J. I., Kim, J., Lee, J. Y., & Park, J. B. (2004). Rho is involved in superoxide formation during phagocytosis of opsonized zymosans. *The*

Journal of Biological Chemistry, 279(20), 21589-21597. doi:10.1074/jbc.M308386200

Kogo, R., Mimori, K., Tanaka, F., Komune, S., & Mori, M. (2011). Clinical significance of miR-146a in gastric cancer cases. *Clinical Cancer Research : An Official Journal of the American Association for Cancer Research, 17*(13), 4277-4284. doi:10.1158/1078-0432.CCR-10-2866; 10.1158/1078-0432.CCR-10-2866

Kuang, W., Tan, J., Duan, Y., Duan, J., Wang, W., Jin, F., . . . Liu, Y. (2009). Cyclic stretch induced miR-146a upregulation delays C2C12 myogenic differentiation through inhibition of numb. *Biochemical and Biophysical Research Communications, 378*(2), 259-263. doi:10.1016/j.bbrc.2008.11.041; 10.1016/j.bbrc.2008.11.041

Labbaye, C., Spinello, I., Quaranta, M. T., Pelosi, E., Pasquini, L., Petrucci, E., . . . Peschle, C. (2008). A three-step pathway comprising PLZF/miR-146a/CXCR4 controls megakaryopoiesis. *Nature Cell Biology, 10*(7), 788-801. doi:10.1038/ncb1741; 10.1038/ncb1741

Lai, E. C., Wiel, C., & Rubin, G. M. (2004). Complementary miRNA pairs suggest a regulatory role for miRNA:miRNA duplexes. *RNA (New York, N.Y.), 10*(2), 171-175.

Laine, J., Marc, M. E., Sy, M. S., & Axelrad, H. (2001). Cellular and subcellular morphological localization of normal prion protein in rodent cerebellum. *The European Journal of Neuroscience, 14*(1), 47-56.

Landreth, G. E., & Reed-Geaghan, E. G. (2009). Toll-like receptors in alzheimer's disease. *Current Topics in Microbiology and Immunology, 336*, 137-153. doi:10.1007/978-3-642-00549-7_8; 10.1007/978-3-642-00549-7_8

Lee, J., Kim, S. Y., Hwang, K. J., Ju, Y. R., & Woo, H. J. (2013). Prion diseases as transmissible zoonotic diseases. *Osong Public Health and Research Perspectives, 4*(1), 57-66. doi:10.1016/j.phrp.2012.12.008

Lee, Y., Ahn, C., Han, J., Choi, H., Kim, J., Yim, J., . . . Kim, V. N. (2003). The nuclear RNase III drosha initiates microRNA processing. *Nature, 425*(6956), 415-419. doi:10.1038/nature01957

Lee, Y., Kim, M., Han, J., Yeom, K. H., Lee, S., Baek, S. H., & Kim, V. N. (2004). MicroRNA genes are transcribed by RNA polymerase II. *The EMBO Journal, 23*(20), 4051-4060. doi:10.1038/sj.emboj.7600385

Lemaire, J., Mkannez, G., Guerfali, F. Z., Gustin, C., Attia, H., Sghaier, R. M., . . . Renard, P. (2013). MicroRNA expression profile in human macrophages in response to leishmania major infection. *PLoS Neglected Tropical Diseases, 7*(10), e2478. doi:10.1371/journal.pntd.0002478; 10.1371/journal.pntd.0002478

Lewis, B. P., Shih, I. H., Jones-Rhoades, M. W., Bartel, D. P., & Burge, C. B. (2003). Prediction of mammalian microRNA targets. *Cell, 115*(7), 787-798.

Li, Y., Vandenboom, T. G.,2nd, Wang, Z., Kong, D., Ali, S., Philip, P. A., & Sarkar, F. H. (2010). miR-146a suppresses invasion of pancreatic cancer cells. *Cancer*

Research, 70(4), 1486-1495. doi:10.1158/0008-5472.CAN-09-2792; 10.1158/0008-5472.CAN-09-2792

Liberski, P. P., Yanagihara, R., Nerurkar, V., & Gajdusek, D. C. (1994). Further ultrastructural studies of lesions produced in the optic nerve by tumor necrosis factor alpha (TNF-alpha): A comparison with experimental creutzfeldt-jakob disease. *Acta Neurobiologiae Experimentalis, 54*(3), 209-218.

Lin, S. L., Chiang, A., Chang, D., & Ying, S. Y. (2008). Loss of mir-146a function in hormone-refractory prostate cancer. *RNA (New York, N.Y.), 14*(3), 417-424. doi:10.1261/rna.874808; 10.1261/rna.874808

Linden, R., Martins, V. R., Prado, M. A., Cammarota, M., Izquierdo, I., & Brentani, R. R. (2008). Physiology of the prion protein. *Physiological Reviews, 88*(2), 673-728. doi:10.1152/physrev.00007.2007; 10.1152/physrev.00007.2007

Liu, B., & Hong, J. S. (2003). Role of microglia in inflammation-mediated neurodegenerative diseases: Mechanisms and strategies for therapeutic intervention. *The Journal of Pharmacology and Experimental Therapeutics, 304*(1), 1-7. doi:10.1124/jpet.102.035048

Liu, S., Liu, Y., Hao, W., Wolf, L., Kiliaan, A. J., Penke, B., . . . Fassbender, K. (2012). TLR2 is a primary receptor for alzheimer's amyloid beta peptide to trigger neuroinflammatory activation. *Journal of Immunology (Baltimore, Md.: 1950), 188*(3), 1098-1107. doi:10.4049/jimmunol.1101121; 10.4049/jimmunol.1101121

Liu, Y., Chen, Q., Song, Y., Lai, L., Wang, J., Yu, H., . . . Wang, Q. (2011). MicroRNA-98 negatively regulates IL-10 production and endotoxin tolerance in macrophages after LPS stimulation. *FEBS Letters, 585*(12), 1963-1968. doi:10.1016/j.febslet.2011.05.029; 10.1016/j.febslet.2011.05.029

Llewelyn, C. A., Hewitt, P. E., Knight, R. S., Amar, K., Cousens, S., Mackenzie, J., & Will, R. G. (2004). Possible transmission of variant creutzfeldt-jakob disease by blood transfusion. *Lancet, 363*(9407), 417-421. doi:10.1016/S0140-6736(04)15486-X

Loo, D. T., Copani, A., Pike, C. J., Whittemore, E. R., Walencewicz, A. J., & Cotman, C. W. (1993). Apoptosis is induced by beta-amyloid in cultured central nervous system neurons. *Proceedings of the National Academy of Sciences of the United States of America, 90*(17), 7951-7955.

Luers, A. J., Loudig, O. D., & Berman, J. W. (2010). MicroRNAs are expressed and processed by human primary macrophages. *Cellular Immunology, 263*(1), 1-8. doi:10.1016/j.cellimm.2010.03.011; 10.1016/j.cellimm.2010.03.011

Luhr, K. M., Nordstrom, E. K., Low, P., Ljunggren, H. G., Taraboulos, A., & Kristensson, K. (2004). Scrapie protein degradation by cysteine proteases in CD11c+ dendritic cells and GT1-1 neuronal cells. *Journal of Virology, 78*(9), 4776-4782.

Lukiw, W. J., Dua, P., Pogue, A. I., Eicken, C., & Hill, J. M. (2011). Upregulation of micro RNA-146a (miRNA-146a), a marker for inflammatory neurodegeneration, in sporadic creutzfeldt-jakob disease (sCJD) and gerstmann-straussler-scheinker (GSS)

syndrome. *Journal of Toxicology and Environmental Health.Part A, 74*(22-24), 1460-1468. doi:10.1080/15287394.2011.618973; 10.1080/15287394.2011.618973

Lukiw, W. J., Zhao, Y., & Cui, J. G. (2008). An NF-kappaB-sensitive micro RNA-146a-mediated inflammatory circuit in alzheimer disease and in stressed human brain cells. *The Journal of Biological Chemistry, 283*(46), 31315-31322. doi:10.1074/jbc.M805371200; 10.1074/jbc.M805371200

Maglio, L. E., Perez, M. F., Martins, V. R., Brentani, R. R., & Ramirez, O. A. (2004). Hippocampal synaptic plasticity in mice devoid of cellular prion protein. *Brain Research.Molecular Brain Research, 131*(1-2), 58-64. doi:10.1016/j.molbrainres.2004.08.004

Manson, J. C., Clarke, A. R., Hooper, M. L., Aitchison, L., McConnell, I., & Hope, J. (1994). 129/ola mice carrying a null mutation in PrP that abolishes mRNA production are developmentally normal. *Molecular Neurobiology, 8*(2-3), 121-127. doi:10.1007/BF02780662

McHattie, S. J., Brown, D. R., & Bird, M. M. (1999). Cellular uptake of the prion protein fragment PrP106-126 in vitro. *Journal of Neurocytology, 28*(2), 149-159.

Mead, S., Stumpf, M. P., Whitfield, J., Beck, J. A., Poulter, M., Campbell, T., . . . Collinge, J. (2003). Balancing selection at the prion protein gene consistent with prehistoric kurulike epidemics. *Science (New York, N.Y.), 300*(5619), 640-643. doi:10.1126/science.1083320

Medori, R., Montagna, P., Tritschler, H. J., LeBlanc, A., Cortelli, P., Tinuper, P., . . . Gambetti, P. (1992). Fatal familial insomnia: A second kindred with mutation of prion protein gene at codon 178. *Neurology, 42*(3 Pt 1), 669-670.

Medori, R., Tritschler, H. J., LeBlanc, A., Villare, F., Manetto, V., Chen, H. Y., . . . Cortelli, P. (1992). Fatal familial insomnia, a prion disease with a mutation at codon 178 of the prion protein gene. *The New England Journal of Medicine, 326*(7), 444-449. doi:10.1056/NEJM199202133260704

Mei, J., Bachoo, R., & Zhang, C. L. (2011). MicroRNA-146a inhibits glioma development by targeting Notch1. *Molecular and Cellular Biology, 31*(17), 3584-3592. doi:10.1128/MCB.05821-11; 10.1128/MCB.05821-11

Merrill, J. E., Ignarro, L. J., Sherman, M. P., Melinek, J., & Lane, T. E. (1993). Microglial cell cytotoxicity of oligodendrocytes is mediated through nitric oxide. *Journal of Immunology (Baltimore, Md.: 1950), 151*(4), 2132-2141.

Michaud, J. P., Richard, K. L., & Rivest, S. (2011). MyD88-adaptor protein acts as a preventive mechanism for memory deficits in a mouse model of alzheimer's disease. *Molecular Neurodegeneration, 6*(1), 5-1326-6-5. doi:10.1186/1750-1326-6-5; 10.1186/1750-1326-6-5

Miele, G., Alejo Blanco, A. R., Baybutt, H., Horvat, S., Manson, J., & Clinton, M. (2003). Embryonic activation and developmental expression of the murine prion protein gene. *Gene Expression, 11*(1), 1-12.

Montag, J., Hitt, R., Opitz, L., Schulz-Schaeffer, W. J., Hunsmann, G., & Motzkus, D. (2009). Upregulation of miRNA hsa-miR-342-3p in experimental and idiopathic prion disease. *Molecular Neurodegeneration, 4*, 36-1326-4-36. doi:10.1186/1750-1326-4-36; 10.1186/1750-1326-4-36

Moore, R. C., Lee, I. Y., Silverman, G. L., Harrison, P. M., Strome, R., Heinrich, C., . . . Westaway, D. (1999). Ataxia in prion protein (PrP)-deficient mice is associated with upregulation of the novel PrP-like protein doppel. *Journal of Molecular Biology, 292*(4), 797-817. doi:10.1006/jmbi.1999.3108

Moser, M., Colello, R. J., Pott, U., & Oesch, B. (1995). Developmental expression of the prion protein gene in glial cells. *Neuron, 14*(3), 509-517.

Mouillet-Richard, S., Ermonval, M., Chebassier, C., Laplanche, J. L., Lehmann, S., Launay, J. M., & Kellermann, O. (2000). Signal transduction through prion protein. *Science (New York, N.Y.), 289*(5486), 1925-1928.

Mourelatos, Z., Dostie, J., Paushkin, S., Sharma, A., Charroux, B., Abel, L., . . . Dreyfuss, G. (2002). miRNPs: A novel class of ribonucleoproteins containing numerous microRNAs. *Genes & Development, 16*(6), 720-728. doi:10.1101/gad.974702

Muhleisen, H., Gehrmann, J., & Meyermann, R. (1995). Reactive microglia in creutzfeldt-jakob disease. *Neuropathology and Applied Neurobiology, 21*(6), 505-517.

Nahid, M. A., Satoh, M., & Chan, E. K. (2011). MicroRNA in TLR signaling and endotoxin tolerance. *Cellular & Molecular Immunology, 8*(5), 388-403. doi:10.1038/cmi.2011.26; 10.1038/cmi.2011.26

Nathan, C. (1992). Nitric oxide as a secretory product of mammalian cells. *FASEB Journal : Official Publication of the Federation of American Societies for Experimental Biology, 6*(12), 3051-3064.

Nicolas, O., Gavin, R., & del Rio, J. A. (2009). New insights into cellular prion protein (PrPc) functions: The "ying and yang" of a relevant protein. *Brain Research Reviews, 61*(2), 170-184. doi:10.1016/j.brainresrev.2009.06.002; 10.1016/j.brainresrev.2009.06.002

O'Connell, R. M., Chaudhuri, A. A., Rao, D. S., & Baltimore, D. (2009). Inositol phosphatase SHIP1 is a primary target of miR-155. *Proceedings of the National Academy of Sciences of the United States of America, 106*(17), 7113-7118. doi:10.1073/pnas.0902636106; 10.1073/pnas.0902636106

O'Connell, R. M., Rao, D. S., Chaudhuri, A. A., & Baltimore, D. (2010). Physiological and pathological roles for microRNAs in the immune system. *Nature Reviews.Immunology, 10*(2), 111-122. doi:10.1038/nri2708; 10.1038/nri2708

O'Connell, R. M., Taganov, K. D., Boldin, M. P., Cheng, G., & Baltimore, D. (2007). MicroRNA-155 is induced during the macrophage inflammatory response. *Proceedings of the National Academy of Sciences of the United States of America, 104*(5), 1604-1609. doi:10.1073/pnas.0610731104

O'Neill, L. A., Sheedy, F. J., & McCoy, C. E. (2011). MicroRNAs: The fine-tuners of toll-like receptor signalling. *Nature Reviews.Immunology, 11*(3), 163-175. doi:10.1038/nri2957; 10.1038/nri2957

Packer, A. N., Xing, Y., Harper, S. Q., Jones, L., & Davidson, B. L. (2008). The bifunctional microRNA miR-9/miR-9* regulates REST and CoREST and is downregulated in huntington's disease. *The Journal of Neuroscience : The Official Journal of the Society for Neuroscience, 28*(53), 14341-14346. doi:10.1523/JNEUROSCI.2390-08.2008; 10.1523/JNEUROSCI.2390-08.2008

Pan, K. M., Baldwin, M., Nguyen, J., Gasset, M., Serban, A., Groth, D., . . . Cohen, F. E. (1993). Conversion of alpha-helices into beta-sheets features in the formation of the scrapie prion proteins. *Proceedings of the National Academy of Sciences of the United States of America, 90*(23), 10962-10966.

Perry, M. M., Moschos, S. A., Williams, A. E., Shepherd, N. J., Larner-Svensson, H. M., & Lindsay, M. A. (2008a). Rapid changes in microRNA-146a expression negatively regulate the IL-1beta-induced inflammatory response in human lung alveolar epithelial cells. *Journal of Immunology (Baltimore, Md.: 1950), 180*(8), 5689-5698.

Perry, M. M., Moschos, S. A., Williams, A. E., Shepherd, N. J., Larner-Svensson, H. M., & Lindsay, M. A. (2008b). Rapid changes in microRNA-146a expression negatively regulate the IL-1beta-induced inflammatory response in human lung alveolar epithelial cells. *Journal of Immunology (Baltimore, Md.: 1950), 180*(8), 5689-5698.

Perry, V. H., Cunningham, C., & Boche, D. (2002). Atypical inflammation in the central nervous system in prion disease. *Current Opinion in Neurology, 15*(3), 349-354.

Poltorak, A., He, X., Smirnova, I., Liu, M. Y., Van Huffel, C., Du, X., . . . Beutler, B. (1998). Defective LPS signaling in C3H/HeJ and C57BL/10ScCr mice: Mutations in Tlr4 gene. *Science (New York, N.Y.), 282*(5396), 2085-2088.

Ponomarev, E. D., Maresz, K., Tan, Y., & Dittel, B. N. (2007). CNS-derived interleukin-4 is essential for the regulation of autoimmune inflammation and induces a state of alternative activation in microglial cells. *The Journal of Neuroscience : The Official Journal of the Society for Neuroscience, 27*(40), 10714-10721. doi:10.1523/JNEUROSCI.1922-07.2007

Ponomarev, E. D., Novikova, M., Maresz, K., Shriver, L. P., & Dittel, B. N. (2005). Development of a culture system that supports adult microglial cell proliferation and maintenance in the resting state. *Journal of Immunological Methods, 300*(1-2), 32-46. doi:10.1016/j.jim.2005.02.011

Ponomarev, E. D., Shriver, L. P., & Dittel, B. N. (2006). CD40 expression by microglial cells is required for their completion of a two-step activation process during central nervous system autoimmune inflammation. *Journal of Immunology (Baltimore, Md.: 1950), 176*(3), 1402-1410.

Ponomarev, E. D., Veremeyko, T., Barteneva, N., Krichevsky, A. M., & Weiner, H. L. (2011). MicroRNA-124 promotes microglia quiescence and suppresses EAE by deactivating macrophages via the C/EBP-alpha-PU.1 pathway. *Nature Medicine, 17*(1), 64-70. doi:10.1038/nm.2266; 10.1038/nm.2266

Prinz, M., Heikenwalder, M., Schwarz, P., Takeda, K., Akira, S., & Aguzzi, A. (2003). Prion pathogenesis in the absence of toll-like receptor signalling. *EMBO Reports, 4*(2), 195-199. doi:10.1038/sj.embor.embor731

Prusiner, S. B. (1982). Novel proteinaceous infectious particles cause scrapie. *Science (New York, N.Y.), 216*(4542), 136-144.

Prusiner, S. B. (1998). Prions. *Proceedings of the National Academy of Sciences of the United States of America, 95*(23), 13363-13383.

Punj, V., Matta, H., Schamus, S., Tamewitz, A., Anyang, B., & Chaudhary, P. M. (2010). Kaposi's sarcoma-associated herpesvirus-encoded viral FLICE inhibitory protein (vFLIP) K13 suppresses CXCR4 expression by upregulating miR-146a. *Oncogene, 29*(12), 1835-1844. doi:10.1038/onc.2009.460; 10.1038/onc.2009.460

Qi, J., Qiao, Y., Wang, P., Li, S., Zhao, W., & Gao, C. (2012). microRNA-210 negatively regulates LPS-induced production of proinflammatory cytokines by targeting NF-kappaB1 in murine macrophages. *FEBS Letters, 586*(8), 1201-1207. doi:10.1016/j.febslet.2012.03.011; 10.1016/j.febslet.2012.03.011

Qin, H., Wilson, C. A., Lee, S. J., Zhao, X., & Benveniste, E. N. (2005). LPS induces CD40 gene expression through the activation of NF-kappaB and STAT-1alpha in macrophages and microglia. *Blood, 106*(9), 3114-3122. doi:10.1182/blood-2005-02-0759

Quinn, E. M., Wang, J. H., O'Callaghan, G., & Redmond, H. P. (2013). MicroRNA-146a is upregulated by and negatively regulates TLR2 signaling. *PloS One, 8*(4), e62232. doi:10.1371/journal.pone.0062232; 10.1371/journal.pone.0062232

Radhakrishna, H., & Donaldson, J. G. (1997). ADP-ribosylation factor 6 regulates a novel plasma membrane recycling pathway. *The Journal of Cell Biology, 139*(1), 49-61.

Radovanovic, I., Braun, N., Giger, O. T., Mertz, K., Miele, G., Prinz, M., . . . Aguzzi, A. (2005). Truncated prion protein and doppel are myelinotoxic in the absence of oligodendrocytic PrPC. *The Journal of Neuroscience : The Official Journal of the Society for Neuroscience, 25*(19), 4879-4888. doi:10.1523/JNEUROSCI.0328-05.2005

Rossi, D., Cozzio, A., Flechsig, E., Klein, M. A., Rulicke, T., Aguzzi, A., & Weissmann, C. (2001). Onset of ataxia and purkinje cell loss in PrP null mice inversely correlated with dpl level in brain. *The EMBO Journal, 20*(4), 694-702. doi:10.1093/emboj/20.4.694

Saba, R., Goodman, C. D., Huzarewich, R. L., Robertson, C., & Booth, S. A. (2008). A miRNA signature of prion induced neurodegeneration. *PloS One, 3*(11), e3652. doi:10.1371/journal.pone.0003652; 10.1371/journal.pone.0003652

Saba, R., Gushue, S., Huzarewich, R. L., Manguiat, K., Medina, S., Robertson, C., & Booth, S. A. (2012). MicroRNA 146a (miR-146a) is over-expressed during prion disease and modulates the innate immune response and the microglial activation

state. *PloS One, 7*(2), e30832. doi:10.1371/journal.pone.0030832; 10.1371/journal.pone.0030832

Sakaguchi, S., Katamine, S., Nishida, N., Moriuchi, R., Shigematsu, K., Sugimoto, T., . . . Noda, T. (1996). Loss of cerebellar purkinje cells in aged mice homozygous for a disrupted PrP gene. *Nature, 380*(6574), 528-531. doi:10.1038/380528a0

Schnitger, A. K., Machova, A., Mueller, R. U., Androulidaki, A., Schermer, B., Pasparakis, M., . . . Papadopoulou, N. (2011). Listeria monocytogenes infection in macrophages induces vacuolar-dependent host miRNA response. *PloS One, 6*(11), e27435. doi:10.1371/journal.pone.0027435; 10.1371/journal.pone.0027435

Schwarz, D. S., Hutvagner, G., Du, T., Xu, Z., Aronin, N., & Zamore, P. D. (2003). Asymmetry in the assembly of the RNAi enzyme complex. *Cell, 115*(2), 199-208.

Scott, M., Foster, D., Mirenda, C., Serban, D., Coufal, F., Walchli, M., . . . Prusiner, S. B. (1989). Transgenic mice expressing hamster prion protein produce species-specific scrapie infectivity and amyloid plaques. *Cell, 59*(5), 847-857.

Selbach, M., Schwanhausser, B., Thierfelder, N., Fang, Z., Khanin, R., & Rajewsky, N. (2008). Widespread changes in protein synthesis induced by microRNAs. *Nature, 455*(7209), 58-63. doi:10.1038/nature07228; 10.1038/nature07228

Sethi, S., Lipford, G., Wagner, H., & Kretzschmar, H. (2002). Postexposure prophylaxis against prion disease with a stimulator of innate immunity. *Lancet, 360*(9328), 229-230. doi:10.1016/S0140-6736(02)09513-2

Sheedy, F. J., Palsson-McDermott, E., Hennessy, E. J., Martin, C., O'Leary, J. J., Ruan, Q., . . . O'Neill, L. A. (2010). Negative regulation of TLR4 via targeting of the proinflammatory tumor suppressor PDCD4 by the microRNA miR-21. *Nature Immunology, 11*(2), 141-147. doi:10.1038/ni.1828; 10.1038/ni.1828

Sikorska, B., & Liberski, P. P. (2012). Human prion diseases: From kuru to variant creutzfeldt-jakob disease. *Sub-Cellular Biochemistry, 65*, 457-496. doi:10.1007/978-94-007-5416-4_17; 10.1007/978-94-007-5416-4_17

Soto, C. (2003). Unfolding the role of protein misfolding in neurodegenerative diseases. *Nature Reviews.Neuroscience, 4*(1), 49-60. doi:10.1038/nrn1007

Soto, C., Estrada, L., & Castilla, J. (2006). Amyloids, prions and the inherent infectious nature of misfolded protein aggregates. *Trends in Biochemical Sciences, 31*(3), 150-155. doi:10.1016/j.tibs.2006.01.002

Soto, C., Saborio, G. P., & Anderes, L. (2002). Cyclic amplification of protein misfolding: Application to prion-related disorders and beyond. *Trends in Neurosciences, 25*(8), 390-394.

Spinner, D. S., Cho, I. S., Park, S. Y., Kim, J. I., Meeker, H. C., Ye, X., . . . Kascsak, R. J. (2008). Accelerated prion disease pathogenesis in toll-like receptor 4 signaling-mutant mice. *Journal of Virology, 82*(21), 10701-10708. doi:10.1128/JVI.00522-08; 10.1128/JVI.00522-08

Spinner, D. S., Kascsak, R. B., Lafauci, G., Meeker, H. C., Ye, X., Flory, M. J., . . . Kascsak, R. J. (2007). CpG oligodeoxynucleotide-enhanced humoral immune

response and production of antibodies to prion protein PrPSc in mice immunized with 139A scrapie-associated fibrils. *Journal of Leukocyte Biology, 81*(6), 1374-1385. doi:10.1189/jlb.1106665

Stansley, B., Post, J., & Hensley, K. (2012). A comparative review of cell culture systems for the study of microglial biology in alzheimer's disease. *Journal of Neuroinflammation, 9*, 115-2094-9-115. doi:10.1186/1742-2094-9-115; 10.1186/1742-2094-9-115

Steele, A. D., Emsley, J. G., Ozdinler, P. H., Lindquist, S., & Macklis, J. D. (2006). Prion protein (PrPc) positively regulates neural precursor proliferation during developmental and adult mammalian neurogenesis. *Proceedings of the National Academy of Sciences of the United States of America, 103*(9), 3416-3421. doi:10.1073/pnas.0511290103

Streit, W. J. (2002a). Microglia and the response to brain injury. *Ernst Schering Research Foundation Workshop, (39)*(39), 11-24.

Streit, W. J. (2002b). Microglia as neuroprotective, immunocompetent cells of the CNS. *Glia, 40*(2), 133-139. doi:10.1002/glia.10154

Sun, S. G., Zheng, B., Han, M., Fang, X. M., Li, H. X., Miao, S. B., . . . Wen, J. K. (2011). miR-146a and kruppel-like factor 4 form a feedback loop to participate in vascular smooth muscle cell proliferation. *EMBO Reports, 12*(1), 56-62. doi:10.1038/embor.2010.172; 10.1038/embor.2010.172

Taganov, K. D., Boldin, M. P., Chang, K. J., & Baltimore, D. (2006). NF-kappaB-dependent induction of microRNA miR-146, an inhibitor targeted to signaling proteins of innate immune responses. *Proceedings of the National Academy of Sciences of the United States of America, 103*(33), 12481-12486. doi:10.1073/pnas.0605298103

Tahara, K., Kim, H. D., Jin, J. J., Maxwell, J. A., Li, L., & Fukuchi, K. (2006). Role of toll-like receptor signalling in abeta uptake and clearance. *Brain : A Journal of Neurology, 129*(Pt 11), 3006-3019. doi:10.1093/brain/awl249

Takeda, K., & Akira, S. (2004). TLR signaling pathways. *Seminars in Immunology, 16*(1), 3-9.

Tal, Y., Souan, L., Cohen, I. R., Meiner, Z., Taraboulos, A., & Mor, F. (2003). Complete freund's adjuvant immunization prolongs survival in experimental prion disease in mice. *Journal of Neuroscience Research, 71*(2), 286-290. doi:10.1002/jnr.10474

Thiel, V. E., & Audus, K. L. (2001). Nitric oxide and blood-brain barrier integrity. *Antioxidants & Redox Signaling, 3*(2), 273-278. doi:10.1089/152308601300185223

Tichopad, A., Pfaffl, M. W., & Didier, A. (2003). Tissue-specific expression pattern of bovine prion gene: Quantification using real-time RT-PCR. *Molecular and Cellular Probes, 17*(1), 5-10.

Tili, E., Michaille, J. J., Cimino, A., Costinean, S., Dumitru, C. D., Adair, B., . . . Croce, C. M. (2007). Modulation of miR-155 and miR-125b levels following lipopolysaccharide/TNF-alpha stimulation and their possible roles in regulating the

response to endotoxin shock. *Journal of Immunology (Baltimore, Md.: 1950), 179*(8), 5082-5089.

Tzircotis, G., Braga, V. M., & Caron, E. (2011). RhoG is required for both FcgammaR- and CR3-mediated phagocytosis. *Journal of Cell Science, 124*(Pt 17), 2897-2902. doi:10.1242/jcs.084269; 10.1242/jcs.084269

Van Acker, T., Eyckerman, S., Vande Walle, L., Gerlo, S., Goethals, M., Lamkanfi, M., . . . Peelman, F. (2014). The small GTPase Arf6 is essential for the tram/trif pathway in TLR4 signaling. *The Journal of Biological Chemistry, 289*(3), 1364-1376. doi:10.1074/jbc.M113.499194; 10.1074/jbc.M113.499194

Van Aelst, L., & D'Souza-Schorey, C. (1997). Rho GTPases and signaling networks. *Genes & Development, 11*(18), 2295-2322.

Vilhardt, F. (2005). Microglia: Phagocyte and glia cell. *The International Journal of Biochemistry & Cell Biology, 37*(1), 17-21. doi:10.1016/j.biocel.2004.06.010

Vinther, J., Hedegaard, M. M., Gardner, P. P., Andersen, J. S., & Arctander, P. (2006). Identification of miRNA targets with stable isotope labeling by amino acids in cell culture. *Nucleic Acids Research, 34*(16), e107. doi:10.1093/nar/gkl590

Walker, W. S., Gatewood, J., Olivas, E., Askew, D., & Havenith, C. E. (1995). Mouse microglial cell lines differing in constitutive and interferon-gamma-inducible antigen-presenting activities for naive and memory CD4+ and CD8+ T cells. *Journal of Neuroimmunology, 63*(2), 163-174.

Will, R. G., Ironside, J. W., Zeidler, M., Cousens, S. N., Estibeiro, K., Alperovitch, A., . . . Smith, P. G. (1996). A new variant of creutzfeldt-jakob disease in the UK. *Lancet, 347*(9006), 921-925.

Williams, A. E., Lawson, L. J., Perry, V. H., & Fraser, H. (1994). Characterization of the microglial response in murine scrapie. *Neuropathology and Applied Neurobiology, 20*(1), 47-55.

Wu, J. Y., & Kuo, C. C. (2012). Pivotal role of ADP-ribosylation factor 6 in toll-like receptor 9-mediated immune signaling. *The Journal of Biological Chemistry, 287*(6), 4323-4334. doi:10.1074/jbc.M111.295113; 10.1074/jbc.M111.295113

Wyss-Coray, T., & Mucke, L. (2002). Inflammation in neurodegenerative disease--a double-edged sword. *Neuron, 35*(3), 419-432.

Xiang, W., Windl, O., Wunsch, G., Dugas, M., Kohlmann, A., Dierkes, N., . . . Kretzschmar, H. A. (2004). Identification of differentially expressed genes in scrapie-infected mouse brains by using global gene expression technology. *Journal of Virology, 78*(20), 11051-11060. doi:10.1128/JVI.78.20.11051-11060.2004

Yang, Y., Chaerkady, R., Beer, M. A., Mendell, J. T., & Pandey, A. (2009). Identification of miR-21 targets in breast cancer cells using a quantitative proteomic approach. *Proteomics, 9*(5), 1374-1384. doi:10.1002/pmic.200800551; 10.1002/pmic.200800551

Yang, Y., Chaerkady, R., Kandasamy, K., Huang, T. C., Selvan, L. D., Dwivedi, S. B., . . . Pandey, A. (2010). Identifying targets of miR-143 using a SILAC-based proteomic

approach. *Molecular bioSystems, 6*(10), 1873-1882. doi:10.1039/c004401f; 10.1039/c004401f

Zhang, Q., Cox, D., Tseng, C. C., Donaldson, J. G., & Greenberg, S. (1998). A requirement for ARF6 in fcgamma receptor-mediated phagocytosis in macrophages. *The Journal of Biological Chemistry, 273*(32), 19977-19981.

Zhang, Y., Zhang, M., Zhong, M., Suo, Q., & Lv, K. (2013). Expression profiles of miRNAs in polarized macrophages. *International Journal of Molecular Medicine, 31*(4), 797-802. doi:10.3892/ijmm.2013.1260; 10.3892/ijmm.2013.1260